DESIGN AND FATIGUE OF A STRUCTURAL

WOOD-PLASTIC COMPOSITE

By

Andrew Edward Slaughter

A thesis submitted in partial fulfillment of
the requirements for the degree of

MASTER OF SCIENCE IN CIVIL ENGINEERING

WASHINGTON STATE UNIVERSITY
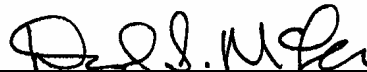Department of Civil and Environmental Engineering
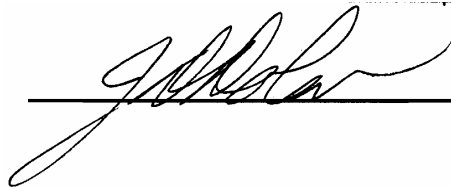
AUGUST 2004

To the Faculty of Washington State University:

The members of the Committee appointed to examine the thesis of

ANDREW EDWARD SLAUGHTER find it satisfactory and recommend that it

be accepted.

_____
Chair

_____

_____

ii

ACKNOWLEDGMENTS

DESIGN AND FATIGUE OF A STRUCTURAL

WOOD-PLASTIC COMPOSITE

Abstract

by Andrew Edward Slaughter, M.S.
Washington State University
August 2004

Chair: Michael P. Wolcott

Wood-plastic composites (WPCs) have emerged as a viable replacement for industrial structural applications such as waterfront structures and bridge decking due to its resistance to moisture and decay. In this study, procedures for assigning allowable design stresses were developed, including adjustments in design values for load duration, moisture, and temperature effects. The proposed procedures were applied to an extruded composite material determined by evaluating twenty-two maple and pine polypropylene formulations for mechanical and physical properties. The resulting allowable design stresses were used to determine required section properties for AASHTO loadings, resulting in the creation of span tables. The influences of coupling agents, test frequency, and stress ratio on the fatigue life were investigated. Results show that fatigue life and internal heating increased with increasing test frequency; however, strain to failure remained relatively constant. Comparing the static and fatigue test distributions indicated that the uncoupled formulation displays different mechanisms controlling short- and long-term failures, unlike those for the formulation containing co-polymer coupling agents. Finally, fatigue testing indicated that the selected WPC formulation is suitable for pedestrian bridge applications.

TABLE OF CONTENTS

LIST OF TABLES

LIST OF FIGURES

CHAPTER 1 – INTRODUCTION

1.1 Background

Wood-plastic composites (WPCs) are defined as filled thermoplastics consisting primarily of wood fiber and thermoplastic polymer (Wolcott, 2001). Thermoplastics such as polyethylene (PE), polyvinyl chloride (PVC), and polypropylene (PP) are currently being utilized for a variety of commercial products, including automotive trim, window frames, and roof singles. However, the largest and fastest growing market for WPCs is extruded residential decking and railing (Clemons, 2002; Wolcott, 2001).

When compared to timber, WPCs exhibit increased durability with minimal maintenance (Clemons, 2002). Wolcott (2001) found that the addition of 40-50% wood improved thermal stability, while the thermoplastic component improved moisture and thermal formability. When exposed to moisture, WPCs absorb less moisture at a slower rate, leading to superior fungal resistance, and dimensional stability when compared to timber (Clemons, 2002). Waterfront applications have also demonstrated that WPC materials exhibit improved durability with respect to checking, decay, termites, and marine organisms in contrast to timber (Balma and Bender, 2001).

Preservative treatment of wood to resist fungal decay has been identified as a leading problem for utilization of timber in certain applications (Smith and Cesa, 1998), thus, providing an incentive to employ WPCs as a timber replacement. Leading wood preservative treatment manufactures, in an agreement with the Environmental Protection Agency (EPA), voluntarily withdrew the use of chromated copper arsenate (CCA) for consumer applications (Southern, 2002). Consequently, next-generation treatments are

now being applied at a higher cost, which has narrowed the cost gap between timber and composites.

Research of high-strength engineered plastics has been performed, and Wolcott (2001) concludes that WPCs should not be limited to nonstructural applications. Therefore, expansion of the WPC market for structural applications is appropriate, provided societal incentive exists and feasible applications are developed and accepted by industry.

1.2 Incentive

Research indicates that the market for WPC decking for residential purposes is well established and expanding beyond traditional residential use. Application of these materials for structurally demanding applications, such as marine pier components, has been successfully demonstrated. Current research is focused on expanding the market to light vehicular or pedestrian bridges such as those found along recreational pathways. To develop engineering acceptance of WPCs and progress into a new structural market, a societal need must exist.

One example outlining this need is the Wood in Transportation Program (WIT). The WIT began in 1989 and has contributed substantially to the expansion of markets for various engineered wood components in transportation infrastructure (Smith and Cesa, 1998). Market expansion assists new technologies to become commercially viable, emphasizing the importance of continuing to develop WPC material for structural uses. Smith and Cesa (1998) also discuss the benefits of becoming involved with an initiative such at the WIT Program. Since the beginning of the WIT Program, over $20 million in

funding has been provided for research, construction, and technology advances (Smith and Cesa, 1998). Commercial exposure has been provided through demonstration projects, which have totaled over 340 by 1997 (Smith and Cesa, 1998).

Smith and Cesa (1998) provide additional indications of the societal need for structural WPC materials. Responses were gathered from industry on various open-ended questions. The most significant of these questions addressed the greatest perceived obstacle influencing the advancement of timber in bridge construction. Among the 40 companies that responded (25% produce engineered wood products), the most common response involved the environmental concerns with wood preservatives (Smith and Cesa, 1998). Studies surveying U.S. marine decision makers, U.S. Port Authorities, and engineering consulting firms concluded that a demand exists for strong, cost-effective, durable, and environmentally-benign materials for exposed applications (Smith and Bright, 2002; Bright and Smith, 2002) Overall, industry desires an alternative to treated timber, and research indicates WPCs are a viable solution.

1.3 Research Development

Previous research has investigated the use of WPCs as an alternative to preservative treated wood members in military and civilian marine structures (Haiar, 2000). Research focused on the use of WPC members for waterfront facilities, including a deck board and chock members that were installed at U.S. Navy bases (Haiar et al., 2001).

Although not identical, the Navy loading requirements for the pier decking are similar to those of the American Association of State Highway and Transportation

3

Officials (AASHTO) for bridges in both magnitude and configuration. The U.S. Navy requirements for the deck section studied consist of a distributed load across the entire area of the pier of 600 psf and a concentrated single wheel load of 16,000 lbf (Haiar et al., 2001). For comparison, the minimum requirement for highway bridges for HS20-44 loadings, consists of a distributed load of 640 lbf per foot across the entire lane width as well as a concentrated load of 18,000 lbf for moment and 26,000 lbf for shear (AASHTO, 2002). The similarity in these two load configurations demonstrates the potential to make use of WPCs as a decking material for transportation applications.

Studies conducted by the Florida Department of Transportation (FDOT) have shown that gross weight, axle weight, and axle configuration of trucks affect the service life of bridge superstructures, with the most damage found in the bridge deck (Wang, 2000). The extensive use of highways and the growing frequency of heavy trucks contribute significantly to fatigue damage (Wang, 2000). Gong and Smith (2003) cite that between 80% and 90% of structural failures occur from fatigue, reinforcing the importance of the cyclic loading conditions in determining structural performance. Both studies concluded that fatigue is an issue that needs to be considered in the design of bridge decks.

A potential problem with using thermoplastic composites in structural applications involves their fatigue reliability under various environmental and loading conditions. Fatigue reliability is an area of research that is gaining increased attention for civil structures, especially in the area of fiber-reinforced composites (FRP). Specifically for WPCs, minimal research exists regarding fatigue, of which nearly all concentrate on small coupon specimens.

Considering the possibility of using wood-plastic composites for structural bridge elements, such as bridge decks, an understanding of the fatigue performance of full-scale WPC members is needed. If WPCs are to be accepted by industry as a building material, the service life of the material is an important parameter to qualify the material as a viable solution.

1.4 Objectives

Previous research has found that society desires an alternative for preservative-treated timber, and implementation of WPCs in structural applications indicates that WPCs are a possible solution. Further development of WPCs for commercial use as a timber alternative requires significant research to provide an understanding and evidence of the materials capabilities. The research presented herein was conducted with the objective of advancing the acceptance and knowledge of WPC materials. The specific goals were to:

a.) Establish an optimum polypropylene WPC formulation for structural application and design based on measured mechanical and physical properties,

b.) To utilize traditional timber design methodologies and current WPC research to verify the potential of a PP WPC formulation to perform structurally, and

c.) To confirm the ability of PP WPCs to resist cyclic loading as well as to use a power law model for predicting fatigue life and characterizing fatigue failure mechanism.

1.5 References

American Association of State Highway and Transportation Officials (AASHTO). "Standard Specifications for Highway Bridges." 17th Edition, 2002.

Balma, D.A. and Bender, D.A. "Engineering Wood Composites for Naval Waterfront Facilities, Evaluation of Bolted WPC Connections." Materials Development, Task 2J. Project End Report, 2001.

Bright, K.D. and Smith, P.M. "Perceptions of New and Established Waterfront Materials by U.S. Marine Decision Makers." Wood and Fiber Science, 34(2), 2002.

Clemons, C. "Wood-Plastic Composites in the United States, The Interfacing of Two Industries." Forest Product Journal, June 2002, Vol. 52, No. 6., pp. 10-18.

Haiar, K.J. "Performance and Design of Prototype Wood-Plastic Composite Sections." Master Thesis, Washington State University, May 2000.

Haiar, K.J., McLean, D.I., Cofer, W.F. "Analysis and Design of WPC Deckboard Section for NUWC Pier 171." Washington State University, Project End Report, June 2001.

Smith, P.M. and Bright, K.D. "Perceptions of New and Established Waterfront Materials: U.S. Port Authorities and Engineering Consulting Firms." Wood and Fiber Science, 34(1), 2002.

Smith, R.L. and Cesa, E. "An Assessment of 'Technology Push' in the Timber Bridge Industry." Forest Product Journal, Vol. 48, No. 1, 1998.

"Southern Pine by Design, Market News from the Southern Pine Council." Southern Pine Council. Volume 9, Issue 1, 2002.

Tang, H.C., Nguyen, T., Chuang, T., Chin J., Lesko, J. Wu, H.F. "Fatigue Model for Fiber-Reinforced Polymeric Composites." Journal of Materials in Civil Engineering, May 2000, pp. 97-104.

Wolcott, M.P. "Wood-Plastic Composites." Encyclopedia of Materials: Science and Technology, 2001.

CHAPTER 2 – STATIC TESTING OF STRUCTURAL POLYPROPYLENE WOOD-PLASTIC COMPOSITES

2.1 Abstract

Wood-plastic composite materials have surfaced as a suitable replacement for treated lumber in residential applications. A need also exists to utilize wood-plastic composites (WPCs) for industrial structural applications such as bridge decking. In this study, twenty-two maple and pine polypropylene (PP) formulations were evaluated to establish a structural material with superior mechanical and physical properties compared to current composite formulations. The materials tested were composed of various quantities of wood flour, PP, talc, coupling agent, and a lubricant. Flexural strength, shear strength, water absorption, thickness swell, and extrusion characteristics were determined for each formulation. Modulus of rupture ranged from 3200 psi to 8800 psi, shear strength varied between 1400 psi to 3400 psi, and modulus of elasticity ranged from 507,000 psi to 870,000 psi. Results indicate that the relative effects of material composition on mechanical and physical properties are similar for both pine and maple wood flour. A comparison between wood flour species indicates that pine exhibits superior water absorption behavior and extrusion quality, but maple demonstrates higher mechanical properties. Overall, a pine formulation with moderate quantities of each material component was selected as the optimum formulation, based on the measured physical and mechanical properties.

2.2 Introduction

Wood-plastic composites (WPCs), defined as a thermoplastics reinforced with wood or other natural fibers, are principally produced from commodity thermoplastics such as polyethylene (PE), polyvinyl chloride (PVC), or polypropylene (PP) (Wolcott, 2001). Current use of WPC materials includes automotive trim, window frames, roof shingles, and residential decking. Compared to timber, WPCs exhibit greater durability, require less maintenance, absorb less moisture, and provide superior fungal resistances (Clemons, 2002). In addition, the wood filler improves thermal stability in contrast to other polymer composites (Wolcott, 2001).

Industrial structural applications of WPC materials have been limited, but a PVC wood-plastic composite formulation was successful utilized for a marine structure that required significant structural performance (Haiar et al., 2001). Benefits exist for using an environmentally-benign material for marine applications, principally in reducing the permitting time and costs currently imposed on treated timber (Smith and Bright, 2002). The bridge industry also recognizes preservative treatment as the greatest hindrance for utilization of timber for bridge construction (Smith and Cesa, 1998), reinforcing the motivation for developing structural WPCs. To reach this goal, these materials must resist a variety of structural loads while also maintaining resistance to moisture exposure and fungal decay (Wolcott, 2001; Clemons, 2002).

Gaining acceptance for the use of WPCs within the structural design community requires a significant quantity of testing, analysis, and demonstrated use. Mechanical testing of WPCs developed for commercial use has been performed on other polymer types, including PE and PVC (Adcock et al., 2001; Haiar, 2000). The work presented

here builds on this previous research with the specific objective of establishing a PP-based WPC formulation that exhibits adequate extrusion characteristics, material properties, and water absorption. Such formulations would improve utilization of this emerging material class for structural applications.

2.3 Materials

Twenty-two polypropylene formulations of wood-plastic composite were produced and evaluated. Two species of wood fiber were utilized, maple (*Acer spp.*) and pine (*Pinus spp.*). Both wood fibres were obtained commercially as 60-mesh wood flour and subsequently dried to approximately 2% moisture content using a conical counter-rotating twin-screw extruder (Cincinnati-Milacron TC86). The composite materials produced were comprised of varying weight percentages of wood fiber, PP, maleated polypropylene coupling agent (MAPP), talc, and lubricant. Product details for each material are included in Table 2.1. Specific material quantities for the various formulations are summarized in Table 2.2, and each formulation is assigned identification, P or M, to denote pine or maple, respectively.

Material components were blended in powdered form using a 4-ft diameter drum mixer in 51 lb batches. The dry blend was direct-extruded at a rate of 3.5 rpm using a conical counter-rotating twin-screw extruder (Cincinnati-Milacron TC86) controlled at a predetermined screw and barrel temperature profile (Table 2.3). The extrusion process included the use of a stranding die (Laver, 1996) to shape the 1 in. by 5.5 in. solid deck board profile depicted in Fig. 2.1.

2.4 Physical and Mechanical Properties

Flexural strength, strain at failure, modulus of elasticity (MOE), and modulus of rupture (MOR) were determined following ASTM D6109 (2002). Load was applied with a 30-kip universal electromechanical test machine (Instron 4400R). Sample size and modulus of elasticity were modified from the standard to conform to the Acceptance Criteria for Deck Board Span Ratings and Guardrail Systems (AC174, 2002). However, the sample size was increased from 5 to 15, and modulus of elasticity was calculated using the secant method between 20% and 40% of ultimate load. On account of poor extrusion performance, formulations M7, M9, and M10 were machined to achieve a regular cross section by removing the snake-skin edges. The cross-sectional area and moment of inertia were calculated using methods described in Appendix A and Appendix B includes images of typical test setups for each for the tests performed in this research (Slaughter, 2004).

Shear parallel to the extrusion direction was determined using two test methods, ASTM D143 (2002) and ASTM D3846 (2002). The shear block method (ASTM D143) was modified by altering the specimen width from 2 in. to 1 in. and excluded moisture content measurements. The coupon shear method (ASTM D3846) prescribes measuring the shear length between notches in the specimen following failure, but for ease and accuracy of measurement, the shear length was determined prior to testing. This method neglects shortening of the shear zone due to compression of the member, which was deemed negligible for the coupon tests. Sample size for both methods was increased to 15 to be consistent with the flexure experiments. Tests were performed with a 30-kip and

2-kip universal electromechanical test machine for the shear block and coupon shear strength methods (Instron 4400R and 4466), respectively.

Thickness swell and water absorption characteristics were determined following a modification of ASTM D1037 (2002). Specimen size, conditioning prior to testing, and measuring techniques varied from the standard. Tested specimens nominally measured 1 in. wide by 5 in. long and 0.25 in. thick. All specimens were conditioned for 40 hr at 73.4 ± 3.6°F prior to submersion. Thickness was measured at four points using digital calipers. Five specimens of each formulation were measured at various time intervals until the average percent increase in absorbed water and thickness swell remained constant. The initial measurements were taken two hours after submersion to minimize size variation caused by the temperature gradient between the conditioning room and water.

2.5 Results

2.5.1 Extrusion Quality

Three classes of extrusion defects were noted during processing of the twenty-two formulations: surface fracture, die swelling, and splitting (Fig. 2.2). Severe surface fractures and die swell existed in formulations M7, M9, and M10 eliminating these formulations from commercial consideration and excluding them from further section quality comparisons. Formulations M2 and M3 demonstrated significant splitting, formulations P7, P10, P11, and M1 had observable swelling, and formulation M11 exhibited surface fracturing. The remaining formulations extruded reasonably well and revealed no obvious production problems.

11

To further quantify extrusion quality, the difference from nominal depth and width of each non-defective formulation was calculated. The absolute values of the depth and width difference were then summed and assumed to be an indicator of extrusion quality (Table 2.4). Based upon this measurement, and limiting comparison to formulations without obvious defects, the least deviation occurred for P4, which contains low amounts of polymer and no coupling agent. Surprisingly, the corresponding maple formulation (M4) exhibited the largest deviation from nominal. The second lowest difference occurred in formulations 5 and 6 for both maple and pine. These formulations are identical except for wood flour type. Although P5 and P6 exhibited a smoother surface compared to that for the maple counterparts, both of these pine and maple formulations are acceptable.

In general, formulations containing pine exhibited superior extrusion quality compared to that for maple. In addition, formulations containing median levels of each material component had the most reliable extrusion characteristics. Disregarding wood species, formulations 5 and 6 exhibited the best extrusion quality.

2.5.2 Mechanical Properties

Mean modulus of elasticity, modulus of rupture, strain at failure, and shear strengths are summarized in Table 2.5 for each formulation. Load-deflection plots for each formulation are included in Appendix B (Slaughter, 2004). A consistent variation of shear strength existed between the values obtained using the two standard test methods. The shear block strength averages 25% lower than those from the coupon shear test. Because both testing methods test the shear strength parallel to extrusion direction, the

12

same strength would be expected. A significant number of coupon specimens did not display a clear shear failure, and were therefore culled. In addition, the coupon shear test is more difficult to perform due to machining and setup time. Considering these factors, shear strength corresponding to those obtained using the shear block method were used as a conservative estimate.

The effects of formulation remain reasonably consistent throughout both wood species; i.e., the largest value of a property within a species group tended to occur for the same formulation in each species. Considering the range of material quantities tested, the best performing formulations contained approximately the median amount of each material. The addition of the coupling agent (MAPP) caused the largest affect on mechanical properties, specifically MOR. Two formulations did not contain MAPP (4 and 9), both of which demonstrated significantly lower MOR. Excluding the formulations without MAPP, MOR for maple varied between 6324 psi and 8800 psi, whereas formulations 4 and 9 equaled 3336 psi and 4655 psi, respectively. The same trend exists for pine, where MOR ranged between 5918 psi and 7557 psi, whereas formulations 4 and 9 equaled 3205 psi and 4685 psi, respectively.

As with MOR, formulations containing the median material quantities demonstrated the largest MOE, strain to failure, and shear strength; however, these properties varied less when compared to variation in MOR. For example, the minimum MOR for maple is 38% of the maximum, and the minimum MOE for maple is 60% of the maximum. MOE ranged from 507,000 psi to 850,000 psi and 540,000 psi to 870,000 psi for maple and pine, respectively. Strain at failure varied between 0.87% and 1.85% for

maple and 0.96% and 1.92% for pine. Finally, shear strength was nearly equivalent for both species, which ranged between 1363 psi and 3423 psi.

Haiar (2000) tested WPCs composed of PVC (polyvinyl chloride) and HDPE (high-density polyethylene). These formulations exhibited inferior mechanical properties compared to the best performing PP-based WPCs tested in this research. The mean MOR for PVC- and HDPE-based WPCs are 5171 psi and 1822 psi, respectively. The mean shear strengths for the same formulations are 2931 psi and 1133 psi, respectively. Finally, the MOE of the PVC and HDPE formulations tested by Haiar (2000) are 754,000 psi and 360,000 psi, respectively.

The two formulations without coupling agent (4 and 9) are exceptions to the trend that formulations with moderate quantities demonstrated greater mechanical properties. The minimum strain to failure occurs in formulation 4, but 4 exhibits a much higher MOE than the minimum, which occurs in formulation 9. In addition, formulation 9 exhibited the largest strain at failure. It seems that formulation 4, which contained the largest quantity of polymer, produced a more ductile material resulting in higher strain to failure with a relatively low MOE. In contrast, formulation 9 contained the largest quantity of filler, resulting in a more brittle material with a low strain at failure and relatively high MOE. The preceding observations indicate that MOE and strain at failure are influenced significantly by polymer and wood flour content in the absence of a coupling agent.

The addition of a coupling agent seemingly reduces the relation between polymer and wood filler content on the strain to failure compared to the two formulations without MAPP. Formulation M1 contains 69.5% filler and has a strain to failure of 1.2%, while

formulation M7 contains 56.4% filler and fails at 1.4% strain. Comparatively, formulations without MAPP (M4 and M9) contain 74% and 54% filler and have a strain to failure of 0.9% and 1.85%, respectively. These results indicate that ductility decreases with increasing filler, but a direct comparison cannot be established because the quantity of MAPP was relatively similar, 4.5% and 3.7% for formulations M1 and M7, respectively.

A t-test was used to determine statistical differences for the mechanical properties between the matching maple and pine formulations (Snedecor and Cochran, 1989). The results verified that, in each case, maple formulations exhibited greater mechanical properties (MOE, MOR, and strain to failure) than pine formulations. Example t-test calculations and results are included in Appendix H of Slaughter (2004). For practical purposes, the difference had little significance. Comparing wood flour species in general, maple formulations exhibited slightly higher mechanical properties when compared to the same formulation produced with pine. Shear strength, strain at failure, and MOE were nearly the same for the maple and pine formulations. Species had a slightly larger influence on MOR with the pine values averaging 93% of maple.

2.5.3 – Physical Properties

The mean specific gravity for each formulation remained relatively constant at 1.15 with a range of 1.08 to 1.22 (Table 2.6). The average specific gravities for the pine and maple formulations were 1.1 and 1.2, respectively. In general, formulations with median quantities of each material also exhibited specific gravity near the average.

Higher amounts of wood fiber resulted in lower specific gravity, with the exception of formulation 4 and 9 where the opposite was true.

Values for the maximum thickness swell and water absorption are summarized in Table 2.6. Thickness swell, defined as percent change in thickness, remained relatively constant over the formulations. The most noticeable exception was again for formulation 4, which swelled 2-3% more than the average for maple and pine formulations, respectively. Absorption, defined as percent water absorbed on a dry-weight basis, decreased with decreasing filler content. On average, the pine formulations, when compared to maple, exhibited a 0.5% and 1.0% decrease in swell and absorption, respectively.

The swelling coefficient is defined here as the change in swell per unit change in absorption, or the slope of the swell versus absorption plot. A noticeable change in slope at approximately 5% absorption exists for each formulation (Fig. 2.3). Therefore, two swell coefficients were calculated, one for the slope when absorption is less than 5% (β_1) and the other for the slope when absorption is greater than 5% (β_2) (Table 2.6). A change in swell coefficient indicates that a change in material behavior may be occurring, such as a breakdown of internal bonding. Both wood fiber species formulations exhibited similar behavior, a relatively constants β_1 and then a varying β_2. However, compared to the averages, formulations with a high β_1 also had a high β_2. The average β_1 for maple and pine was 1.2 and 1.0, respectively. β_2 seemed to vary negatively with polymer content (decreasing as polymer content increases). The average β_2 values for maple and pine were 2.4 and 2.6, respectively. Comparing the average β values between maple and pine

indicated that maple tends to swell more initially, and then swell less as absorption increases.

2.6 Conclusions

Comparing the differences between maple and pine for a given formulation demonstrates that pine exhibits superior performance based on extrusion quality, swell, and absorption. On the other hand, maple demonstrates superior mechanical properties. Establishing the affects of material composition within a species is a more difficult process; however, the behavior is consistent between wood flour species. In general, extrusion quality, mechanical properties, and physical properties tend to be the best for formulations with median amounts of each material. The exclusion of MAPP within a formulation caused the largest reduction in mechanical properties, compared to any other material present. In conclusion, the pine formulation containing 58.8% wood flour, 33.8% PP, 4.0% talc, 2.3% MAPP, and 1.0% lubricant (P5 and P6) was deemed the optimum formulation by maximizing the mechanical and physical properties in addition to providing quality extrusion characteristics.

2.7 References

AC174. "Acceptance Criteria for Deck Board Span Ratings and Guardrail Systems (Guards and Handrails)." ICBO Evaluation Service, Inc., April 2002.

Adcock, T., Hermanson, J.C., and Wolcott, M.P. "Engineered Wood Composites for Naval Waterfront Facilities." Washington State University, Project End Report. June, 2001.

ASTM D143-97. "Standard Test Methods for Small Clear Specimens of Timber." American Society of Testing and Materials, Vol. 04.01, 2002.

ASTM D1037. "Standard Test Methods for Evaluating Properties of Wood-Base Fiber and Particle Panel Materials." American Society of Testing and Materials, Vol. 04.10, 1999.

ASTM D3846-02. "Standard Test Method for Coupon Shear Strength of Reinforced Plastics." American Society of Testing and Materials, Vol. 08.02, 2003.

ASTM D6109-97. "Standard Test Methods for Flexural Properties of Unreinforced and Reinforced Plastic Lumber." American Society for Testing and Materials, Vol. 08.03, 2002.

Clemons, C. "Wood-Plastic Composites in the United States, The Interfacing of Two Industries." Forest Product Journal, June 2002, Vol. 52, No. 6., pp. 10-18.

Haiar, K.J., McLean, D.I., Cofer, W.F. "Analysis and Design of WPC Deckboard Section for NUWC Pier 171." Washington State University, Project End Report, June 2001.

Haiar, K.J. "Performance and Design of Prototype Wood-Plastic Composite Sections." Master Thesis, Washington State University, May 2000.

Slaughter, A.E. "Design and Fatigue of a Structural Wood-Plastic Composites." Washington State University; Master Thesis, August 2004.

Smith, R.L. and Cesa, E. "An Assessment of 'Technology Push' in the Timber Bridge Industry." Forest Product Journal, Vol. 48, No. 1, 1998.

Snedecor, G.W. and Cochran, W.G. "Statistical Methods, Eighth Edition." Iowa State University Press, 1989.

Wolcott, M.P. "Wood-Plastic Composites." Encyclopedia of Materials: Science and Technology, 2001.

Table 2.1. Product details for extruded materials

Material	Manufacturer	Product
Polypropylene	Solvay	HB9200
Maple	American Wood Fibers	#6010
Pine	American Wood Fibers	#6020
Talc	Luzenac	Nicron 403
Coupling Agent	Honeywell	950P
Lubricant	Honeywell	OP100

Table 2.2. Material composition for each extruded formulation

I.D.*	Run Order**	Wood	PP	Talc	MAPP	OP100
M1	9	69.5%	25.0%	0.0%	4.5%	1.0%
M2	11	69.5%	25.0%	0.0%	4.5%	1.0%
M3	10	64.4%	31.4%	2.0%	1.2%	1.0%
M4	5	64.0%	25.0%	10.0%	0.0%	1.0%
M5	7	58.8%	33.8%	4.0%	2.3%	1.0%
M6	8	58.8%	33.8%	4.0%	2.3%	1.0%
M7	2	54.4%	38.9%	2.0%	3.7%	1.0%
M8	4	54.4%	36.4%	7.0%	1.2%	1.0%
M9	1	54.0%	45.0%	0.0%	0.0%	1.0%
M10	3	50.0%	34.0%	10.0%	5.0%	1.0%
M11	6	50.0%	34.0%	10.0%	5.0%	1.0%
P1	12	69.5%	25.0%	0.0%	4.5%	1.0%
P2	18	69.5%	25.0%	0.0%	4.5%	1.0%
P3	21	64.4%	31.4%	2.0%	1.2%	1.0%
P4	15	64.0%	25.0%	10.0%	0.0%	1.0%
P5	20	58.8%	33.8%	4.0%	2.3%	1.0%
P6	22	58.8%	33.8%	4.0%	2.3%	1.0%
P7	16	54.4%	38.9%	2.0%	3.7%	1.0%
P8	17	54.4%	36.4%	7.0%	1.2%	1.0%
P9	13	54.0%	45.0%	0.0%	0.0%	1.0%
P10	14	50.0%	34.0%	10.0%	5.0%	1.0%
P11	19	50.0%	34.0%	10.0%	5.0%	1.0%

M represents maple and P represents pine

*** Run order denotes the order of which the formulations were extruded*

Table 2.3. Extruder
temperature profile utilized for
all formulations produced

		Temperature (°F)
Barrel Zone	1	370
	2	370
	3	365
	4	360
Screw		360
Die Zone	1	360
	2	365
	3	370

Table 2.4. Sum of difference of depth and width as each
varies from the nominal cross section dimensions

I.D.	Average Width	Difference	Average Depth	Difference	Sum of Difference
	(in)	*(%)*	*(in)*	*(%)*	
Nominal	**5.50**		**1.00**		
M4	5.54	0.6%	1.03	3.4%	4.1%
M5	5.40	-1.9%	1.00	0.4%	2.3%
M6	5.40	-1.8%	1.00	0.2%	1.9%
M8	5.43	-1.2%	1.02	1.9%	3.1%
P1	5.42	-1.4%	1.02	2.3%	3.8%
P2	5.42	-1.4%	0.99	-0.7%	2.1%
P3	5.45	-0.9%	1.02	2.3%	3.2%
P4	5.46	-0.8%	1.00	0.0%	0.8%
P5	5.44	-1.0%	1.01	1.1%	2.1%
P6	5.45	-1.0%	1.02	1.6%	2.6%
P8	5.43	-1.3%	0.98	-2.4%	3.8%
P9	5.45	-0.8%	1.01	1.4%	2.3%

Table 2.5. Average mechanical properties for each formulation including coefficient of variation and sample size

| I.D. | Flexure Tests | | | | | | | | Shear Block Shear | | | Coupon Shear Stress | | |
| | Sample Size | ε_{max} | | MOE | | MOR | | | Sample Size | τ_{max} | | Sample Size | τ_{max} | |
	n	(%)	*COV*	(psi)	*COV*	(psi)	*COV*		*n*	(psi)	*COV*	*n*	(psi)	*COV*
M1	14	1.17%	13.2%	718,326	5.7%	6,342	14.4%		15	2,677	9.5%	15	3,334	12.0%
M2	15	1.15%	15.3%	725,340	6.5%	6,327	15.2%		15	2,558	7.8%	15	3,358	36.7%
M3	14	1.55%	5.7%	796,527	1.3%	8,047	3.9%		15	3,292	3.6%	15	4,774	8.8%
M4	15	0.87%	8.4%	741,410	7.5%	3,342	9.5%		15	1,371	5.8%	15	1,570	12.9%
M5	15	1.65%	5.3%	794,689	1.4%	8,628	3.0%		13	3,234	14.5%	13	4,173	16.0%
M6	15	1.68%	4.8%	809,730	1.3%	8,819	2.1%		13	3,322	5.4%	13	4,059	16.9%
M7	15	1.38%	8.9%	693,080	6.6%	7,162	8.2%		15	3,428	6.9%	15	4,052	13.2%
M8	15	1.42%	7.8%	803,839	2.1%	7,698	3.4%		15	2,882	6.6%	15	4,076	7.3%
M9	15	1.85%	13.4%	506,964	10.5%	4,663	7.0%		15	2,615	2.3%	15	3,971	12.9%
M10	14	1.11%	9.7%	851,551	6.5%	7,282	4.3%		15	2,952	6.9%	15	4,404	9.6%
M11	15	1.40%	4.2%	780,336	3.0%	7,625	3.5%		15	3,007	9.3%	15	4,149	5.6%
P1	15	1.07%	20.2%	778,232	2.1%	5,988	2.9%		15	2,665	7.5%	15	3,690	8.9%
P2	15	1.00%	8.0%	866,129	3.8%	6,658	6.0%		15	2,840	5.3%	15	3,891	8.7%
P3	15	1.33%	4.8%	676,435	4.2%	5,921	7.3%		15	2,837	4.1%	15	3,538	9.2%
P4	15	0.96%	4.7%	702,412	2.3%	3,217	0.8%		15	1,604	8.9%	15	2,113	5.5%
P5	15	1.50%	3.6%	794,652	1.5%	7,209	2.4%		15	3,128	5.3%	15	3,892	14.7%
P6	13	1.48%	2.9%	718,402	1.2%	7,027	2.9%		14	3,279	4.8%	14	4,190	13.8%
P7	15	1.36%	8.9%	757,265	2.5%	7,567	4.6%		15	3,061	5.4%	15	3,971	13.4%
P8	15	1.39%	4.6%	785,676	3.1%	7,137	3.1%		15	3,151	8.1%	15	4,069	7.5%
P9	15	1.92%	10.8%	540,410	4.0%	4,693	5.4%		15	2,325	2.5%	15	3,137	7.5%
P10	15	1.33%	4.0%	821,111	8.0%	7,628	6.4%		15	3,068	6.7%	15	4,373	9.1%
P11	15	1.52%	6.8%	727,705	1.6%	7,239	3.0%		15	3,307	3.1%	15	4,280	18.4%

Table 2.6. Average physical properties for each formulation produced

I.D.	Specific Gravity	Swell		Absorption		Swelling Coefficent*			
		(%)	COV	(%)	COV	β_1	COV	β_2	COV
M1	1.1	9.30	5.6%	25.76	7.2%	1.36	9.5%	3.24	9.8%
M2	1.1	9.60	2.9%	24.21	5.3%	1.41	10.2%	2.79	23.0%
M3	1.2	9.63	8.5%	19.43	3.2%	1.00	20.3%	3.07	15.8%
M4	1.2	11.15	1.5%	24.06	3.0%	1.07	11.7%	2.57	7.2%
M5	1.2	8.78	5.6%	15.90	2.0%	0.99	9.4%	2.60	15.6%
M6	1.2	8.50	4.4%	16.12	1.2%	1.32	25.2%	2.31	17.2%
M7	1.1	10.24	11.2%	13.55	1.4%	1.18	19.4%	1.19	24.8%
M8	1.2	9.55	4.0%	14.34	1.3%	0.99	10.3%	1.93	11.1%
M9	1.1	5.59	16.4%	14.25	2.9%	1.60	25.3%	3.59	18.9%
M10	1.2	8.64	7.0%	13.22	2.0%	1.19	20.0%	1.68	20.1%
M11	1.2	8.11	6.2%	12.80	0.8%	1.04	8.2%	1.91	19.1%
P1	1.1	9.57	8.3%	22.50	4.1%	1.22	20.6%	3.07	15.0%
P2	1.2	9.21	3.5%	20.75	4.3%	0.97	4.3%	3.66	16.2%
P3	1.1	8.69	1.5%	18.06	2.4%	0.89	10.1%	2.59	11.1%
P4	1.2	11.82	3.7%	23.67	0.7%	0.89	15.8%	2.83	5.8%
P5	1.2	8.05	15.5%	15.70	26.0%	0.98	11.3%	2.08	23.8%
P6	1.2	8.13	5.3%	15.47	0.7%	0.99	17.2%	2.50	30.6%
P7	1.1	7.35	1.3%	13.50	1.3%	1.06	15.8%	2.29	30.0%
P8	1.2	8.07	6.8%	14.33	2.8%	0.97	10.8%	2.51	29.5%
P9	1.1	7.76	5.1%	14.48	4.8%	1.02	25.2%	2.16	29.9%
P10	1.2	8.07	6.4%	12.84	4.1%	0.92	7.5%	2.27	13.3%
P11	1.2	7.07	4.6%	12.88	3.2%	1.13	16.2%	2.58	36.9%

* β_1 denotes coefficient below 5% absorbed water, and β_2 is greater than 5% absorbed water
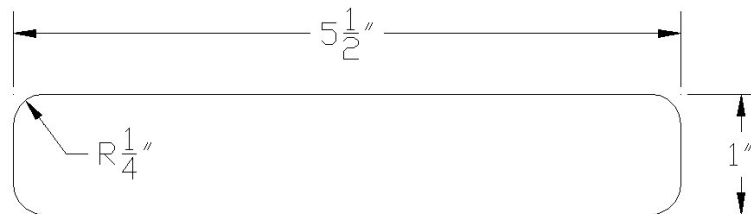

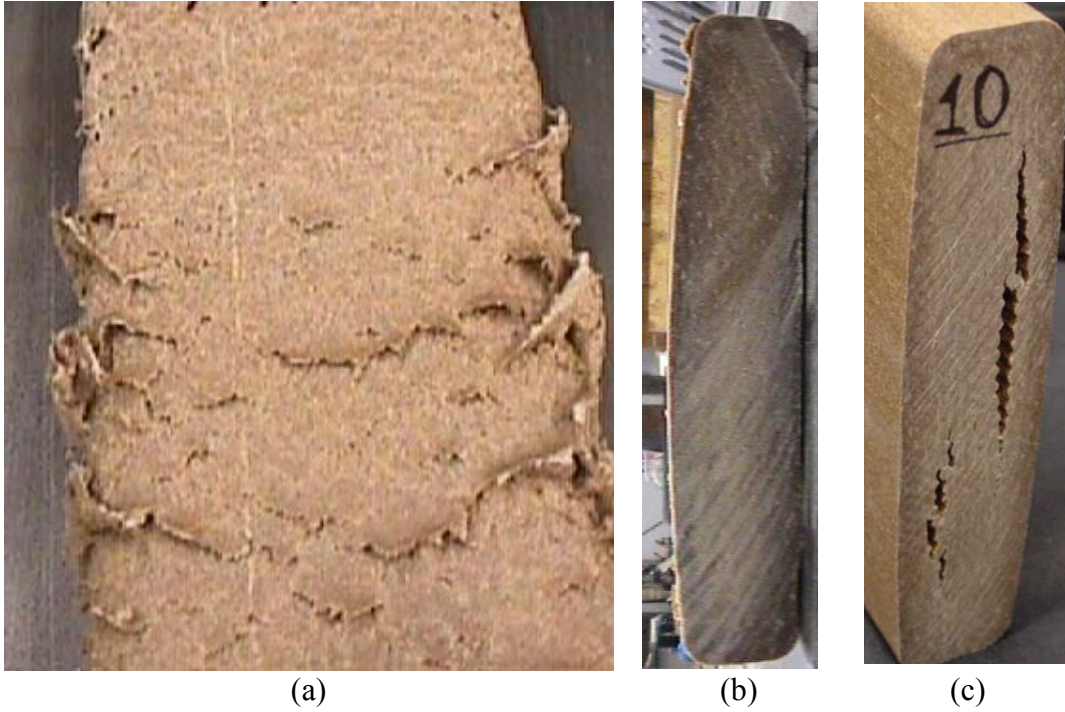**Fig. 2.1.** Deck board extrusion die profile including nominal member dimensions

Fig. 2.2. Three classes of extrusion failure exhibited during processing: (a) surface fracture, (b) swelling, and (c) splitting
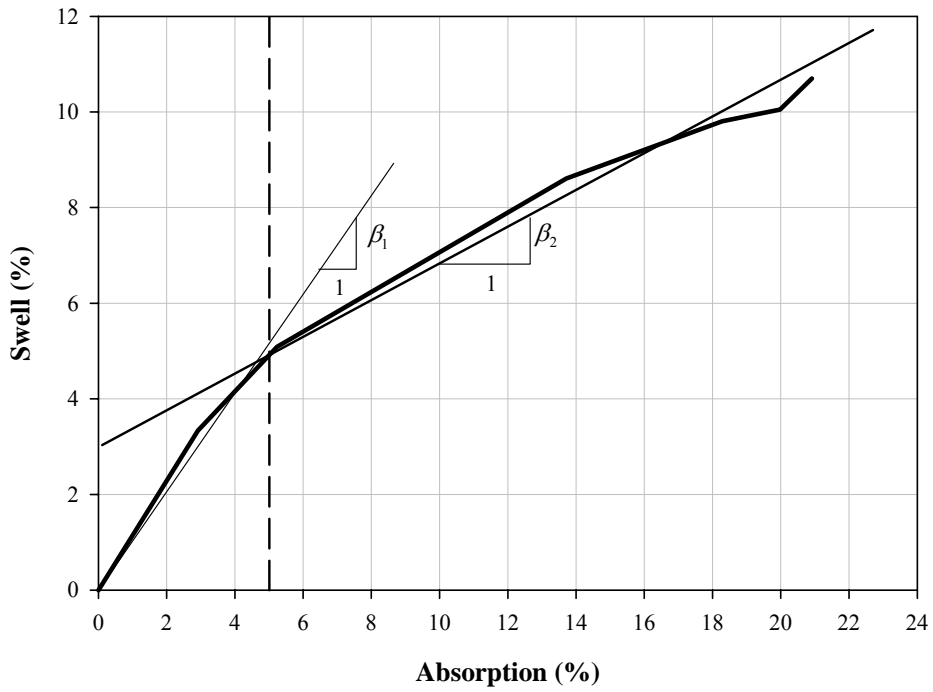

Fig. 2.3. Example plot for determination of swelling coefficients

CHAPTER 3 - DESIGN OF A WOOD-PLASTIC COMPOSITE

BRIDGE DECK MEMBER

3.1 Abstract

Preservative treatment is often a necessary criteria when utilizing timber in exterior components of structures. In the last decade, timber composites have been shown to be an excellent material for replacing exterior structures, but the dependence on pesticide treatment has created a need for a substitute material. For residential structures, wood-plastic composites (WPCs) have emerged as a viable replacement due to its superior resistance to moisture and decay when compared to timber. To assess the potential for utilizing this new class of hybrid composite material in industrial structures, procedures for establishing allowable design stresses are developed including adjustments for load duration, moisture, and temperature effects. The proposed procedures are then applied to a recently developed polypropylene-wood formulation and compared to section stresses developed under AASHTO loadings for continuous span bridge decks. Span tables are constructed for various members and design assumptions for load duration factors. Based on this evaluation, WPCs are shown to be adequate for a typical pedestrian bridge deck.

3.2 Introduction

The greatest perceived obstacle to increased use of timber for bridge applications is the environmental concern regarding the use of preservative treatment to resist fungal decay (Smith and Cesa, 1998). Similar concerns were also expressed by engineers and

owners of marine structures, citing the need for a strong, cost-effective, durable, and environmentally-benign material for use in exposed conditions (Smith and Bright, 2002). Recently, the Environmental Protection Agency (EPA) prohibited the use of chromated copper arsenic (CCA) for consumer and residential applications (Southern, 2002). Although the EPA allows CCA for continued use in industrial structures, many public agencies are eliminating their use of the chemical in response to public perception and potential exposure risks. Finally, the increased costs and corrosion potential of replacement chemicals provide additional motivation for a replacement material.

Based upon these environmental concerns, WPCs are emerging as a replacement for preservative treated timber in residential construction and have potential application in industrial structures as well. When compared to timber, WPCs exhibit increased durability, require less maintenance, absorb less moisture, and demonstrate superior fungal resistance (Clemons, 2002). For exposed conditions such as marine applications, WPCs exhibit improved resistance to checking, decay, termites, and marine organisms (Balma and Bender, 2001).

WPCs are hybrid composite materials traditionally composed of a natural fiber reinforced thermoplastic, such as polyethylene (PE), polyvinyl chloride (PVC), or polypropylene (PP). The natural fiber is most typically wood flour, but other agricultural fibers may be used (Wolcott, 2001). Production of such composites involves a two-stage process, beginning with compounding or dispersing the wood filler into the molten polymer and additives (Clemons, 2002). The raw materials are then processed into a final product using plastics processing techniques such as extrusion, compression molding, or injection molding. Current use of WPC materials includes automotive trim,

window frames, and roof shingles; however, extruded residential decking and railing products comprise the largest and fastest growing sector of the market in the United States (Wolcott, 2001; Clemons, 2002).

Recent research has shown that WPCs may be successfully utilized in industrial waterfront applications (Haiar et al., 2001; Wolcott, 2001). The demonstrated application of a PVC wood-plastic composite indicates that WPCs are capable of resisting significant load demands like those found on an industrial pier deck subjected to forklift travel consisting of a 16,000-lbf wheel load with a 600-lbf/ft distributed load (Haiar et al., 2001). The similarity of this forklift-loading scenario with the American Associations of State Highway and Transportation Officials (AASHTO) minimum required loadings (AASHTO, 2002) for interstate highways supports the potential to utilize WPC materials for bridge decking.

Overall, WPCs exhibit superior moisture and decay resistance when compared to other timber composites. To date, engineered applications of wood-plastic composite materials have been limited. For residential deck board and railing applications, the International Council of Building Officials (ICBO) has developed product acceptance criteria that establishes prescribed mechanical and physical performance (AC174, 2002). Consequently, to move WPC materials into engineered applications such as bridge structures, an accepted design procedure must exist. The development of such a design procedure is the main objective for this research. While developing engineering standards for the design of WPC structural elements, the specific goals of this research were to:

1. Assign allowable design stresses using a proposed procedure,

2. Assess section stresses resulting from a variety of AASHTO loads and flexure spans for a bridge deck,

3. Compute span tables for a variety of extruded WPC cross-sections, and

4. Implement the design procedure in a case study for a typical pedestrian bridge converted from a railroad trestle.

3.3 Background

Utilizing timber for rural and pedestrian bridges is common practice. According to Smith and Cesa (1998), an estimated 400 to 500 timber bridges are built every year in the United States. Two classifications of timber bridges were investigated: rural highway and pedestrian. Examples of each type were considered, each using variations of the standard AASHTO HS20-44 live load and constructed of treated timbers.

Detailed papers have been written on specific projects for different types of bridge structures. Manbeck et al. (1999) discusses a typical highway bridge, which was constructed using red oak glulam and designed to resist a HS25-44 live load, replacing a 44-year old concrete bridge. The bridge spans 35 ft, supports two lanes of traffic, and was constructed on existing stone abutments. The entire structure, including superstructure, railings, and parapets, was constructed using red oak glulam treated with a creosote solution. Pedestrian bridges have also been designed to improve existing cycling or pedestrian trails and provide vehicular access for emergency and maintenance. Collins and Fishchetti (1996) described two Kingpost truss bridges constructed of CCA treated Hemlock and White Pine that were designed to resist an HS8-44 live load and spans approximately 14 ft.

Preservative treatment of the wood components played an important role in each of the previously discussed projects. Manbeck et al. (1999) explains the preservative treatment process involved two stages of application: field repair for glue line separations, and core borings to insure penetration of the pesticide. Collins and Fishchetti (1996) noted that all timber joinery, including mortises, tenons, pin holes, and nail holes, were completed before pressure treatment of the Kingpost trusses. Pre-treating of the bridge members in such a way requires the bridge to be constructed completely without any modifications that would require field treatment application.

Fiber-reinforced polymer (FRP) composite bridges provide an additional option to steel and concrete while negating any need for pesticide treatment. In contrast to modern timber construction, FRP composites offer performance benefits due to high strength-to-weight ratio, quick installation, and reduced maintenance requirements (Foster et al., 2000). To demonstrate the abilities of FRP composites, a 33-ft span two-lane structure was designed and constructed to resist an HS20-44 live load. Using FRP beams reduced construction time by 4 weeks, minimizing both labor costs and traffic disruptions when compared to a more traditional reinforced concrete structure.

Design of a composite panel (inorganic phosphate cement) structure was conducted to investigate the potential of replacing a steel pedestrian bridge (De Roover et al. 2003). Inorganic phosphate cements (IPCs) are defined as a structural ceramic, which were reinforced with glass fibers, and have added benefits including low manufacturing cost, environmentally friendly compositions, and chemical resistance (De Roover et al., 2003). The composite bridge spans 44 ft and utilizes a concrete deck with three

28

supporting girders composed of IPC sandwich panels. The pedestrian bridge is designed

to support a load nearly equivalent to an HS4-44 live load.

In general, both timber and composite structures provide effective replacement

options for obsolete concrete and steel bridges. One advantage of synthetic composite

versus timber structures is removal of the need for pesticide treatment, but in most cases

these structures have significantly increased raw materials cost. As discussed, the

AASHTO HS live load system is utilized for both rural highway and pedestrian bridges.

Structures carrying significant truck traffic are designed for the minimum highway load

HS20-44 live load. Structures with less demand, such as pedestrian bridges, utilize live

loading near HS10-44, which allows for emergency and maintenance vehicular access

only.

3.4 Design Procedures

3.4.1 Allowable Design Stress

Limited research has been conducted towards developing design stresses for WPC

materials. Haiar (2000) developed a design equation (3.1) for determining allowable

design stresses, which modifies equations found in the 2001 National Design

Specification for Wood Construction (NDS). Note that Eq. (3.1) includes the

characteristic design value (B), as well as factors to adjust for the appropriate mechanical

property (C_a), temperature (C_t), moisture (C_m), and member volume (C_v).

$$F_a = BC_aC_tC_mC_v \qquad\qquad (3.1)$$

The characteristic design value accounts for material variability and is derived from an estimate of the lower fifth percentile. Using a non-parametric estimate, this quantity is equivalent to the lowest value of a sample containing 28 specimens. Assuming a normal distribution, Eq. (3.2) is used for calculation of the characteristic design value (B) from the sample mean (X), coefficient of variation (COV), and confidence factor (k) (ASTM D2915, 1998). The confidence factor depends on sample size and is tabulated for various confidence levels in ASTM D2915 (1998).

$$B = X - X\left(k \cdot COV\right) \tag{3.2}$$

The procedures developed by Haiar (2000) for establishing allowable design stresses prescribes a constant property adjustment factor (C_a) of 0.48 for both flexure and shear. This factor is derived from timber design procedures, and includes a load duration and safety component (ASTM D245, 2002). The property adjustment for timber is calculated using Eq. (3.3) where the value 1.3 is taken as a safety factor. The load duration component (X_{10yr}) calibrates the design value to a 10-year load duration, which is considered normal use. In design, the allowable stresses are adjusted for abnormal load durations. For timber, the X_{10yr} is set at 1.6 leading to a C_a equal to 0.48.

$$C_a = \frac{1}{X_{10yr} \cdot 1.3} \tag{3.3}$$

Brandt and Fridley (2003) studied the load duration response of composite formulations based on either PVC or HDPE and found significantly different behavior when compared to timber. These findings warrant the use of a different load-duration factor than those used by timber. Values proposed by Brandt and Fridley are presented in Table 3.1. Comparing the proposed constant property adjustment factor of 0.48 with research conducted by Brandt and Fridley (2003) indicates that this assumption can significantly under or over predict the actual load duration performance. For this reason, the load duration factor (C_D) proposed by Brandt and Fridley (2003) and a property adjustment factor with a load duration basis (Eq. (3.3)) are applied to Eq. (3.1), resulting in Eq. (3.4).

$$F_a = BC_a C_D C_t C_m C_v \qquad (3.4)$$

Haiar (2000) found that temperature effects are greater for HDPE-based WPCs compared to timber, and proposed a factor of 0.6 for in-service temperatures ranging between 130°F and 150°F, a factor of 0.75 for temperatures between 100°F and 130°F, and a factor of 0.85 for temperatures below 100°F. Billmeyer (1984) shows that PP has a greater heat-deflection temperature (140°F) compared to HDPE (130°F); therefore, the temperature adjustment factors proposed by Haiar (2000) are assumed to be conservative estimates of the factor expect for PP-based WPCs. Haiar (2000) also suggested that, based on engineering judgment, moisture effects are minimal for applications where the WPC component is not submerged in water. This assumption is assumed valid for the materials in this study. A moisture adjustment factor equal to 1.0 is, therefore, assumed

31

for bridge decking. Finally, the volume adjustment factor was determined following procedures outlined in ASTM D5456 (2002), which adjusts for the effect of member size on flexural and tensile performance. It is important to note that the adjustment factors presented in this research regarding load duration, moisture, and temperature are derived from preliminary studies of HDPE- and PVC-based WPC formulations and further research is recommended to verify the validity of these factors.

To compare the design capacity with the applied internal moment and shear forces from an AASHTO load class, the adjusted allowable bending (F_b) and shear (F_v) stresses must be converted to allowable moment (M) and shear force (V), respectively (NDS, 2001). Equations (3.5) and (3.6) utilize the section modulus (S) and cross-sectional area (A), respectively. The factor of 2/3 is applicable to a rectangular cross section and would be different for other cross-sectional shapes.

$$M = F_b S \qquad (3.5)$$

$$V = \frac{2}{3} F_v A \qquad (3.6)$$

3.4.2 AASHTO Applied Load

The following description of the process for determining the applied load for a deck system is derived from the American Association of State Highway and Transportation Officials Standard Specification for Highway Bridges (AASHTO, 2002). The AASTHO standard specifies the minimum interstate highway loading as an HS20-44. The number following the HS specifies the gross weight in tons of the tractor and may be increased or decreased proportionally. For example, an HS10-44 loading is 50% of a HS20-44 loading.

32

Assuming WPCs behave similar to timber for design purposes, the applied load simplifies to include only the lane live load. This simplification includes omitting the overload provision because the member comprises a roadway deck, dead load is neglected because the self weight of the member is minimal in comparison to the live load, the decking is oriented perpendicular to the bridge span, and that the impact factor is 1.0. An HS20-44 lane load consists of two portions: a wheel load (18,000 lbf for moment and 26,000 lbf for shear) and a distributed load (640 lbf/ft). According to AASHTO, the wheel load is distributed transversely over a 20-in. width and longitudinally over the width of the plank, but not less than 10 in. Therefore, if a deck member is less than 10 in. wide, the load may be reduced proportionally. The maximum bending moment shall be assumed to equal 80% of a simple span for continuous systems (more than two spans), which is a conservative estimate of the moments in a continuous span system.

The resulting applied moment and shear stresses were calculated using traditional beam theory. Two possible scenarios exist for continuous spans: those less than 20 in. and spans greater than 20 in. For spans less than 20 in., the lane loading simplifies to one distributed load consisting of the wheel load and uniform loading. Eq. (3.7) and Eq. (3.8) are the general equations for applied moment and shear stress for spans less than or equal 20 in. Eq. (3.9) and Eq. (3.10) are the general equations for applied moment and shear stress for spans greater than 20 in. Each equation is a function of a HS load classification (i.e., 10 for HS10-44), span (L) in inches, and width (w) in inches. If the width of the deck board is greater than 10 in., the ratio of width to 10 is neglected or assumed to equal

1.0. Appendix C (Slaughter, 2004) includes complete derivation of the general moment (calculated as lbf·in.) and shear force (calculated as lbf) equations.

$$M_{\leq 20"} = 95.3L^2 \cdot \left(\frac{w}{10}\right)\left(\frac{HS}{20}\right) \tag{3.7}$$

$$V_{\leq 20"} = 676.6L \cdot \left(\frac{w}{10}\right)\left(\frac{HS}{20}\right) \tag{3.8}$$

$$M_{>20"} = \left[5.34L^2 + 3600L - 36000\right] \cdot \left(\frac{w}{10}\right)\left(\frac{HS}{20}\right) \tag{3.9}$$

$$V_{>20"} = \left[26.7L + 26000 - \frac{260000}{L}\right] \cdot \left(\frac{w}{10}\right)\left(\frac{HS}{20}\right) \tag{3.10}$$

3.5 Application

3.5.1 Allowable Design Stress of a WPC

Slaughter (2004) determined the mechanical properties of a polypropylene-based WPC formulation (Table 3.2). The average modulus of rupture (MOR) is 7125 psi and the mean shear strength, as determined by shear block tests, is 3201 psi. Table 3.3 summarizes the mechanical properties. Applying Eq. (3.2) to the mean values obtained from static testing and assuming a 99% confidence limit, the characteristic design values for flexure and shear are estimated as 6597 psi and 2751 psi, respectively.

The 10-year load duration factor is assumed to be 3.0 (Table 3.1), as determined by Brandt and Fridley (2003) for HDPE 8, which exhibited similar mechanical properties in regards to load duration as the PP formulation used in this investigation. In addition, a safety factor of 1.3 is applied to remain consistent with traditional timber design

methodologies. Therefore, the property adjustment factor (C_a) utilized for design is calculated from Eq. (3.4) and determined to be 0.26.

The volume factor was determined from ASTM D5456 (2002) and Eq. (3.11). The factor, m, is defined as the shape parameter of a 2-parameter Weibull distribution. The depth of the unit volume member (d_1) is the deck board section tested by Slaughter (2004) that is nominally 1 in. deep. The depth of application member (d) is the depth of the member to which the adjustment and design equation are being applied. The flexural test data used for this work had a COV of 0.028 (Table 3.3); hence, the shape factor was calculated using test data and determined to equal to 40.2. Appendix E (Slaughter, 2004) includes the calculation of the shape parameter following the methods presented in Law and Kelton (1999).

$$C_v = \left(\frac{d_1}{d} \right)^{2/m} \tag{3.11}$$

ASTM D5456 limits the m factor to a maximum of 8 for samples with a coefficient of variation (COV) less than 0.15. This limitation is to encourage multiple-size testing for determination of the volume adjustment factor. Limiting the shape factor in this manner results in a significant reduction applied to cross sections deeper than the unit member, which is not expected for the materials presented in this research. Considering the objectives of the research presented, the non-limited shape factor is utilized in order to estimate the allowable design stresses expected.

Table 3.4 summarizes the allowable design stresses, excluding the volume adjustment factor, for various temperature factors and load durations. Appendix D of Slaughter (2004) includes an example calculation of allowable design stress.

3.5.2 Span Tables

A review of the literature indicates that utilizing a HS-type live load is reasonable for bridge deck designs and static testing of a PP-based WPC has provided allowable design values suitable for design. Four major variables exist when designing a bridge deck: span, cross section, load, and load duration. Therefore, span tables for various cross sections were produced to simplify the design process. A maximum span was determined by substituting the allowable design moment and shear into the applied load equations (Eq. (3.7) through Eq. (3.10)) and solving for span. The allowable values assume a temperature adjustment factor of 0.75, which assumes that in-service temperature will be less than 120°F. The minimum calculated span for shear or moment was utilized for each load duration and load classification.

Three cross sections were chosen for the span tables: a traditional solid deck member, a three-box hollow section, and a larger hollow 4 in. deep by 6 in. wide (4x6) structural member (Fig. 3.1). The deck board and three-box sections nominally measure 5.5-in. wide by 1-in. deep and 6.5-in. wide by 1.8-in. deep with a 0.4-in. wall thickness, respectively. The computed section properties for each cross section are provided in Table 3.5.

Maximum spans for the deck board, three-box, and 4x6 cross sections are included in Table 3.6 for various load scenarios. Load duration factors are provided for

two minutes to ten years based on research results by Brandt and Fridley (2003) and HS classification ranges from an HS5 to HS25 that covers the range of pedestrian to highway loading scenarios.

3.5.3 Example Application

Abandoned railroads across the United States are being converted to paved pedestrian trails, for use by individuals on foot as well as by bicycles. Converted paths typically include railroad bridges that require a conversion to provide adequate and safe passage over waterways and roads. Figure 3.2(a) shows a typical railroad bridge that requires conversion to allow for a pedestrian trail to traverse the structure.

Often, the existing railroad ties and supporting structure are adequate to carry pedestrian traffic, and modification in the form of a bridge deck and railings is the only requirement. One method of such a modification involves the placement of a nominal 4-in. by 8-in. timber (4x8) between each rail tie, as illustrated in Fig. 3.2(b). The original railroad bridge is constructed of 8-in. wide ties supported by two large timber girders. The ties are roughly spaced 15 in. on center. The addition of the nominal 4x8 timbers results in a 2-in. average spacing between the railroad tie and 4x8 timbers, as illustrated in Fig. 3.2(b).

To allow for bicycle tires to traverse the bridge easily, decking materials should not be placed perpendicular to supports. A possible solution is installing the decking material at a 22.5° angle, as illustrated in Fig. 3.2(b). Placing decking at an angle increases the clear span compared to a deck placed perpendicular to the supporting structure. For design purposes, the span shall be calculated according to AASHTO

(2002), which states that the span consists of the clear span plus one half the width of one

stringer, but not to exceed the clear span plus the depth of the member. The additional

value added to the clear span shall be labeled c, which is 1 in. for this application.

Applying the deck angle as well as the AASTHO requirements for span results in the

design span (L) given by Eq. (3.12). Using Eq. (3.12) to determine a span of the solid

deck board section results in a design span of 6.2 in. Then, Table 3.6 demonstrates that

the deck board section is capable of resisting an HS10-44 loading with a 10-year load

duration factor, which is considered as an appropriate duration for application to a

pedestrian structure (Collins and Fischetti, 1996)

$$L = \frac{2}{\sin(22.5)} + c \qquad (3.12)$$

In addition to strength requirements, AASTHO (2002) states that members having

continuous spans should be designed so deflection due to service loads does not exceed

L/500. Examining the example pedestrian bridge with a span of 6.2 in., the maximum

applied moment equals 1008 lbf·in. Deflection may be estimated using Eq. (3.13), which

was derived from traditional beam theory.

$$\Delta = \frac{23L^2 M}{216 EI} \qquad (3.13)$$

Substituting the applied moment (M), the modulus of elasticity (E), and moment

of inertia (I) into Eq. (3.13), results in a deflection of approximately 0.012 in. This

deflection is equivalent to L/523, which is less than the AASHTO (2002) specified deflection limit. De Roover (2003) states that acceptable deflection limit states for composite structures range from L/200 to L/300, which indicates the predicted deflection results for the pedestrian bridge application are conservative.

3.6 Conclusions

Procedures for determining the allowable design stress for WPC materials were developed using current WPC research and the NDS (2001). Following timber standards, mean strength is reduced to a 5% exclusion limit, which is then adjusted for temperature, moisture, and size. In addition, the procedure modifies a proposed ASTM standard to include a load duration component that was determined to be significant for a variety of WPC formulations. Applying the proposed procedure to static tests performed by Slaughter (2004), allowable design stresses were calculated for a PP-based formulation.

A review of the literature indicates that the AASHTO (2002) HS load configuration is common for establishing applied loads for highway and pedestrian bridge structures. Span tables were developed for various HS classifications, load durations, and cross sections by combining the allowable moment and shear forces and the applied load equations. The span tables indicate that the selected WPC formulation is capable of resisting loads between HS5-44 and HS25-44 for continuous spans, depending on load duration and cross section. Utilizing the span tables to assess a typical retrofit of a railroad bridge for a pedestrian bridge indicates that the tested formulation is more than adequate for such an application.

3.7 References

AC174. "Acceptance Criteria for Deck Board Span Ratings and Guardrail Systems (Guards and Handrails)." ICBO Evaluation Service, Inc., April 2002.

ASTM D245-00. "Standard Practice for Establishing Structural Grades and Related Allowable Properties for Visually Graded Lumber." American Society of Testing Materials, 2002.

ASTM D5456-01a. "Standard Specification for Evaluation of Structural Composite Lumber Products." American Society of Testing Materials, 2002.

ASTM D2915. "Standard Practice for Evaluating Allowable Properties for Grades of Structural Lumber." American Society of Testing Materials, 1998.

American Association of State Highway and Transportation Officials (AASHTO). "Standard Specifications for Highway Bridges." 17th Edition, 2002.

Balma, D.A. and Bender, D.A. "Engineering Wood Composites for Naval Waterfront Facilities, Evaluation of Bolted WPC Connections." Materials Development, Task 2J. Project End Report, 2001.

Benjamin, J.R. and Cornell, C.A. "Probability, Statistics, and Decision for Civil Engineers." McGraw-Hill, Inc., 1970.

Billmeyer, F.W. "Textbook of Polymer Science." John Wiley & Sons, Inc., pp. 478-479, 1984.

Brandt, C.W. and Fridley, K.J. "Load-Duration Behavior of Wood-Plastic Composites." Journal of Materials in Civil Engineering, Nov/Dec, 2003.

Clemons, C. "Wood-Plastic Composites in the United States, The Interfacing of Two Industries." Forest Product Journal, June 2002, Vol. 52, No. 6., pp. 10-18.

Collins, W.J. and Fischetti, D.C. "Recreational Timber Bridges in Pennsylvania State Parks and Forests." National Conference on Wood Transportation Structures; FPL-GTR-94; Madison, WI, 1996.

De Roover, C., Vantomme, J., Wastiels, J., Croes, K., Taerwe, L., and Blontrock, H. "Modular Pedestrian Bridge with Concrete Deck and IPC Truss Girder." Engineering Structures (25), pp. 449-459, 2003.

Haiar, K.J. "Performance and Design of Prototype Wood-Plastic Composite Sections." Master Thesis, Washington State University, May 2000.

Haiar, K.J., McLean, D.I., Cofer, W.F. "Analysis and Design of WPC Deckboard Section for NUWC Pier 171." Washington State University, Project End Report, June 2001.

Law, A.M. and Kelton, W.D. "Simulation Modeling and Analysis." McGraw-Hill Inc., 3rd Edition, 1999.

Manbeck, H.B., Blankenhorn, P.R., Janowiak, J.J., Witmer, R.W., Labosky, P., Powers, P.S., and Schram, P.D. "Northern Red Oak Glued-Laminated Timber Bridge." Journal of Bridge Engineering, November, 1999.

"National Design Specification for Wood Construction (NDS)." American Forest and Paper Association and the American Wood Council, 2001.

Slaughter, A.E. "Static Testing of PP/wood flour Wood-Plastic Composites." Washington State University; Master Thesis, Ch. 2, August 2004.

Wolcott, M.P. "Wood-Plastic Composites." Encyclopedia of Materials: Science and Technology, 2001.

Table 3.1. Load duration factors for various WPC formulations (Brandt and Fridley, 2003)

	PVC	HDPE 8	HDPE 67.5	HDPE w/MAPE	Timber
2-min	2.50	3.20	3.00	3.15	1.70
10-min	2.35	3.00	2.80	2.90	1.60
7-day	1.65	1.95	1.85	1.90	1.25
2-mo	1.40	1.60	1.55	1.60	1.15
5-yr	1.10	1.10	1.10	1.10	1.02
10-yr	1.00	1.00	1.00	1.00	1.00

Table 3.2. Composition of material used for allowable design stress determination

Material	Quantity
Polypropylene	58.8%
Pine	33.8%
Talc	4.0%
Coupling Agent	2.3%
Lubricant	1.0%

Table 3.3. Average mechanical properties for a PP formulation (Slaughter, 2004).

	Density	Stain at failure	MOR	MOE	Shear Strength
	(lb/ft^3)	(%)	(psi)	(psi)	(psi)
Mean	72.0	1.49%	7,125	724,020	3,186
Sample Size	28	28	28	28	29
COV (%)	0.2%	3.4%	2.9%	1.5%	5.1%

Table 3.4. Allowable design stress for various load durations and temperatures factors (C_t) of a PP WPC

		$C_t = 0.60$		$C_t = 0.75$		$C_t = 0.85$	
		Flexure (F_b)	Shear (F_v)	Flexure (F_b)	Shear (F_v)	Flexure (F_b)	Shear (F_v)
		(psi)	(psi)	(psi)	(psi)	(psi)	(psi)
Load Duration	**2-min**	3,248	1,355	4,060	1,693	4,601	1,919
	10-min	3,045	1,270	3,806	1,587	4,314	1,799
	7-day	1,979	825	2,474	1,032	2,804	1,169
	2-mo	1,624	677	2,030	847	2,301	959
	5-yr	1,116	466	1,396	582	1,582	660
	10-yr	1,015	423	1,269	529	1,438	600

Table 3.5. Cross-section properties for typical WPC members including the volume adjustment factor

	Moment of Inertia	Depth	Width	Area	Volume Factor, C_v
	(in^4)	(in)	(in)	(in^2)	
Deckboard	0.46	1.0	5.50	5.45	1.00
Three-Box	2.75	1.8	6.50	6.80	0.97
4x6	28.05	4.0	6.00	15.11	0.93

Table 3.6. Span tables for various load durations, AASHTO HS classifications, and cross sections

		Span (in)*				
		HS5-44	*HS10-44*	*HS15-44*	*HS20-44*	*HS25-44*
Deckboard	2-min	16.8	11.9	9.7	8.4	7.5
	10-min	16.3	11.5	9.4	8.2	7.3
	7-day	13.1	9.3	7.6	6.6	5.9
	2-month	11.9	8.4	6.9	6.0	5.3
	5-year	9.9	7.0	5.7	4.9	4.4
	10-year	9.4	6.7	5.4	4.7	4.1
3-Box Section	2-min	29.3	19.7	16.1	13.9	12.5
	10-min	28.1	19.1	15.6	13.5	12.1
	7-day	21.9	15.4	12.6	10.3	8.3
	2-month	19.7	13.9	11.3	8.5	6.8
	5-year	16.4	11.6	7.8	5.8	4.7
	10-year	15.6	10.6	7.1	5.3	4.2
4 x 6	2-min	95.0	54.8	40.4	33.0	28.5
	10-min	90.2	52.1	38.6	31.6	27.4
	7-day	63.9	37.9	28.8	24.1	19.1
	2-month	54.8	33.0	25.5	19.6	15.7
	5-year	41.3	25.9	18.0	13.5	10.8
	10-year	38.6	24.5	16.3	12.2	9.8

* Shaded area denotes span is controlled by shear criterion
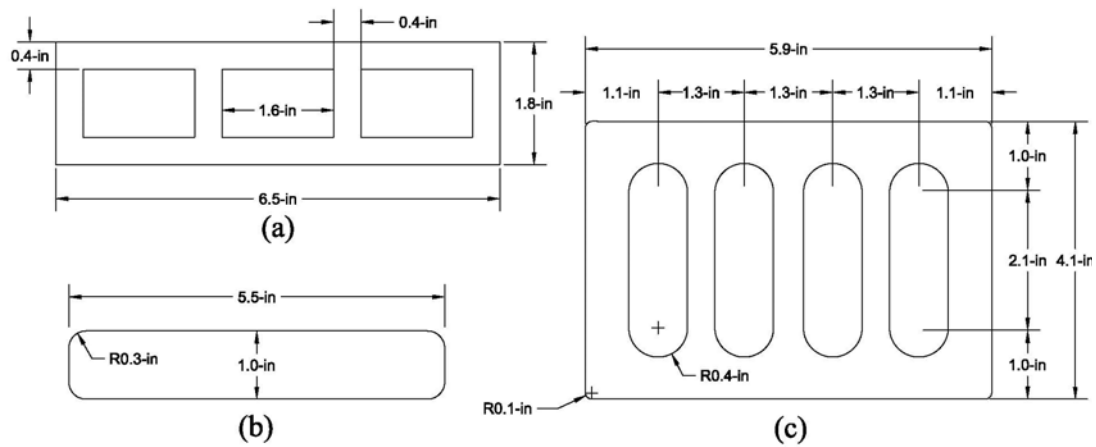
Fig. 3.1. Typical cross sections for WPC materials: (a) 3-box, (b) deck board, and (c) 4 x 6
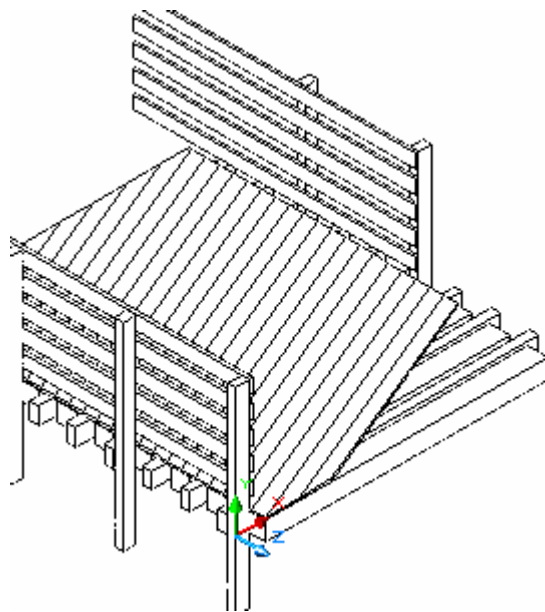
(a)   (b)

Fig. 3.2. Pedestrian bridge retrofit of a typical pedestrian bridge: (a) existing structure and (b) proposed retrofit.

CHAPTER 4 - FATIGUE RESPONSE OF A WOOD-PLASTIC COMPOSITE

4.1 Abstract

Natural fiber reinforced composites are emerging as a viable alternative to preservative-treated timber in both residential and commercial applications. In many transportation structures, repeated loading controls the material failure. Full-scale sections of wood-polypropylene composites were tested in flexural fatigue to investigate the mechanical durability. In this research, the influence of coupling agents, test frequency, and stress ratio on the fatigue life were investigated. Three frequencies, 1.0, 5.2, and 10.4 Hz, were tested at nominal 60% of the ultimate stress. Fatigue life and increased with increasing test frequency, however, the strain to failure remained reasonably constant. Strength-cycle (S-N) data were collected for applied to ultimate stress ratios between 40% and 85% for each formulation at 10-Hz. To compare the failure mechanisms between static and dynamic loading conditions, a power law model was fit to the S-N data and subsequently used to determine a distribution for the apparent static strength. The strength distributions derived from static and fatigue testing were compared. Unlike the formulation containing co-polymer coupling agents, the uncoupled formulation displays different mechanisms controlling the short- and long-term failures.

4.2 Introduction

Recent research has demonstrated the ability to effectively use wood-polypropylene (PP) composites in transportation structures like pedestrian and rural highway bridge decks, (Slaughter, 2004b). Fatigue loading has been identified as a major cause of structural failure for highway structures produced from other materials (Gong

45

and Smith, 2003; Wang, 2000). Fatigue reliability has also gained increasing attention from civil structures (Tang et al., 2000), especially for fiber-reinforced polymer (FRP) composites where mechanical fatigue has been cited as the most common type of failure (Gamstedt et al., 1999). Limited research has been conducted to characterize the fatigue response of WPCs. Thus, to further the understanding of structural performance for wood-plastic composites (WPC), full-scale fatigue testing is considered.

Fatigue research can either utilize full-scale structural sections or small coupons representative of the commercial material. Coupon testing is often used to classify the effects of various parameters inherent to fatigue testing (e.g., stress ratio and frequency) or to develop fundamental material models. On the other hand, full-scale testing is normally aimed at verifying a specific product performance for a given an application (Soudki, 1999; Senne, 2000). Full-scale fatigue research indicates that stress ratio (i.e., $R = \sigma_{min}/\sigma_{max}$) is difficult to maintain at constant levels over a variety of frequencies. This fact, combined with the variability of commercial material components, complicates the use of full-scale specimens for parameter studies (Soudki, 1999; Senne, 2000). These limitations highlight the need for a model capable of incorporating R-ratio and statistical variability to enable full-scale testing to progress beyond specific verification of performance.

Caprino and D'Amore (1998) present various models for predicting fatigue life, including logarithmic and power law relationships. In their research, they focus on the development of a power law model that incorporates the R-ratio. Although an R-ratio of 0.1 is typically used in fatigue research (Soudki et al., 1999; Senne, 2000; Tang et al., 2000; Lewis, 1962; Pooler, 2001), Caprino and D'Amore (1998) performed fatigue tests

on glass-fiber reinforced PP composites with R values between 0.1 and 0.5. Their results confirm that for a given load ratio, fatigue life increases significantly with increasing R.

Fatigue results are usually presented using S-N plots, where S is the ratio of applied stress to ultimate stress and N is the number of cycles to failure. Traditionally, fatigue life is assumed to vary at a given applied stress, but research conducted by Caprino and D'Amore (1998) hypothesized that the fatigue life may be presented using a model with constant variables and the variations noted in a S-N plot were accounted for by the variation in initial strength. Using their prediction model of fatigue life, static strength may be predicted from fatigue data and the variability between short-term static strength and fatigue life may be compared. If the model assumptions are consistent with the material behavior, each distribution should be similar.

Overall, two major incentives exist for conducting fatigue life on full-scale WPC specimens: lack of WPC fatigue data and design verification of full-scale members. Specifically, the objects of this research are threefold:

1. Establishing a baseline study of full-scale WPC members for future fatigue research,

2. Comparing the distributions of static tests and fatigue tests to evaluate the deterministic nature of fatigue life, and

3. Verify the ability of a WPC material to resist a design load for the design lifetime.

4.3 Methods and Materials

Two wood-PP composite formulations, with and without a maleated polypropylene (MAPP) coupling agent, were manufactured according to formulations presented in Table 4.1. Each formulation shall be referred to as PP-MAPP and PP, for

the coupled and uncoupled formulations, respectively. Pine wood fiber (*Pinus* spp.) was obtained commercially and dried to approximately 2% moisture content. All material components were measured and blended in a 4 ft diameter low intensity mixer in 55 lb batches. The dry blend was directly extruded at a rate of 10 rpm using a conical counter-rotating twin-screw extruder (Cincinnati-Milacron TC86). The four barrel zones decreased in temperature from 370 to 360°F with a screw temperature of 360°F. The extrusion process included the use of a stranding die (Laver, 1996) with three temperature zones increasing from 360 to 370°F. The solid section measured a nominal 1 in. by 5.5 in. profile as depicted in Fig. 4.1. Fatigue specimens were cut to length and conditioned for a minimum of 40 hr at 73.4 ± 3.6°F and 50 ± 5% relative humidity prior to testing.

Thirty specimens of each formulation were statically tested according to ASTM Standard D6109 (2002) using a 30-kip electromechanical universal testing machine. The 16-in. clear flexure span was loaded at the third-points. Mean ultimate strength, or modulus of rupture (MOR), of PP-MAPP and PP were determined to be 6494 psi and 4745 psi, respectively. Static strain at failure was calculated from crosshead deflection, using traditional beam theory, and determined to average 1.35% and 1.71% for PP-MAPP and PP, respectively.

Fatigue testing was conducted using a 10-kip servo-hydraulic actuator (MTS Corp.), equipped with a 10-kip load cell, and mounted to a large steel load frame. Cycles were counted continuously from the controlling load signal. Load and actuator displacement (third-point deflection) were acquired by a computer and recorded at predetermined cycles for one to ten second intervals, depending on load frequency (f). Surface temperature of the specimen was record at four top and bottom locations using Type J thermocouples. The parameter S for the fatigue tests ranged from 0.40 to 0.85 for

tests at 10.4 Hz. Tests at 5.2 Hz and 1.0 Hz were conducted at a nominal S of 0.60. The R-ratio ranged from 0.07 to 0.3, depending on formulation and test frequency. Two repetitions at each S were conducted in accordance with ASTM D739 (2002). The mean laboratory conditions during testing were 76.1°F and 27.4% relative humidity.

4.4 Results

Results from each fatigue test performed are summarized in Table 4.2, including the tested S, actual R-ratio, and fatigue life. Establishing a baseline flexure performance focused on comparing the coupled and uncoupled formulations in three areas; internal heating, fatigue life, and strain at failure. Lastly, the relationship of the results to a design application is discussed.

4.4.1 Internal Heating

Specimen temperature increased during testing of the full-scale specimens, with the magnitude of this increase depending on both specimen load and formulation. Temperature increases over the duration of the tests ranged from 4 and 5°F (S = 80%) to 40 and 36°F (S = 50%) for the PP-MAPP and PP formulations, respectively. Specimens loaded at low levels of S and those with uncoupled formulations experienced the largest temperature rise during the test, however, these specimens also experienced the longest fatigue life.

The total magnitude of temperature increase during the test was affected by both the heating rate and the fatigue life. To examine the role of S and formulation on heating rate, the temperature rise was quantified between N = 200 and 1000. This comparison for S, ranging from 50% to 70%, demonstrates that internal heating rate is positively

correlated with S. For instance, over first 1000 cycles, temperature increased 1.1 (S = 50%) and 4.3°F (S = 70%) for the PP-MAPP formulations and 0.9 (S = 50%) and 2.9°F (S = 70%) for the PP formulation. These results also illustrate that the PP formulation heats at a slower rate than the PP-MAPP formulations, especially at increased values of S. The increased heating rate for both the higher values of S and the PP-MAPP formulations are likely related since the PP-MAPP formulations are loaded to higher levels with the higher strength level imparted by the added coupling agent. Higher loads generally produce greater amounts of heat since there is a greater amount of mechanical energy available for converting to thermal energy.

Since noticeable temperature increases were noted for all test conditions, end-use conditions were examined to determine what temperature increase may be acceptable. The current acceptance criterion for deck boards (ICBO AC174) states that allowable load ratings are applicable for in-service temperature of 125°F or less. Thus, internal heating may be acceptable provided the overall temperature of the specimen remains below the maximum service temperature. Because the maximum temperature increase experienced resulted in a specimen temperature of approximately 115°F, this level of internal heating was deemed acceptable for in-service evaluation.

4.4.2 Test Parameters

The PP formulation demonstrated an average fatigue life of 8745, 29,011, and 85,406 for f = 10.4 Hz, 5.2 Hz, and 1.0 Hz, respectively. This compared to the PP-MAPP formulations, which demonstrated shorter average fatigue life of 7718, 13,290, and 29,649 for the same frequencies, respectively. According to Xiao (1999), frequency has dual effects, depending on the magnitude of internal heating. If internal heating is

minimal compared to the material temperature sensitivity, then, fatigue life will increase with frequency. Applying this interpretation to the results presented here indicates that internal heating is not significant enough to affect fatigue life, because the fatigue life increased with frequency for both formulations.

The fatigue life of the WPC tested in this research differs from other composite and construction materials. Xiao (1999) evaluated a continuous carbon fiber composite produced with a high temperature thermoplastic matrix (AS4/PEEK). The fatigue life of this material was found to be 690, 140,000, and 1,300,000 cycles for S = 60% and f = 1, 5, and 10 Hz, respectively. The extended fatigue life of this composite is reasonable since the short-fiber reinforcement of the WPC material places a increased stress on the thermoplastic matrix material and will, therefore, undergo large creep strains during the test. In addition, timber exhibits better fatigue life than the WPC tested here. Tsai and Ansell (1990) performed a literature survey and observed that timber of various species and moisture conditions may exhibit fatigue lives in excess of 2 million cycles for S < 60%. In contrast, other glass-fiber composites have been shown to experience shorter fatigue lives (S = 60% and f = 1 Hz) compared to the WPCs tested. Caprino and D'Amore (1998) tested continuous-fiber PP that exhibited a fatigue life of 7000 cycles, compared to the short-fiber composites test by Horst and Spoormaker (1996) that displayed a fatigue life of 6000 cycles.

Strain to failure remained nearly constant regardless of S, frequency, or R-ratio. The average strains to failure were 0.96% and 1.3% for the PP and PP-MAPP formulations, respectively. Comparing the static and fatigue strain at failure, the difference is approximately 0.4% strain for both formulations, which may be due to the large difference in load rate between the static and fatigue testing. The constant strain at

failure indicates that the long-term failure mechanism may be strain governed. This strong strain dependence also highlights the role creep deflection may play in these fatigue tests. Each fatigue specimen inherently contains a creep component because the specimen is continuously loaded. The creep load is the mean applied load, which is the mid point of the applied waveform.

Figure 4.2 is a typical plot of the minimum and maximum strain of a fatigue specimen. Notice, the plot demonstrates a classic creep behavior including the three zones: primary, secondary, and tertiary creep (Hamel, 1988). Horst and Spoormaker (1996) found a strong correlation between creep rate and tension-tension fatigue strength in short glass fiber reinforced nylon composites. In both the Horst and Spoormaker (1996) and the research presented here, failure seems to occur when a constant strain is achieved. The time required to reach this strain is influenced by the plastic deformation imposed by fatigue damage and the ongoing creep occurring from the mean load of the cycle.

4.4.3 Formulation

Comparing the fatigue life for the two formulations demonstrates that on average the PP formulation material displays a greater fatigue life than the PP-MAPP materials. This difference may, in part, be explained by differences in the actual R-ratio of the two tests. Research indicates that fatigue life increases with increasing R-ratio, which was slightly higher on average for the uncoupled formulation (Caprino and D'Amore, 1998). The slight increase of fatigue life between the two formulations is visible in the S-N plots (Fig. 4.3). This response is the opposite of results found for reinforced glass-fiber polypropylene. Gamstedt et al. (1999) indicates that a coupling agent produced a

minimal difference in static mechanical properties since static strength is dominated by the continuous glass fibers (Gamstedt, et al, 1999). However, the coupled system was determined to be more resistant to fatigue and displayed longer fatigue life when compared to the uncoupled system. Differences in the role of MAPP coupling agents found here and that by Gamstedt may reflect the differences in the role of fiber-matrix interfaces for continuous and short-fiber composites.

4.4.4 Design Considerations

Slaughter (2004b) has established allowable stresses for various bridge load configurations (i.e. pedestrian and rural highway). These design values were found to be approximately 30% of the ultimate strength. To properly use these allowable stresses in design of a transportation structure, a design life must be classified and compared to the fatigue life of the material. The Asphalt Institute establishes a design life based on expected cycles of traffic, which for rural highways is 1 million cycles (Boyer and Hensley, 1999). Therefore, this limit establishes the objective that the tested members should survive 1 million cycles at S > 30%. Fatigue specimens of PP-MAPP were successfully fatigued for 1 million cycles at a S of 40%. In addition, the specimen temperature increased to a maximum of 100°F, which is relative close to the maximum service temperature of 125°F when compared to typical tests in an ambient environment. Although this method for evaluating long term performance is not entirely conclusive, results indicate that fatigue should not be a major factor in failure at design loads for pedestrian and rural highway applications.

4.5 Fatigue Life Analysis

A direct comparison of formulations is difficult from the data of these tests because R of the fatigue tests, mean, and variation of static properties differed between the formulations. A power law fatigue model and statistical a method utilized by Caprino and D'Amore (1998) is emulated here to account for these differences. A critical underlying assumption of this method is that the fatigue life of the material can be described using a mathematical model with constant variables. The variation found in fatigue life of different specimens is then attributed to the inherent variation in static strength, and contributes to under or over estimating the actual S of the specific specimen. The comparison methodology is composed of three steps. First, a fatigue model is chosen and fit to the fatigue data of both formulations. Second, a 3-parameter Weibull distribution is fit to the static testing results. Finally, the fatigue model is assumed to be constant, and is used to predict a static strength distribution, then the predicted distribution is compared to the static Weibull distribution derived from the static testing.

4.5.1 Power Law Model

To analyze the fatigue distribution as it relates to the static strength distribution, a fatigue life model is solved as a function of fatigue life (*N*). A power law model incorporating the influence of R is presented by Caprino and D'Amore (1998):

$$\frac{\sigma_{max}}{\sigma_0} = \left[1 + \alpha \cdot (1-R) \cdot \left(N^\beta - 1 \right) \right]^{-1} \tag{4.1}$$

where σ_{max} is the applied stress, σ_0 is the ultimate static strength, N is the number of cycles to failure, and α and β are material dependant constants. Note that when N = 1, the equation simplifies to $\sigma_{max} = \sigma_o$ indicating that at a fatigue life of one cycle the applied load equals the static strength. Eq. (4.1) is rearranged to produce a linear form with slope α and the left-hand term defined as K:

$$\left(\frac{\sigma_0}{\sigma_{max}} - 1\right) \cdot \frac{1}{1-R} = \alpha \cdot \left(N^\beta - 1\right) \tag{4.2}$$

Material constants can be determined using an iterative process where β is varied to produce the best fitting line between K and $\left(N^\beta - 1\right)$ with slope α (Fig. 4.4). Table 4.3 summarizes the material constants calculated and the corresponding correlation coefficient for each formulation.

4.5.2 Weibull Distribution

A 3-parameter Weibull distribution was fit to the static MOR results using the maximum likelihood method (Kline and Bender, 1990). Table 4.4 summarizes the distribution parameters for calculated and the two formulations. The cumulative distribution function (CDF) for the 3-parameter distributions is provided in Eq. (4.3). In contrast to Caprino and D'Amore, the 3-parameter Weibull distribution was chosen for analysis because a location parameter is included, which shifts the distribution from the origin.

$$F(x) = 1 - e^{-\left(\frac{x-\eta}{\gamma}\right)^\delta} \tag{4.3}$$

where,

$$\delta = \text{Shape parameter,}$$
$$\gamma = \text{Scale parameter, and}$$
$$\eta = \text{Location parameter.}$$

To verify that the Weibull distribution accurately predicts static variability, a Kolmogorov-Smirnov (K-S) goodness-of-fit test was performed for each formulation. The 3-parameter Weibull distribution is demonstrated to predict static MOR to a level of significance greater than 20% for both formulations, which by convention is more than adequate to assume a strong fit (Benjamin and Cornell, 1970).

4.5.3 Predicted Static Strength

To predict static strength from fatigue life, Eq. (4.2) is rearranged to facilitate solving for ultimate strength (σ_0), resulting in Eq. (4.4).

$$\sigma_{0N} = \sigma_{max} \cdot \left[1 + \alpha \cdot (1-R)(N^\beta - 1) \right] \tag{4.4}$$

The calculated ultimate strength from fatigue life is defined here as the predicted strength and assigned the symbol σ_{0N} to avoid confusion. Applying the material constants α and β determined for the model, the predicted static strength may be determined. The predicted static strength is then compared to the 3-parameter Weibull distribution determined from the true static strength results. Figures 4.5 and 4.6 included the CDF in conjunction with the predicted static strength for the coupled and uncoupled formulations, respectively.

The K-S goodness-of-fit method was employed to determine if the predicted static strength was accurately estimated by the static Weibull distribution (Law and Kelton, 1999; Evans et al., 1989). For the PP-MAPP formulation, the Weibull parameters determined from the static strength distribution accurately described the distribution in predicted static strength with a significance level greater than 20% (Fig. 4.5 and 4.7). The mean strength and coefficient of variation (COV) for the static and predicted strength values are also similar (Table 4.4). This result indicates that the variability in fatigue life for the coupled formulation is similar to the variation of static strength, implying the two properties are correlated and likely controlled by the same mechanism.

However, a K-S goodness-of-fit validates that the predicted static strength for the PP formulation can not be adequately described by the Weibull parameters determined from actual static strength. The predicted static strength has greater variability, indicated by the wider spread of data on the CDF plot (Fig. 4.6). For comparison a 3-parameter Weibull distribution was fit to the predicted static strength of the PP formulation (Table 4.3), which was verified for goodness-of-fit using the K-S method. The two probability density functions (PDF) of the actual strength and predicted strength are plotted for comparison in Fig. 4.8. The PDF plots illustrate that large difference in variability between the predicted and actual. The actual data has a narrow range from 4500-psi to 4900-psi, while the predicted data ranges from 4400-psi to 5200-psi.

4.6 Discussion

Horst and Spoormaker (1996) cite differences in the failure modes for static and fatigue loading, with fatigue failures characterized by increased fiber fractures and debonding. The PP formulations tested in our research exhibits greater variability in

57

fatigue failure when compared to the static strength, suggesting that a different failure mechanism controls the two loading modes. The difference in variation is quantified in the coefficient of variation (COV), which is summarized in Table 4.4. The predicted strength COV is 3.4%, which is nearly 3 times the static strength COV of 1.3%. The extremely low COV obtained for the static strength may have resulted from that a sampling error but this is not likely. In contrast, the variability for the PP-MAPP formulation exhibits a close relationship between static strength and fatigue life, indicating the similar failure mechanisms may exist when a coupling agent is used.

The increased variability of the fatigue loaded WPC without the MAPP coupling agent implies that damage may play a larger role in long-term strength of these materials. This phenomenon was also observed in continuous glass-fiber/PP composite tested by Gamstedt et al. (1999). In this research, the uncoupled glass-fiber composites demonstrate a higher degree of damage than coupled materials. Although it is difficult to compare failure mechanisms of continuous and short-fiber composites, these findings suggest that further research is needed to understand the role of the fiber-matrix interphase.

4.7 Conclusions

A minimum sample of PP wood-plastic composites was shown to perform adequately in regards to long term loading. Specimens were cycled to 1 million cycles, which was the estimated design life, at load ratios well above the estimated design load. Thus, results indicate that WPCs may be applicable for a pedestrian bridge application as presented by Slaughter (2004b).

Beyond the design application, a more comprehensive study of fatigue of full-scale specimens was conducted. Coupled and uncoupled formulations of a polypropylene WPC were fatigued at frequencies of 10.4, 5.2, and 1.0 Hz at a nominal load ratio of 60%. Results indicate that cycles to failure increased with increasing frequency, and the uncoupled formulation experienced greater temperature increases due to the greater fatigue life, when compared to the coupled formulation. Comparing the formulations at 1000 cycles indicated that the coupled formulation experienced a faster rate of internal heating when compared to the uncoupled. S-N data was collected from load ratios between 40% and 85% of ultimate for both formulations at a test frequency of 10.4 Hz. The uncoupled formulation exhibited a slightly higher fatigue life, which may be a result of different R-ratios between the formulations tested. Throughout all the fatigue tests, the specimens tended to fail at a constant strain, approximately 1.0% and 1.3% for the coupled and uncoupled formulations, which was 0.4% less than the strain at failure for the static tests.

Static strength was estimated from the fatigue life data, and then compared to the distribution of the static tests. Utilizing the K-S goodness-of-fit method the predicted static strength was compared to a 3-parameter Weibull distribution that closely predicted the static strength distribution. The distribution of the uncoupled static results had a much tighter distribution than the predicted static strengths, demonstrating that different failure mechanisms exist for long- and short-term testing. Comparatively, results indicate similar failure mechanism exists for fatigue and static testing of coupled formulations.

Overall, the work presented indicates the complex nature of fatigue testing as well as the possible benefits of utilizing fatigue testing to analyze material behavior. Fatigue

testing provides additional evidence for gaining acceptance of materials, analyzing failure

mechanisms, as well as relating to other common tests such as creep or static strengths.

4.8 References

American Association of State Highway and Transportation Officials (AASHTO). "Standard Specifications for Highway Bridges." 17th Edition, 2002.

ASTM D6109-97. "Standard Test Methods for Flexural Properties of Unreinforced and Reinforced Plastic Lumber." American Society for Testing and Materials, Vol. 08.03, 2002.

ASTM E739. "Standard Practice for Statistical Analysis of Linear of Linearized Stress-Life (S-N) and Strain-Life (e-N) Fatigue Data." American Society of Testing Materials, 2002.

Benjamin, J.R. and Cornell, C.A. "Probability, Statistics, Decision for Civil Engineers." McGraw Hill Inc., 1970.

Brandt, C.W. and Fridley, K.J. "Effect of Load Rate on Flexural Properties of Wood-Plastic Composites." Wood and Fiber Science, 35(1), pp. 135-147, 2003.

Boyer, B. and Hensley J. "Life-Cycle Performance." Asphalt Contractor, January 1999.

Bright, K.D. and Smith, P.M. "Perceptions of New and Established Waterfront Materials by U.S. Marine Decision Makers." Wood and Fiber Science, 34(2), 2002.

Caprino, G. and D'Amore, A. "Flexural Fatigue Behaviour of Random Continuous-Fibre-Reinforced Thermoplastic Composites." Composite Science and Technology, 1998.

Clemons, C. "Wood-Plastic Composites in the United States, The Interfacing of Two Industries." Forest Product Journal, June 2002, Vol. 52, No. 6., pp. 10-18.

Evans, J.W., Johnson, R.A., and Green, D.W. "Two- and Three- parameter Weibull Goodness-of-fit Tests." Research Paper FPL-RP-493, U.S. Forest Products Laboratory, Madison, WI., 1989.

Gassan, J. "A Study of Fibre and Interface Parameters Affecting the Fatigue Behaviour of Natural Fiber Composites." Composites: Part A 33, pp. 369-374, 2002.

Gong, M. and Smith, I. "Effect of Waveform and Loading Sequence on Low-Cycle Compressive Fatigue Life of Spruce." Journal of Materials in Civil Engineering, January/February, 2003.

Gamstedt, E.K., Berglund, L.A., and Peijs, T. "Fatigue Mechanisms in Unidirectional Glass-Fibre-Reinforced Polypropylene." Composites Science and Technology, 59, pp. 759-768, 1999.

Horst, J.J. and Spoormaker, J.L. "Mechanisms of Fatigue in Short Glass Fiber Reinforced Polyamide 6." Polymer Engineering and Science, Vol. 36, No. 22, Nov. 1996.

ICBO AC174. "Acceptance Criteria for Deck Board Span Ratings and Guardrail Systems (Guards and Handrails)." ICBO Evaluation Service, Inc., April 2002.

Kazanci, M., Marom, D.C., Migliaresi, C., and Pegoretti, A. "Fatigue Characterization of Polyethylene Fiber Reinforced Polyolefin Biomedical Composites." Composites Part A: Applied Science and Manufacturing, 33, pp. 453-458, 2002.

Kline, D.E. and Bender, D.A. "Maximum Likelihood Method for Shifted Weibull and Lognormal Distributions." American Society of Agricultural Engineering. Transactions in Agriculture, 1990.

Launfenberg, T.L. "Structural Composites Under Long-Term Loads." 1988 In: Hamel, M.P., ed. Structural Wood Composites: new technologies for expanding markets: Proceedings 47359, 1987 Nov. 18-20: Memphis, TN. Madison, WI: Forest Products Research Society: 67-71.

Law, A.M. and Kelton, W.D. "Simulation Modeling and Analysis." McGraw-Hill Inc., 3rd Edition, 1999.

Laver, T.C. "Extruded Synthetic Wood Composition and Method for Making Same." Patent Number 5,516,472. 1996.

Lewis, W.C. "Fatigue Resistance of Quarter-Scale Bridge Stingers in Flexure and Shear." Forest Product Laboratory, Report No. 2236, September, 1962.

Pooler, D.J. "The Temperature Dependent Non-Linear Response of A Wood Plastic Composite." Master Thesis, Washington State University, August 2001.

Rangaraj, S.V. and Smith, L.V. "Effects of Moisture on the Durability of a Wood/Thermoplastic Composite." Journal of Thermoplastic Composite Materials, Vol. 13. March, 2000.

Senne, J.L. "Fatigue Life of Hybrid FRP Composite Beams." Masters Thesis, Virginia Polytechnic Institute and State University, July 2000.

Slaughter, A.E. "Design and Fatigue of a Structural Wood-Plastic Composite." Masters Thesis, Chapter Two, Washington State University, August 2004a.

Slaughter, A.E. "Design and Fatigue of a Structural Wood-Plastic Composite." Masters Thesis, Chapter Three, Washington State University, August 2004b.

Smith, R.L. and Cesa, E. "An Assessment of 'Technology Push' in the Timber Bridge Industry." Forest Product Journal, Vol. 48, No. 1, 1998.

Smith, P.M. and Bright, K.D. "Perceptions of New and Established Waterfront Materials: U.S. Port Authorities and Engineering Consulting Firms." Wood and Fiber Science, 34(1), 2002.

Soudki, K.A., Rizkalla, S.H., and Uppal, A.S. "Performance of Bridge Timber Ties under Static and Fatigue Loading." Journal of Bridge Engineering, November 1999.

Tang, H.C., Nguyen, T., Chuang, T., Chin J., Lesko, J. Wu, H.F. "Fatigue Model for Fiber-Reinforced Polymeric Composites." Journal of Materials in Civil Engineering, May 2000, pp. 97-104.

Tsai, K.T. and Ansell, M.P. "The Fatigue Properties of Wood in Flexure." Journal of Materials Science, 25, pp. 865-878, 1990.

Wang, T. "Influence of Heavy Trucks on Highway Bridges." Florida Department of Transportation (FDOT), Summary of Final Report, BC-379, October 2000.

Xiao, X.R. "Modeling of Load Frequency Effect on Fatigue Life of Thermoplastic Composites."   Journal of Composite Materials, Vol. 33, No. 12, 1999.

Table 4.1. Product details and quantities for extruded materials

Material	Quantities		Manufacturer	Product
	A	**B**		
Polypropylene	33.8%	36.2%	Solvay	HB9200
Pine	58.8%	58.8%	American Wood Fibers	#6020
Talc	4.0%	4.0%	Luzenac	Nicron 403
Coupling Agent	2.3%	0.0%	Honeywell	950P
Lubricant	1.0%	1.0%	Honeywell	OP100

Table 4.2. Summary of fatigue test results for coupled and uncoupled formulations

	Formulation					
	PP			**PP-MAPP**		
	R-ratio	**S**	**Fatigue Life**	**R-Ratio**	**S**	**Fatigue Life**
10.4-Hz	0.18	0.48	188,912	0.24	0.45	658,907
	0.18	0.48	194,898	0.23	0.45	802,049
	0.18	0.58	32,001	0.26	0.51	152,494
	0.19	0.57	38,688	0.24	0.49	109,113
	0.16	0.58	18,258	0.23	0.55	68,797
	0.20	0.66	2,884	0.22	0.55	112,451
	0.21	0.66	2,545	0.23	0.55	74,970
	0.21	0.70	3,776	0.23	0.63	16,712
	0.21	0.70	808	0.24	0.63	23,220
	0.21	0.75	385	0.25	0.67	9,943
	0.21	0.75	1,054	0.26	0.67	10,031
	0.19	0.81	261	0.30	0.69	4,105
	0.21	0.80	200	0.30	0.69	4,435
	0.22	0.83	13	0.28	0.73	1,583
	0.22	0.83	18	0.30	0.73	1,012
				0.29	0.77	340
				0.29	0.78	674
5.2-Hz	0.11	0.60	11,352	0.11	0.59	24,138
	0.10	0.61	11,356	0.11	0.60	29,009
	0.10	0.62	17,162	0.10	0.59	33,887
1.04-Hz	0.07	0.62	9,412	0.06	0.62	12,916
	0.08	0.59	6,390	0.07	0.62	6862
	0.07	0.62	7,351	0.06	0.62	6457

Table 4.3. Material
constants for power law
model and Pearson
correlation coefficient (r)

	Formulation	
	PP-MAPP	**PP**
α	0.121	0.153
β	0.384	0.240
r	0.962	0.960

Table 4.4. Three-parameter Weibull distribution
parameters including correlation coefficient

Formulation		PP-MAPP		PP	
		Static	*Predicted*	*Static*	*Predicted*
Parameter	**Shape**	3.38	3.84	11.09	2.11
	Scale	689.72	943.54	543.17	442.08
	Location	5869.30	5637.28	4221.71	4352.14
Correlation Coefficent (r)		0.98	0.97	0.90	0.97

Table 4.5. Mean static strength and predicted strength from
fatigue life results for uncoupled and coupled formulations

	PP-MAPP		PP	
	Actual	*Predicted*	*Actual*	*Predicted*
Mean MOR (psi)	6,494	6,489	4,740	4,744
COV (%)	3.2%	4.1%	1.3%	3.4%
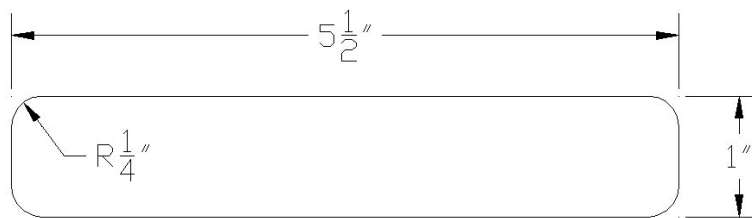
Fig. 4.1. Extruded cross section including nominal
dimensions
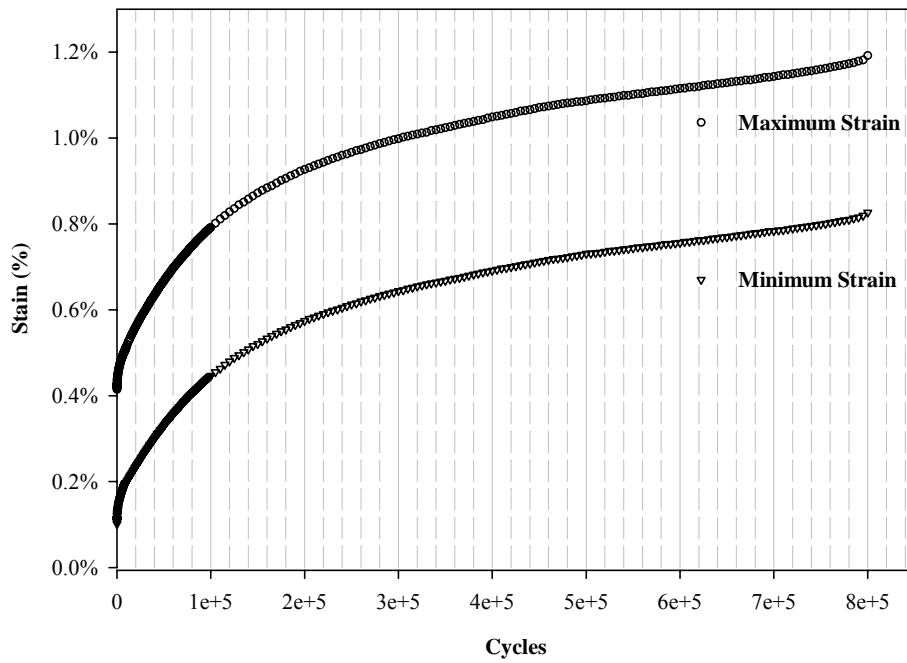
Fig. 4.2. Example creep behavior of a fatigue specimen (PP at 50% S)
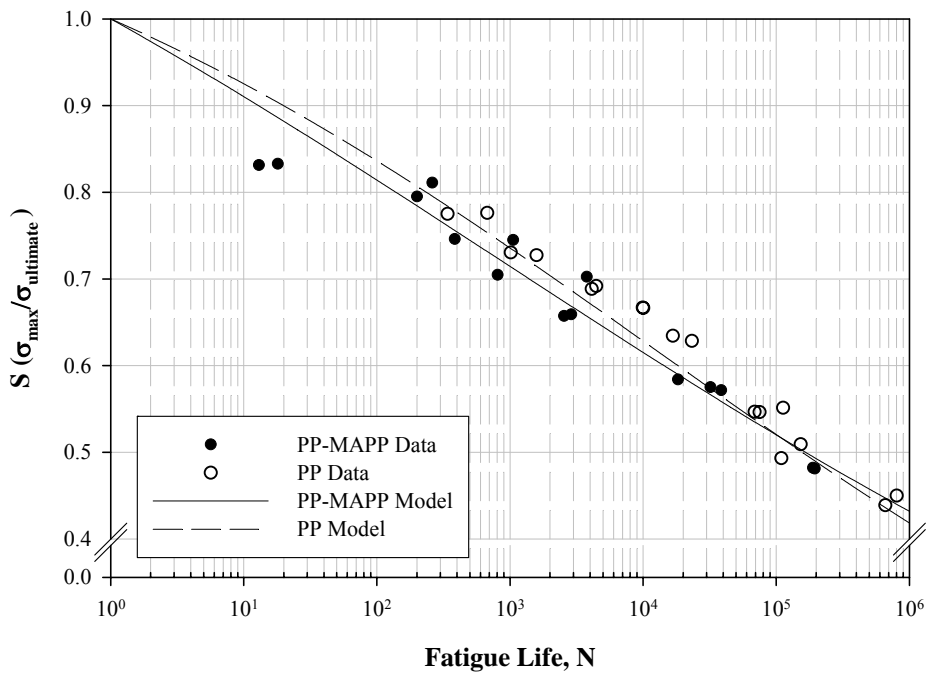
Fig. 4.3. Strength-life (S-N) plot for 10.4-Hz fatigue tests
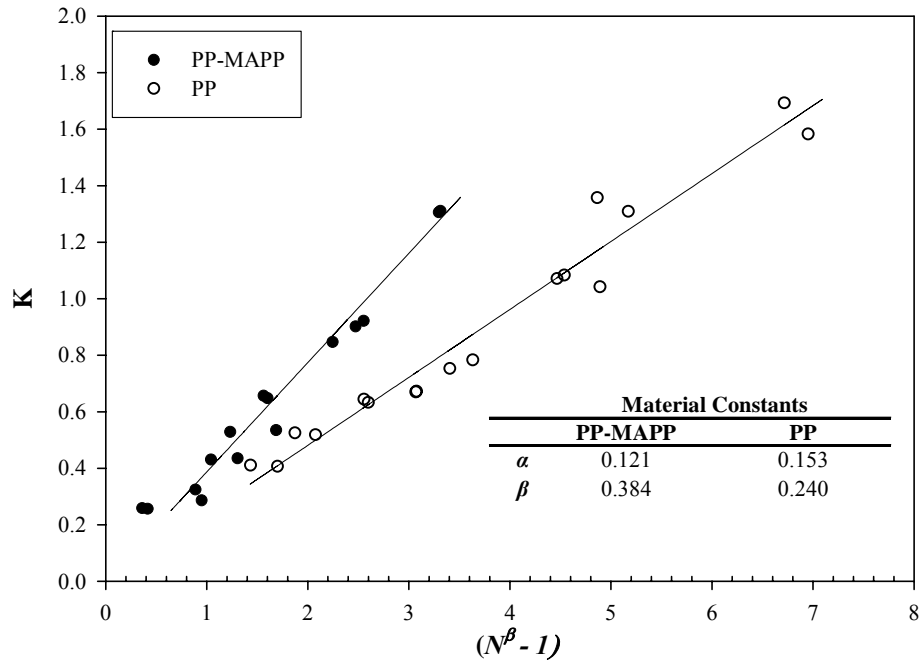
Fig. 4.4. Best-fit estimates for determination of the power law material constants
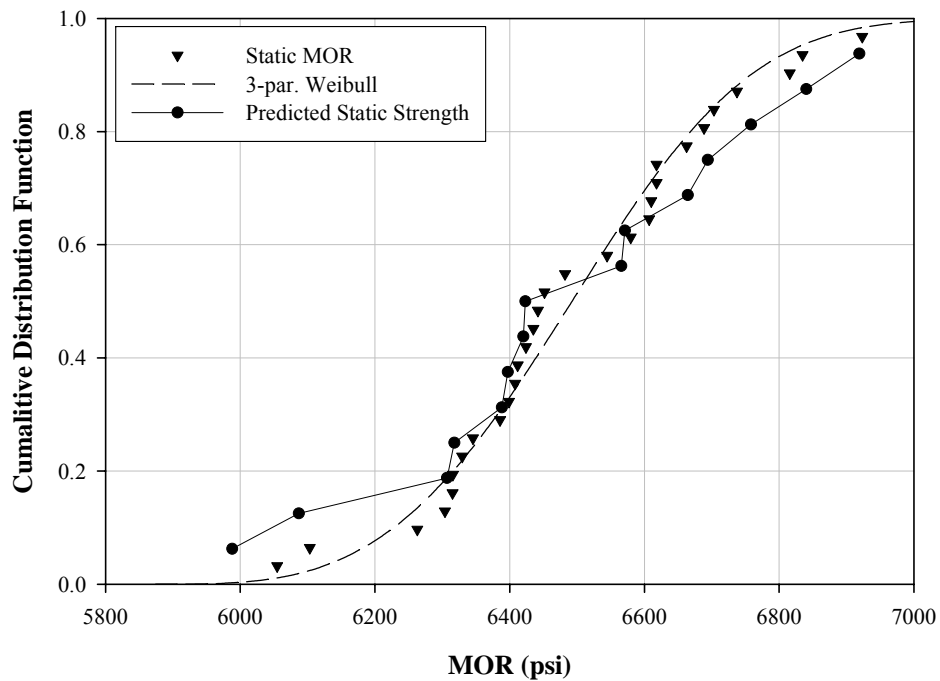
Fig. 4.5. Cumulative distribution function of static strength and predicted static strength for the coupled formulation (PP-MAPP)

67
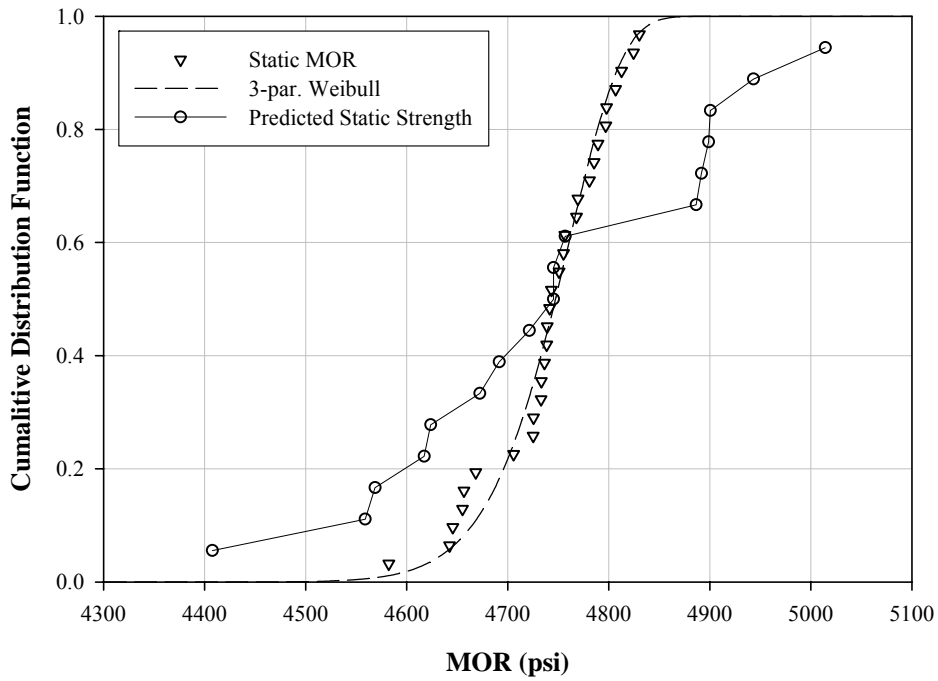
Fig. 4.6. Cumulative distribution function of static strength and predicted static strength for the uncoupled formulation (PP)
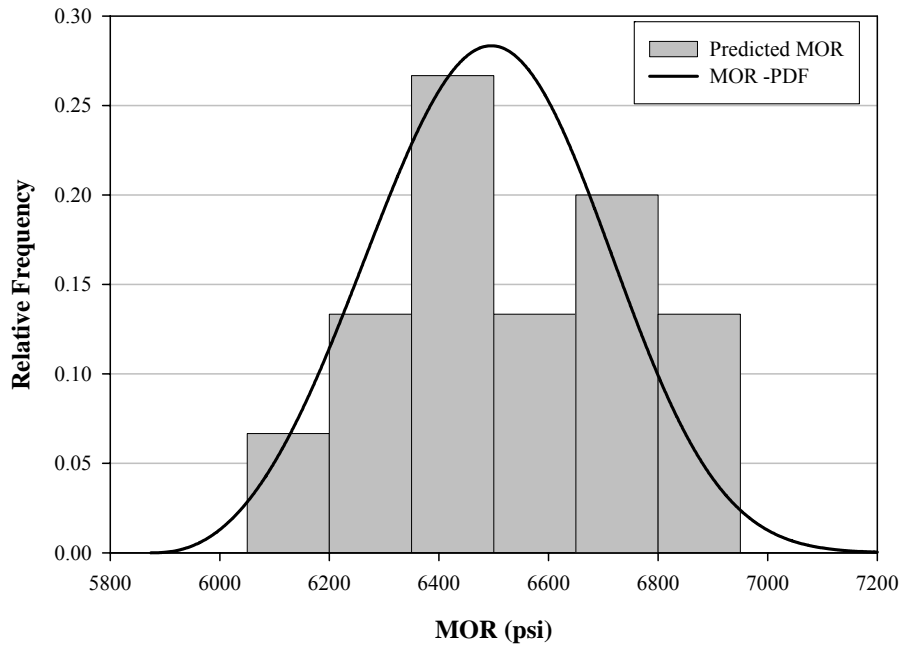
Fig. 4.7. Probability density function of predicated strength and static Weibull for the coupled formulation (PP-MAPP)
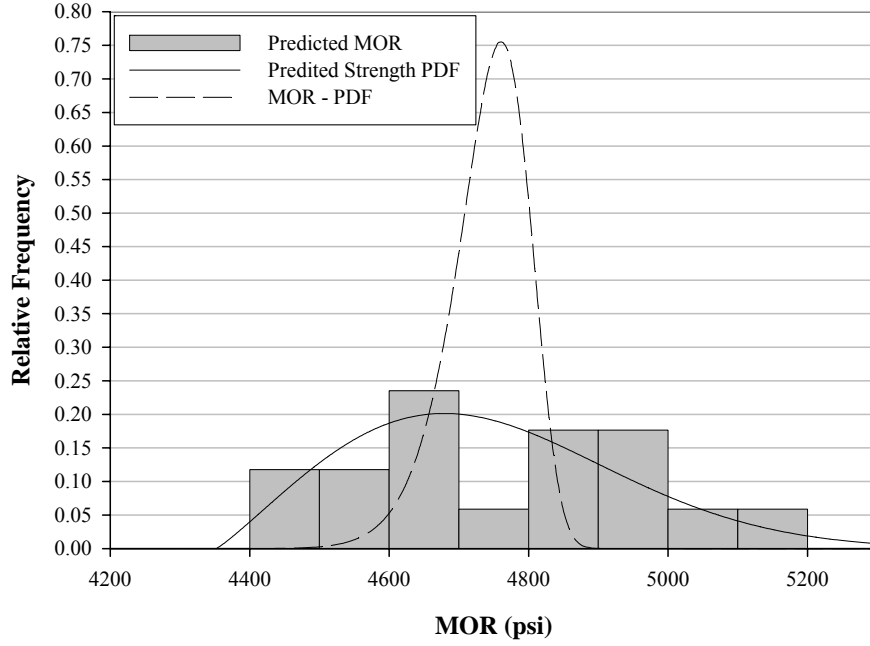
Fig. 4.8. Probability density function of predicated strength, static Weibull and predicted Weibull for the uncoupled formulation (PP)

69

CHAPTER 5 – CONCLUSIONS AND RECOMMENDATIONS

5.1 Conclusions

Wood-plastic composite (WPC) materials are a potential replacement material for treated timber, particularly for bridge and waterfront applications. The research presented in this thesis focuses specifically on the utilization of a WPC deck boards for industrial applications such as bridge decking, including determination of the mechanical and physical performance of various WPC formulations, allowable design stress assignment, and fatigue life behavior.

Previous WPC research focused on high-density polyethylene (HDPE) and polyvinyl chloride (PVC) materials. PVC typically demonstrated excellent mechanical performance but exhibited extremely brittle behavior. In contrast, HDPE exhibited a more ductile behavior but mechanical performance was weak. In an effort to develop a material that incorporates superior strength and ductility compared to PVC and HDPE, a formulation study of polypropylene (PP) was conducted.

Static tests were performed on twenty-two different polypropylene WPC formulations with two different wood flours, maple (*Acer spp.*) and pine (*Pinus spp.*), as well as a coupling agent, talc, and lubricant. Flexure and shear strength were determined in addition to water absorption and thickness swell. In general, the maple formulations exhibited greater mechanical properties, while pine formulations demonstrated superior physical properties including processing quality. The greatest effect on mechanical and physical properties was the exclusion of coupling agent, which resulting in inferior mechanical properties. The water absorption tests demonstrated that two significant

stages exist. The swelling coefficient changed drastically at about 5% water absorption for all formulations, indicating that a change in material behavior may occur at this point. Overall, the best performing formulations contained median levels of each material component (e.g., MAPP ranged from 0% to 5%; thus, the best performing formulation contained a quantity of MAPP close to 2.5%). The optimum formulation determined by mechanical and physical properties was composed of 58.8% pine, 33.8% PP, 4.0% talc, 2.3% MAPP, and 1.0% lubricant.

Design procedures were developed for application of a PP-based WPC for industrial structural use. The design procedures adjust the mean strength, as determined from static testing, to a lower fifth percentile tolerance limit. Next, the allowable design stress is adjusted for load duration, temperature, moisture, member volume, and safety. Finally, the design stress are converted to design moment and shear forces for typical cross sections. The allowable internal forces are compared to applied loading scenarios for timber bridge decking, determined from the American Association of State Highway and Transportation Officials (AASHTO) bridge design manual. Using these proposed procedures, span tables were developed for various load durations. The tables were utilized to demonstrate that a WPC formulation is adequate for application as a typical pedestrian bridge deck.

Research indicates that fatigue is a controlling failure mechanism for numerous civil engineering applications, and therefore fatigue testing of a deck board cross section was conducted. The study verified that a WPC deck board was capable of resisting a load greater than expected for a bridge deck application for the design life of one million cycles. The design life was estimated as the number of trucks expected to traverse a

bridge structure, which was associated to cycles of a fatigue test. In addition to the design verification, a baseline for future fatigue research was developed by performing tests at various frequencies as well as comparing uncoupled and coupled WPC formulations. Internal heating occurred at a faster rate for the coupled formulation, but due to a longer fatigue life the uncoupled formulation experienced greater temperature increases over the extent of fatigue testing. A power law model was implemented to estimate static strength from fatigue life, which allowed for a comparison between the distributions of static and fatigue specimens. The basis for comparison is that variation in fatigue life is caused by a variation is static strength. Therefore, if the fatigue and static data demonstrate similar distributions, the failure mechanisms may be correlated. Results indicate that the same failure mechanism exists for the static and fatigue tested coupled formulation. The uncoupled formulation displayed a much different distribution for the static testing when compared to the fatigue testing.

In summary, industry requires a replacement material for treated timber. WPCs are a quality alternative with superior material behavior regarding moisture as well as structural performance when compared to timber. The proposed design procedures indicate that a WPC formulation is capable of resisting pedestrian and highway bridge loadings.

5.2 Recommendations

The research presented in this thesis is an additional step toward advancing the use of wood-plastic composites to industrial applications. The recommendations presented herein are focused on two needed research areas: material advancement with

72

regards to design and developing further understanding of fatigue in wood-plastic composites.

For allowable design value assignments, two aspects require additional consideration. First, a complete analysis of material properties for the optimum formulation should be conducted, including tension, compression, and dowel bearing. In addition, the effect of shear for bending members warrants further consideration. Secondly, the adjustment factors require verification for the formulation tested in this research. The most significant of these factors includes the load duration factors that require long term testing and the volume adjustment factor that involves testing of various cross sections. Verification of the temperature factor and moisture factors should be included in any such study.

With respect to fatigue, three major areas require future consideration. A typical parameter for analysis of fatigue behavior is damage, as defined as a function of changing modulus of elasticity. The fatigue research conducted in this study included calculation of damage, but because of fluctuating laboratory conditions, reliable data was not available. Therefore, the control and effects of testing environment on fatigue life and damage require additional consideration. Secondly, the strain to failure for the fatigue specimens remained constant, but at values that were lower than the strains determined for static testing. It is speculated that this difference is due to the difference in load rate between the static and fatigue testing, which may also effect the strength of the specimen. Finally, the inherent creep component should be considered in combination with fatigue loading to determine the interaction of the two types of testing.

APPENDIX A – DECK BOARD AREA AND MOMENT OF INERTIA

CALCULATIONS

Deck board cross section:
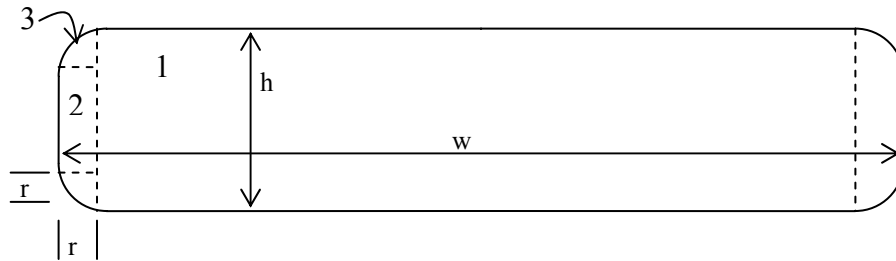
Area Calculation:

$$A_1 = h \cdot (w - 2r)$$
$$A_2 = r \cdot (h - 2r)$$
$$A_3 = \frac{\pi r^2}{4}$$
$$A = A_1 + 2A_2 + 4A_3$$

Moment of Inertia Calculation:

$$I_1 = \frac{1}{12}(w - 2r)h^3$$
$$I_2 = \frac{1}{12}r(h - 2r)^3$$
$$I_3 = \left(\frac{\pi}{16} - \frac{4}{9\pi}\right)r^4 + \left(\frac{\pi r^2}{4}\right)\left[\frac{h}{2} - r + \frac{4r}{3\pi}\right]^2$$
$$I = I_1 + 2I_2 + 4I_3$$

APPENDIX B – STATIC TESTS

B.1 Summary

Twenty-two polypropylene wood-plastic composite formulations were tested to determine modulus of rupture (MOR), modulus of elasticity (MOE), and strain at failure. Tests were performed on a full-scale deck board section nominally measuring 1 in. thick by 5.5 in. wide. Testing procedures conformed to the ASTM D6109 and were performed on a mechanical testing machine (Instron 4400R). In addition, an optimum formulation was chosen based upon mechanical and physical properties (*see* Chapter 2). The optimum formulation was then extruded in greater quantities with and without coupling agent, tested statically, and utilized for fatigue testing (*see* Chapter 4). The following page gives the load-displacement plots for each formulation tested.

B.2 Load-displacement plots for 22 statically tested PP-based WPCs
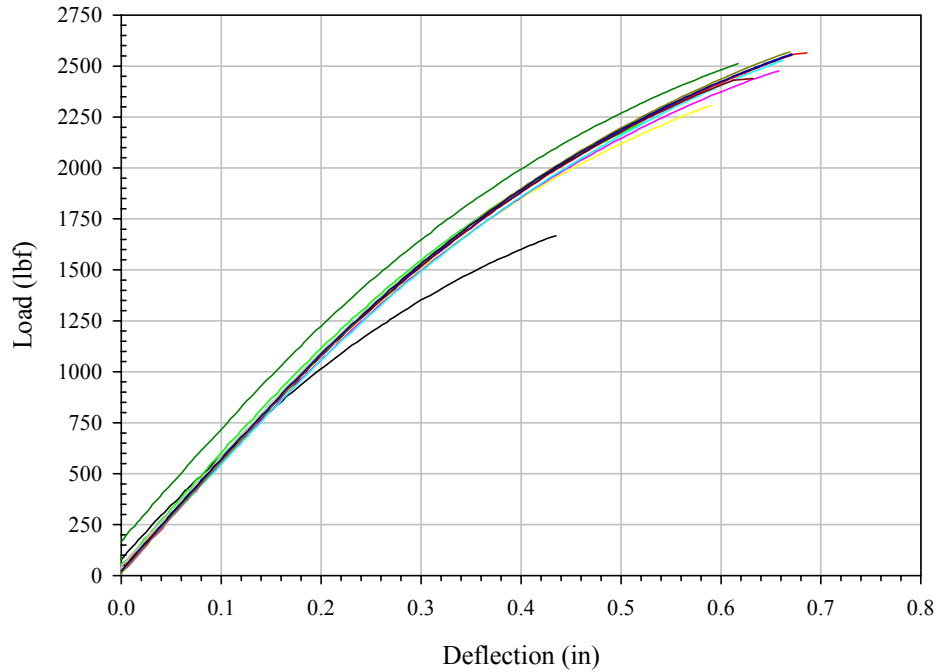
Fig. M1: 69.5% PP / 25.0% Maple / 0.0% Talc / 4.5% MAPP / 1.0% OP100
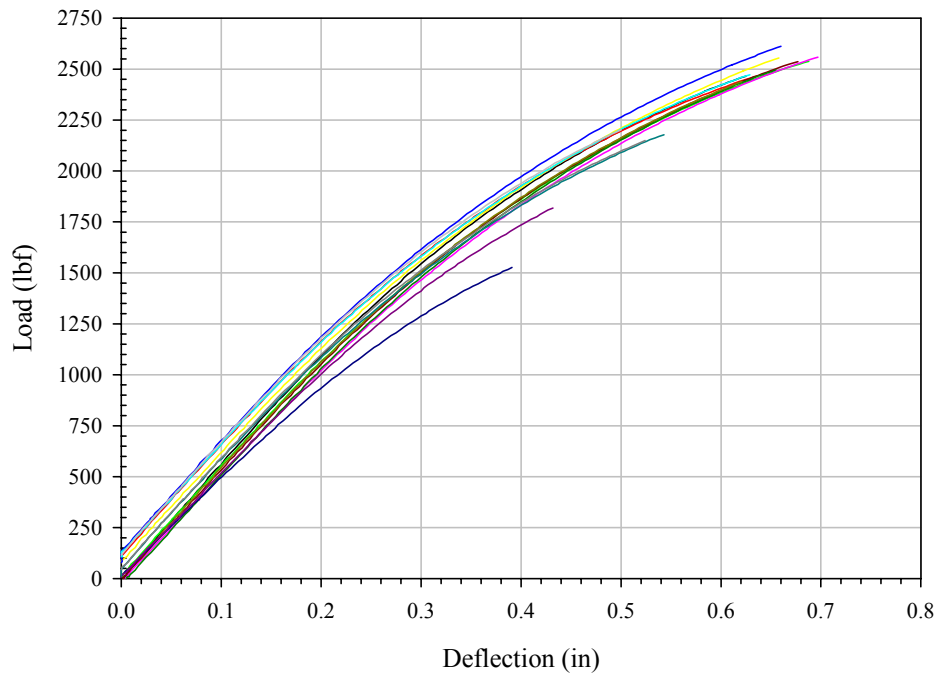
Fig. M2: 69.5% PP / 25.0% Maple / 0.0% Talc / 4.5% MAPP / 1.0% OP100
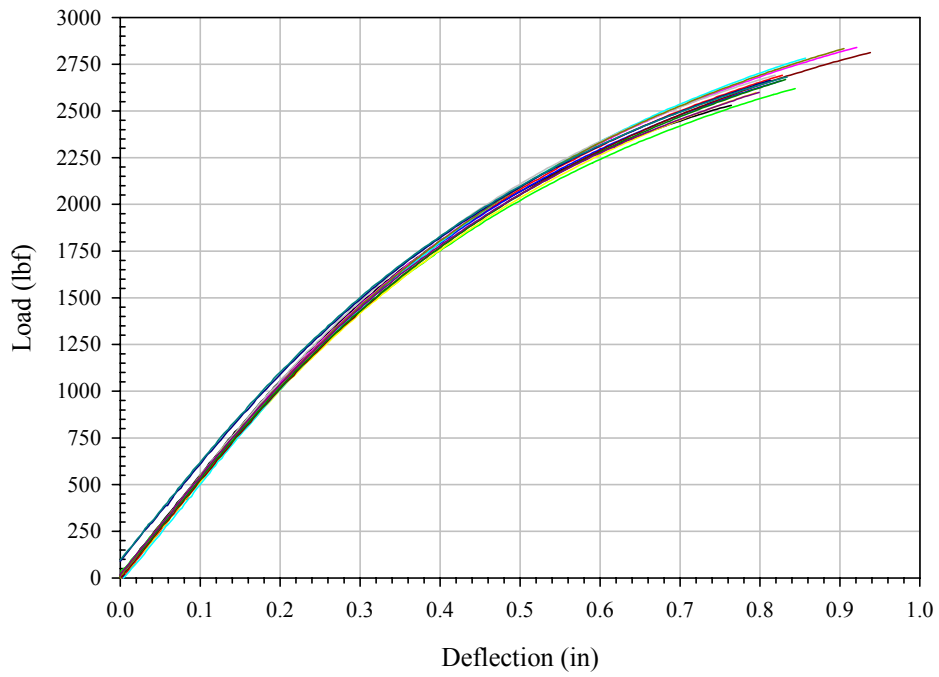
**Fig. M3:** 64.4% PP / 31.4% Maple / 2.0% Talc / 1.2% MAPP / 1.0% OP100
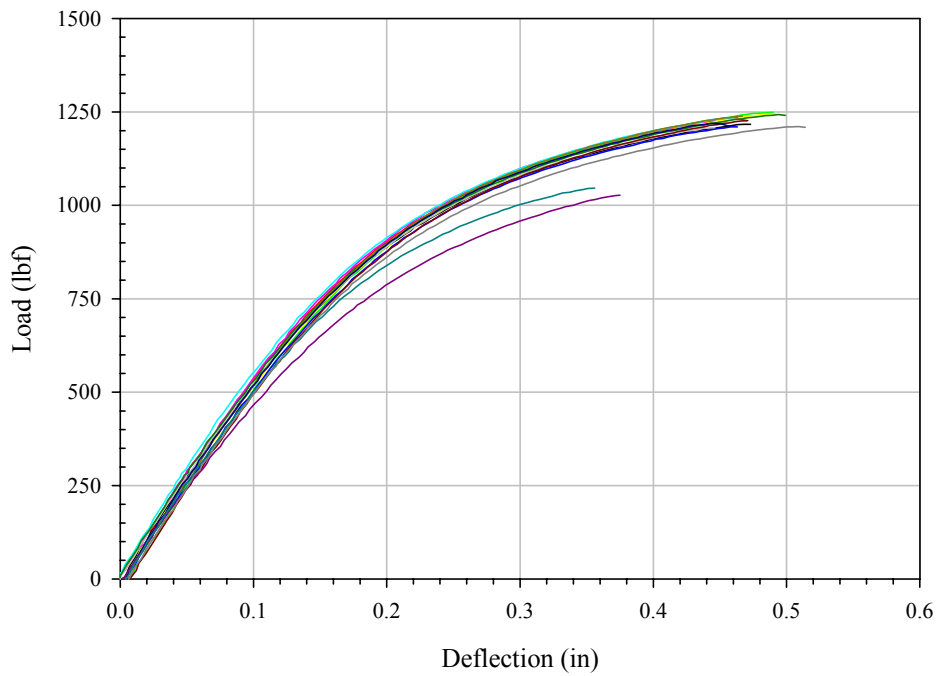
**Fig. M4:** 64.0% PP / 25.0% Maple / 10.0% Talc / 0.0% MAPP / 1.0% OP100
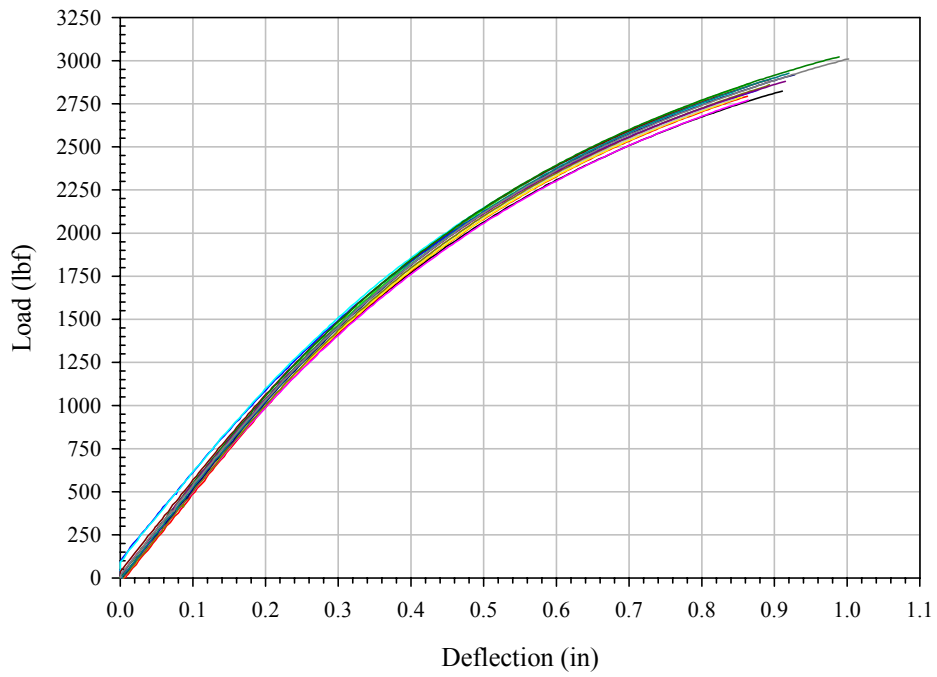
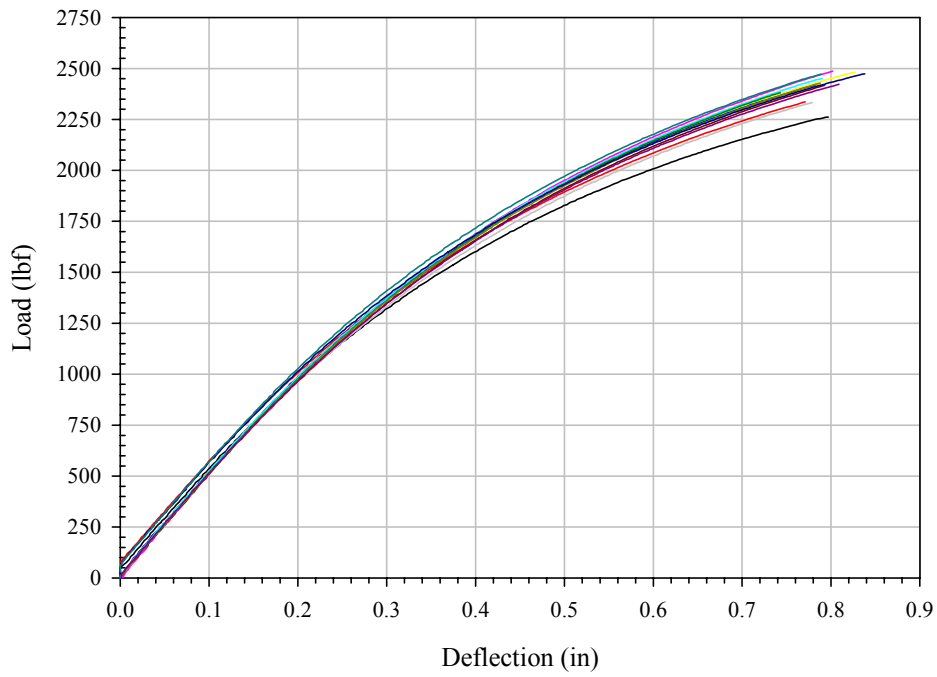**Fig. M5:** 58.8% PP / 33.8% Maple / 4.0% Talc / 2.3% MAPP / 1.0% OP100
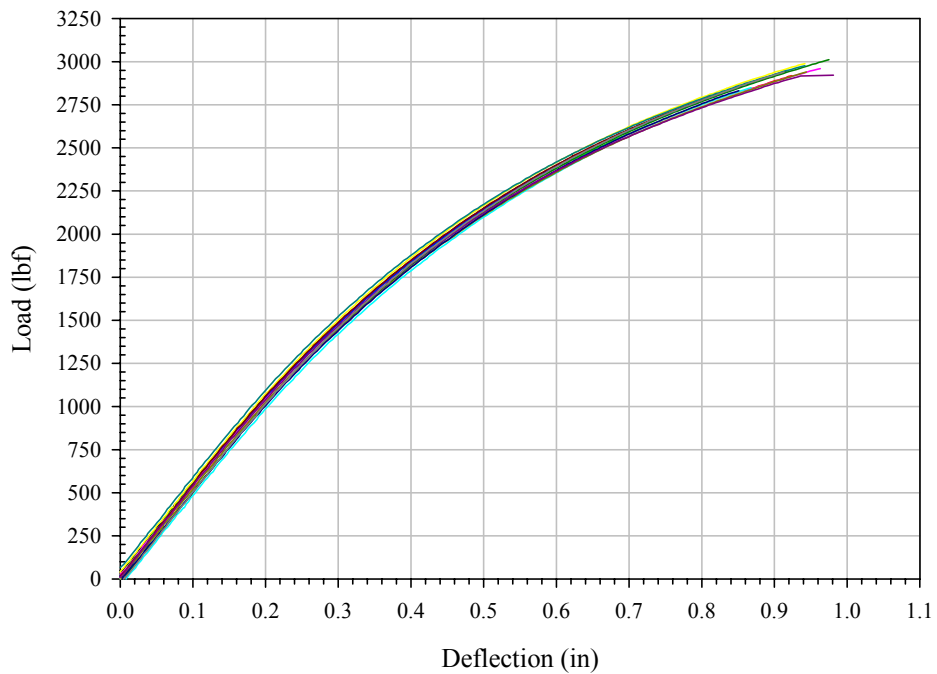
**Fig. M6:** 58.8% PP / 33.8% Maple / 4.0% Talc / 2.3% MAPP / 1.0% OP100
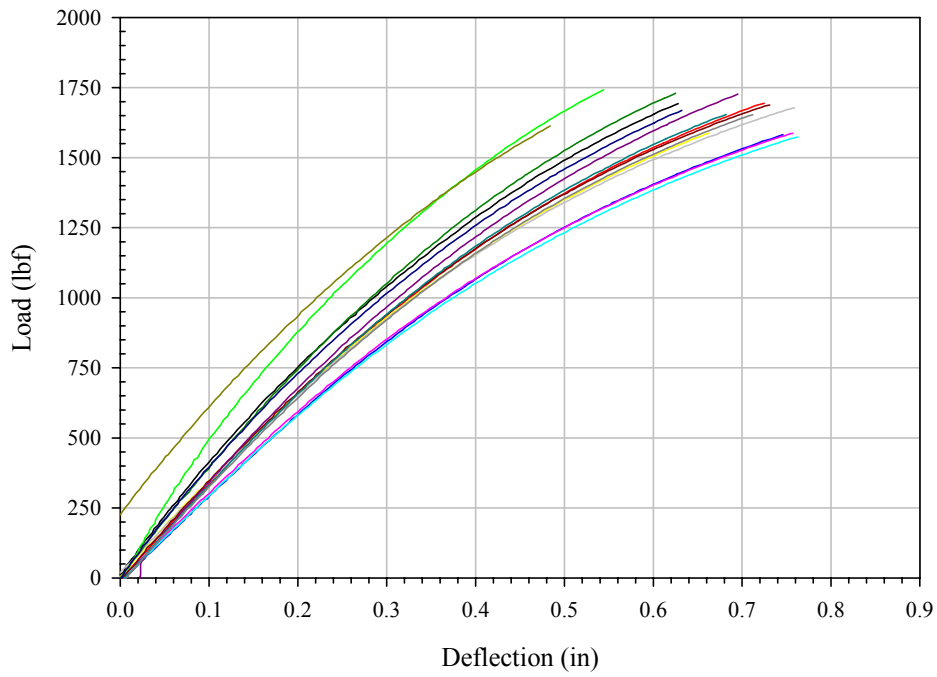
Fig. M7: 54.4% PP / 38.9% Maple / 2.0% Talc / 3.7% MAPP / 1.0% OP100
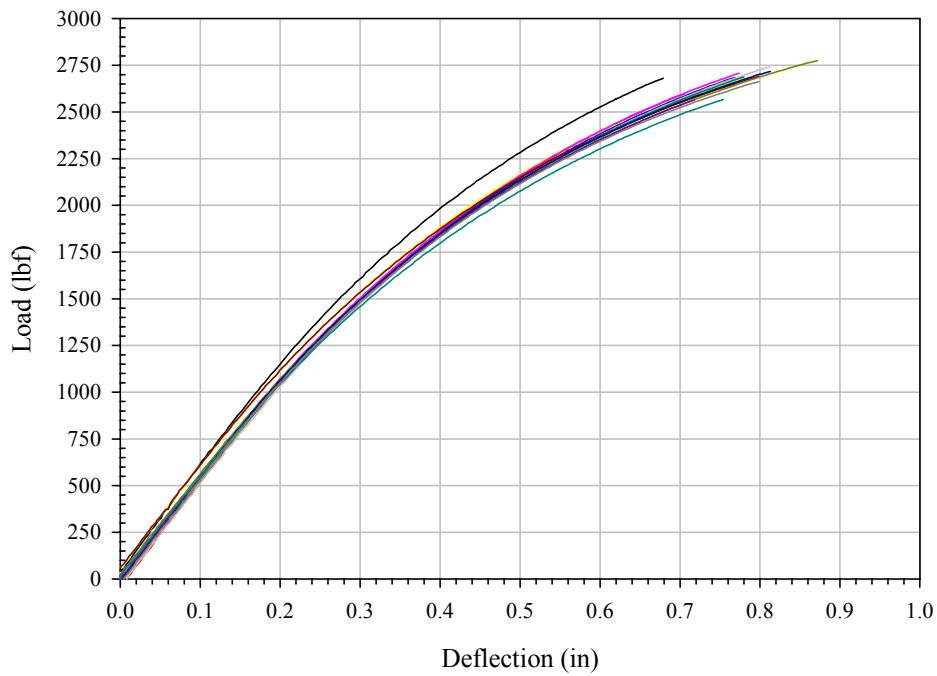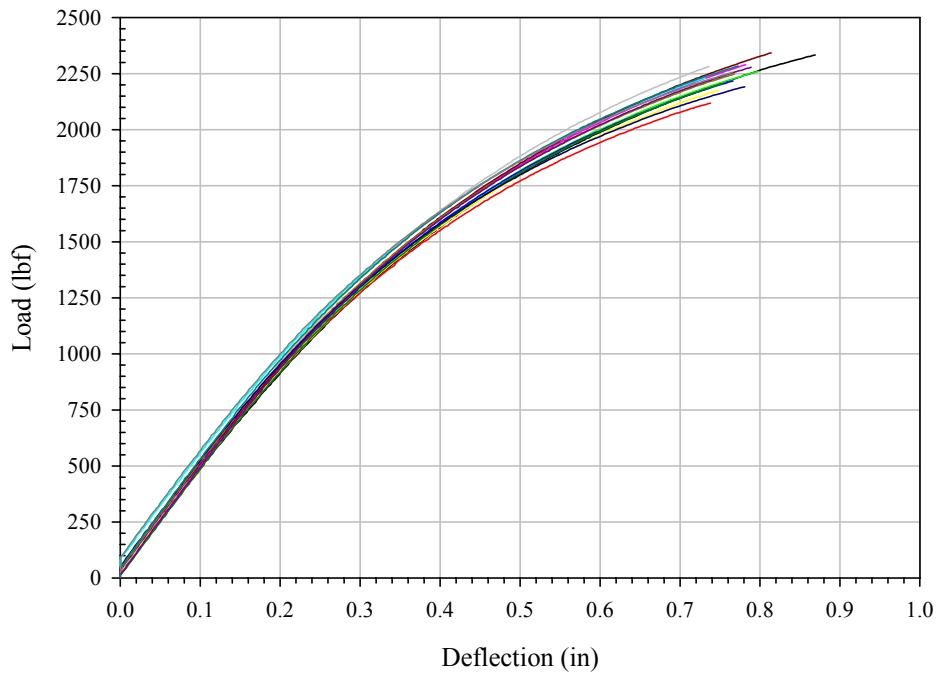

**Fig. M8:** 54.4% PP / 36.4% Maple / 7.0% Talc / 1.2% MAPP / 1.0% OP100
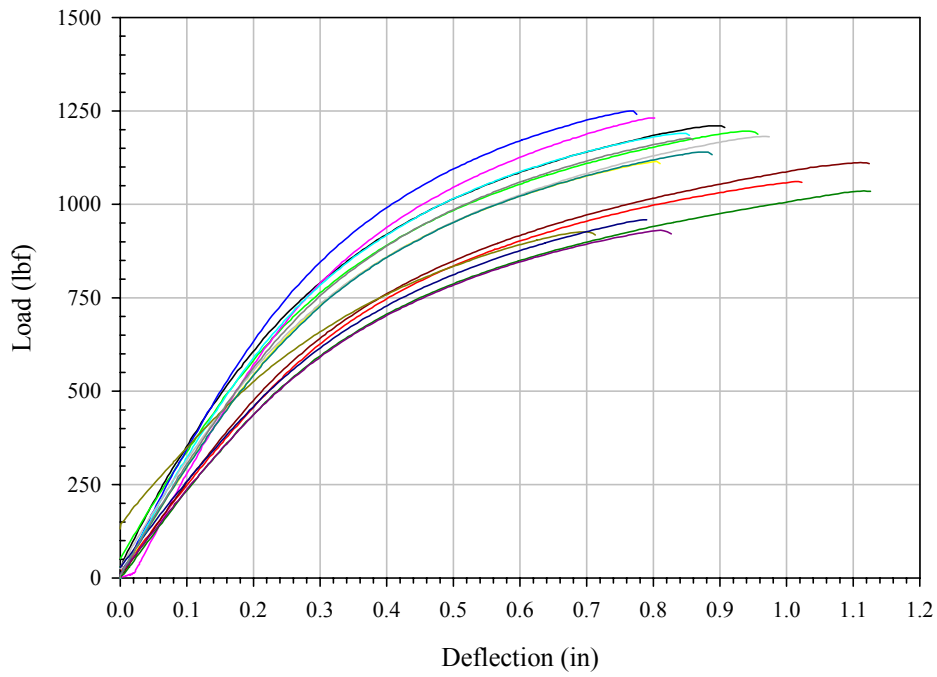
**Fig. M9:** 54.0% PP / 45.0% Maple / 0.0% Talc / 0.0% MAPP / 1.0% OP100
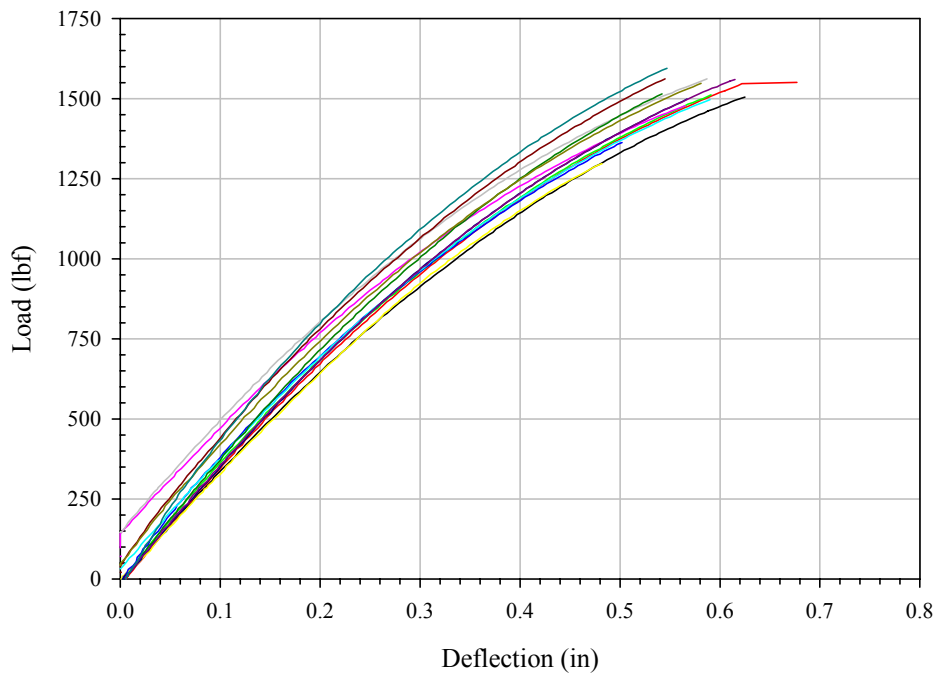
Fig. M10: 50.0% PP / 34.0% Maple / 10.0% Talc / 5.0% MAPP / 1.0% OP100
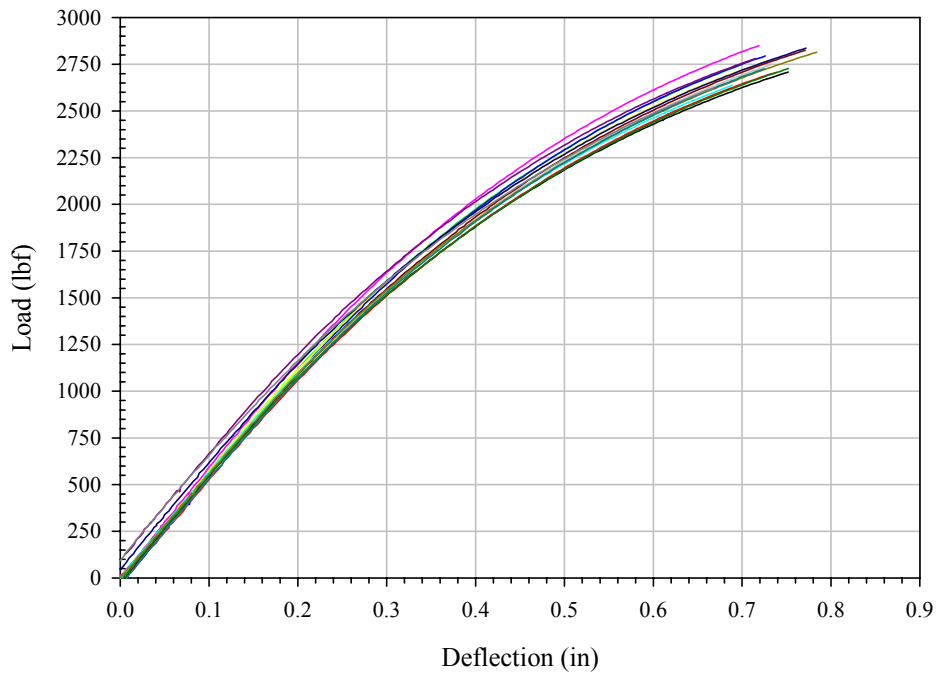
Fig. M11: 50.0% PP / 34.0% Maple / 10.0% Talc / 5.0% MAPP / 1.0% OP100
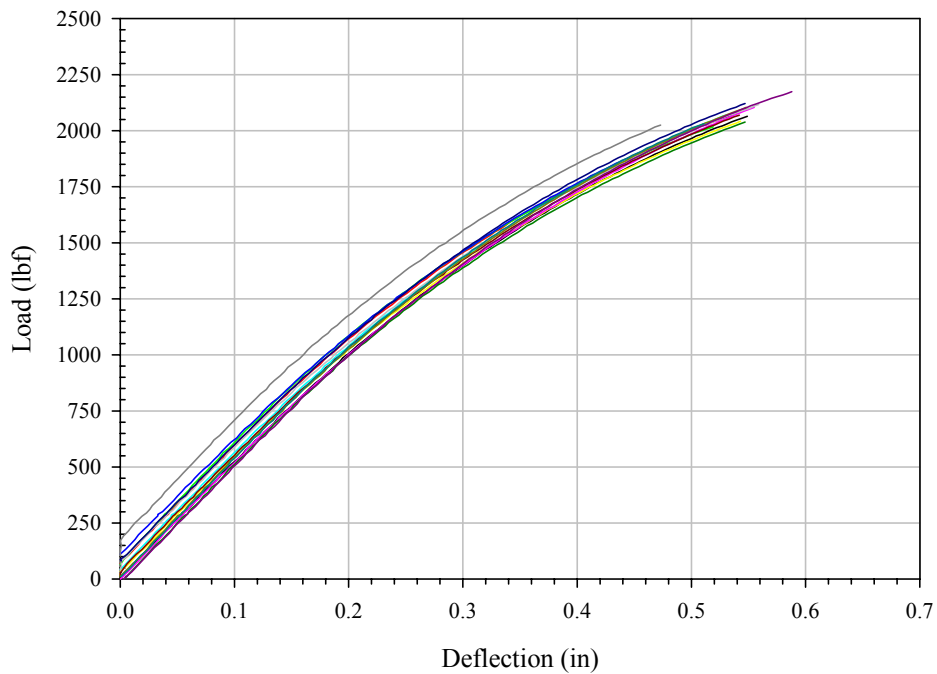
Fig. P1: 69.5% PP / 25.0% Pine / 0.0% Talc / 4.5% MAPP / 1.0% OP100
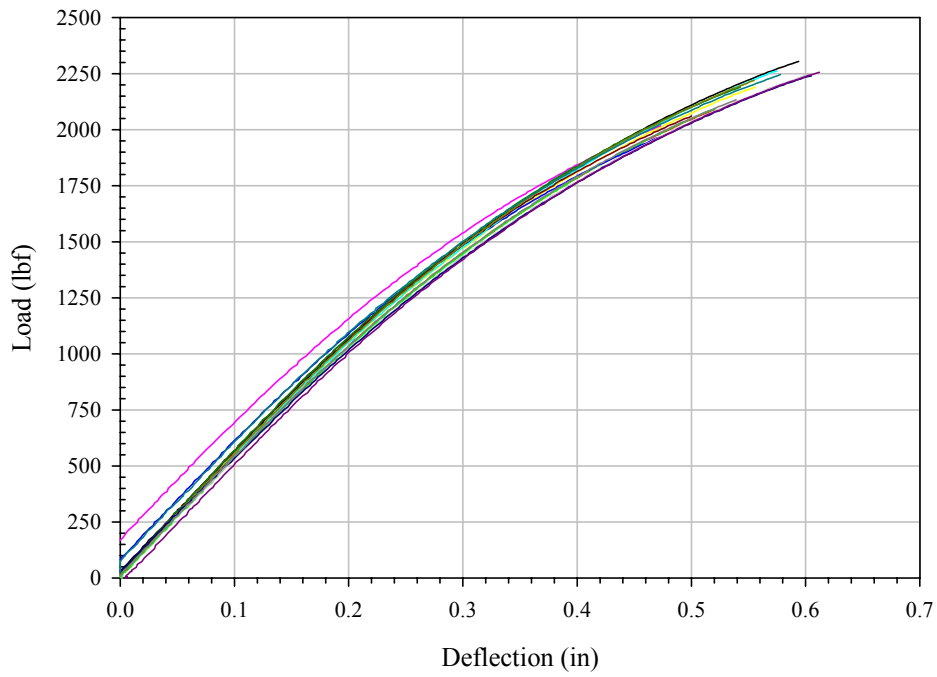
Fig. P2: 69.5% PP / 25.0% Pine / 0.0% Talc / 4.5% MAPP / 1.0% OP100
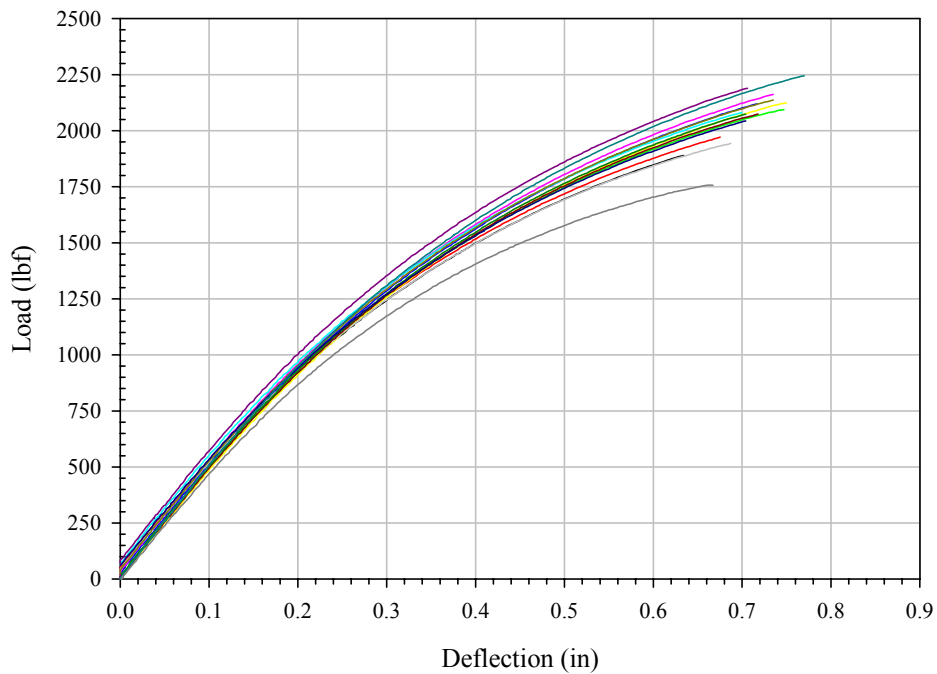
Fig. P3: 64.4% PP / 31.4% Pine / 2.0% Talc / 1.2% MAPP / 1.0% OP100
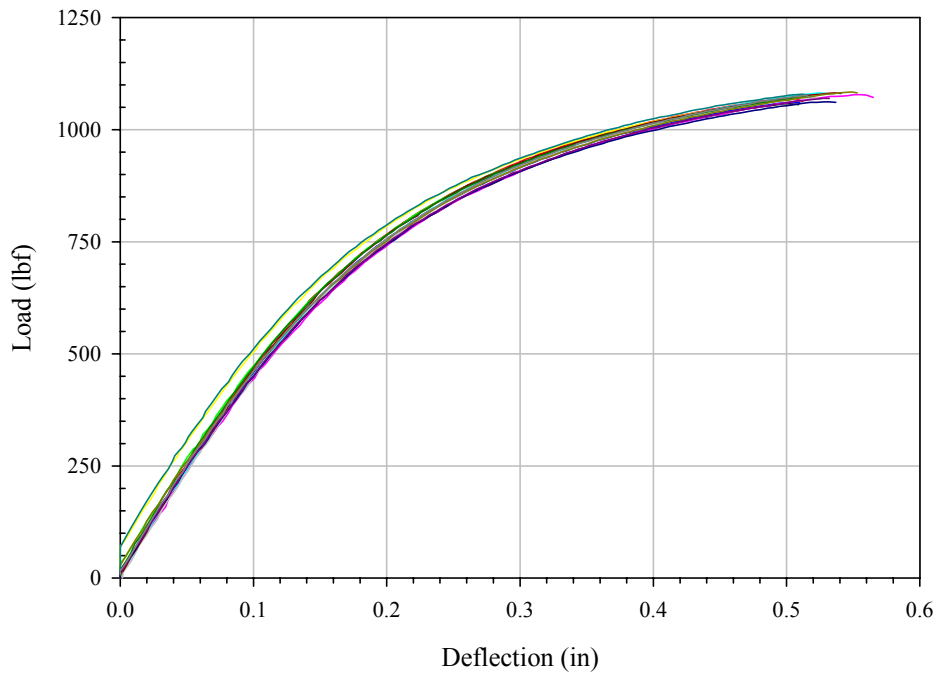
Fig. P4: 64.0% PP / 25.0% Pine / 10.0% Talc / 0.0% MAPP / 1.0% OP100
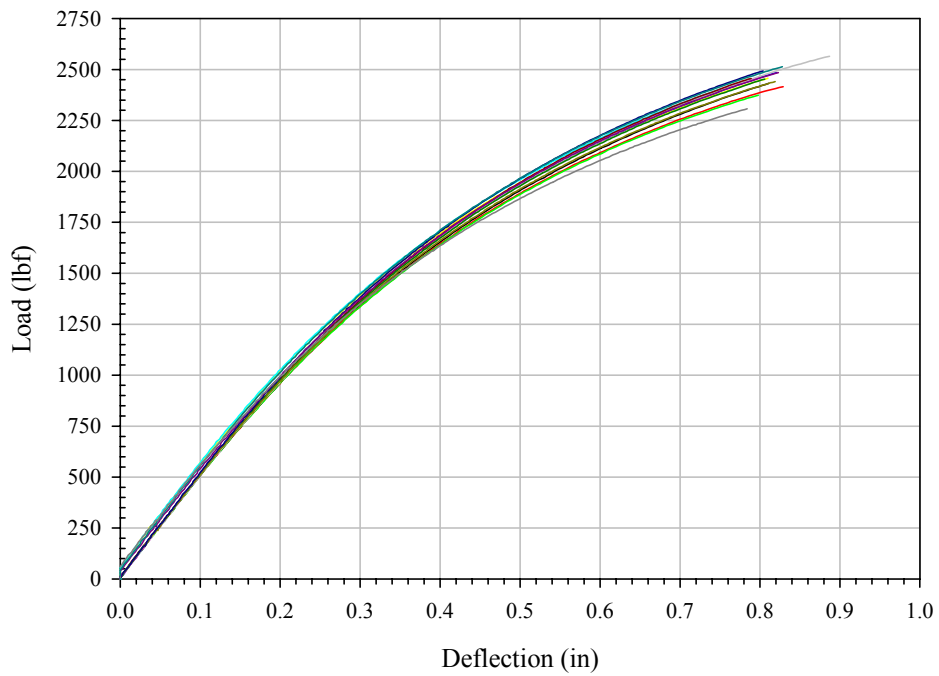
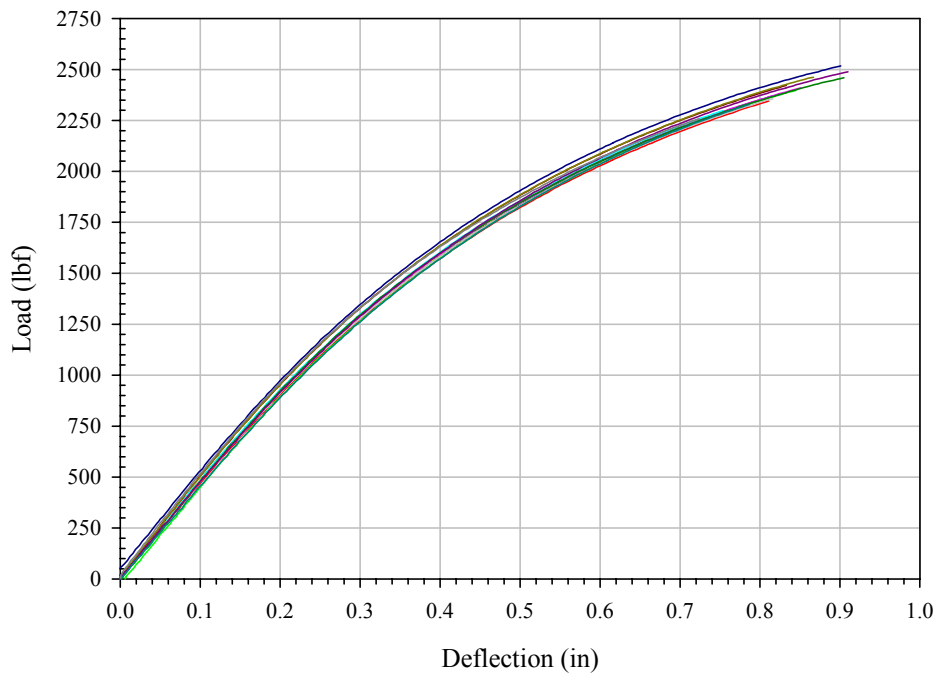**Fig. P5:** 58.8% PP / 33.8% Pine / 4.0% Talc / 2.3% MAPP / 1.0% OP100

Fig. P6: 58.8% PP / 33.8% Pine / 4.0% Talc / 2.3% MAPP / 1.0% OP100
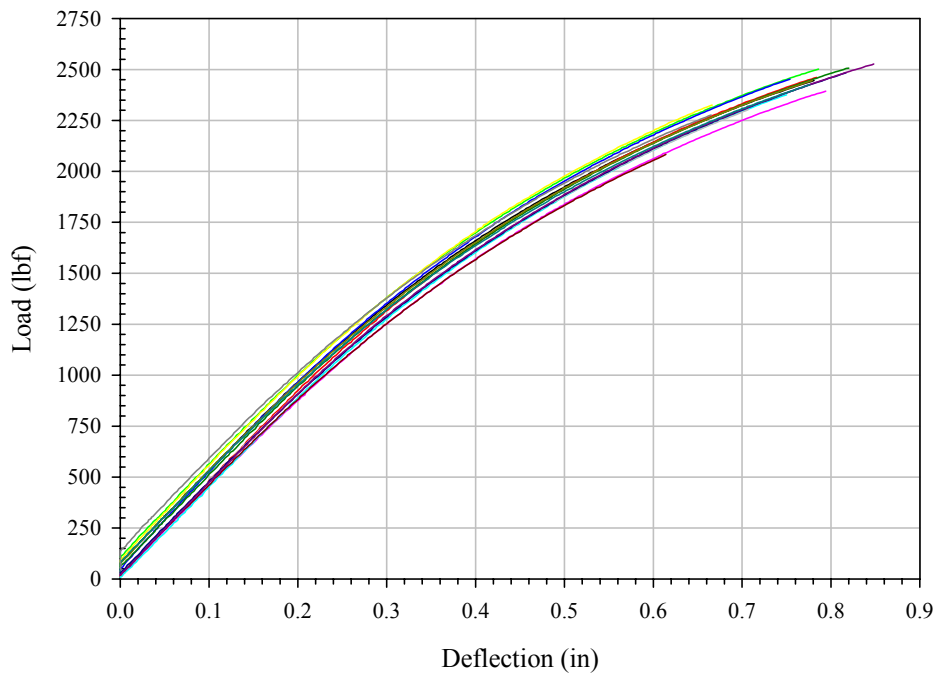
Fig. P7: 54.4% PP / 38.9% Pine / 2.0% Talc / 3.7% MAPP / 1.0% OP100

86

Fig. P8: 54.4% PP / 36.4% Pine / 7.0% Talc / 1.2% MAPP / 1.0% OP100
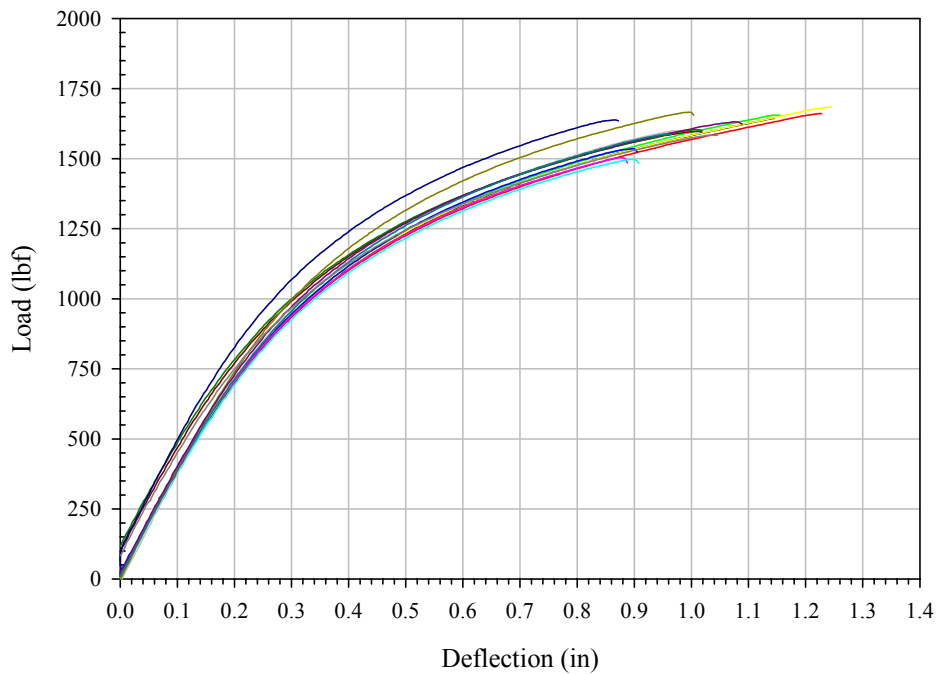
Fig. P9: 54.0% PP / 45.0% Pine / 0.0% Talc / 0.0% MAPP / 1.0% OP100
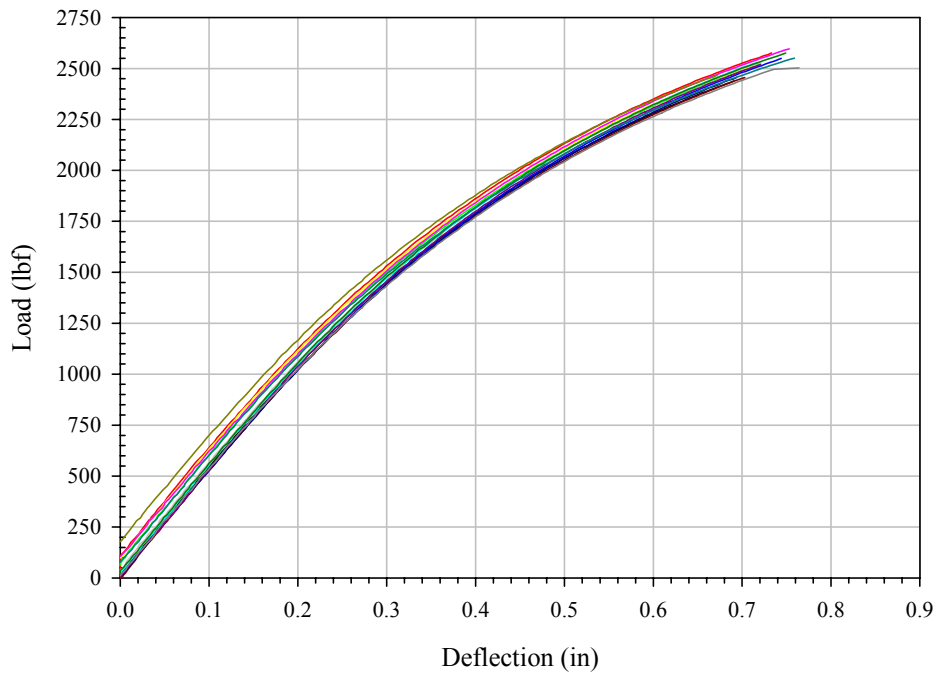
Fig. P10: 50.0% PP / 34.0% Pine / 10.0% Talc / 5.0% MAPP / 1.0% OP100

Fig. P11: 50.0% PP / 34.0% Pine / 10.0% Talc / 5.0% MAPP / 1.0% OP100

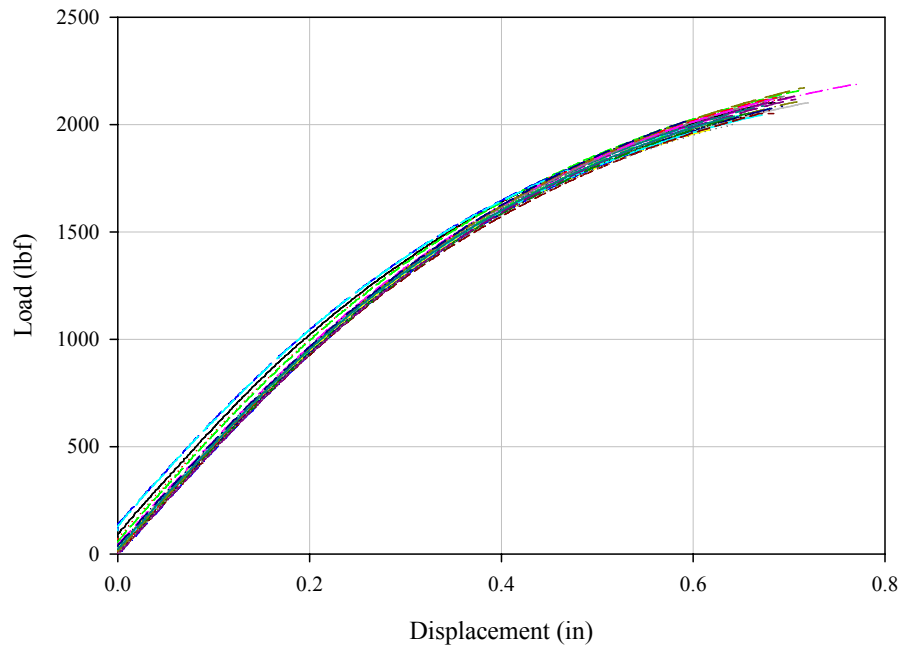**B.3 Load-displacement plots for statically tested PP-WPCs for fatigue testing**

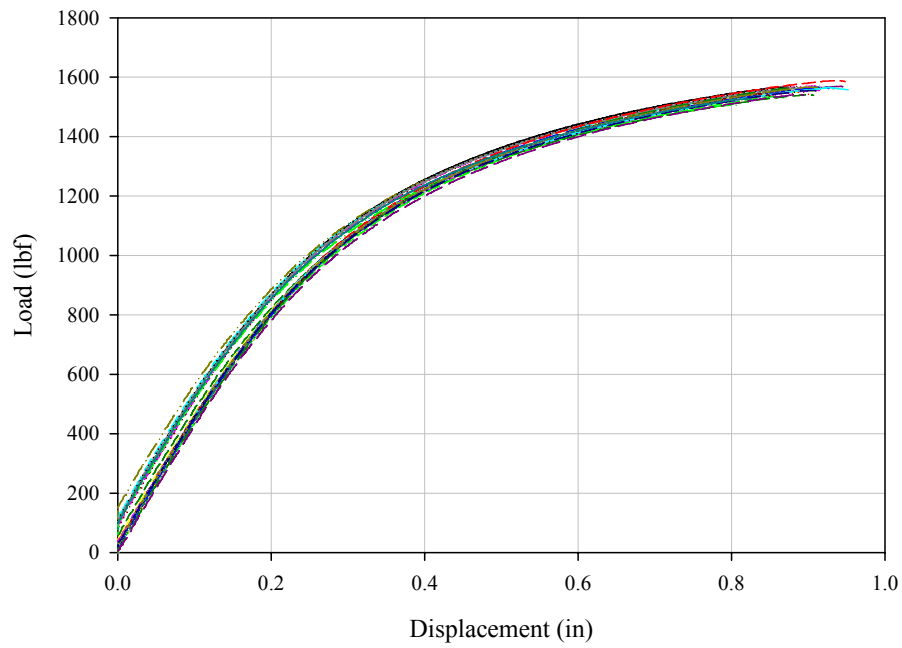**Fig. PP-MAPP:** 58.8% PP / 33.8% Pine / 4.0% Talc / 2.3% MAPP / 1.0% OP100

Fig. PP: 58.8% PP / 36.1% Pine / 4.0% Talc / 0.0% MAPP / 1.0% OP100

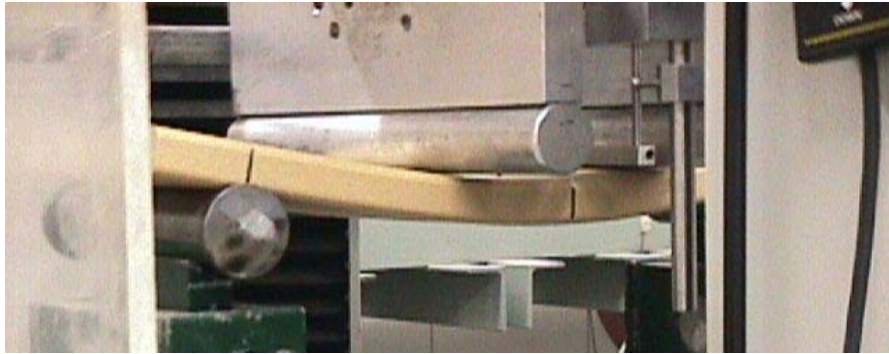**B.4 Typical Test Setups for Flexure and Shear Tests Conducted**

Fig. A Typical test setup of for static flexure testing

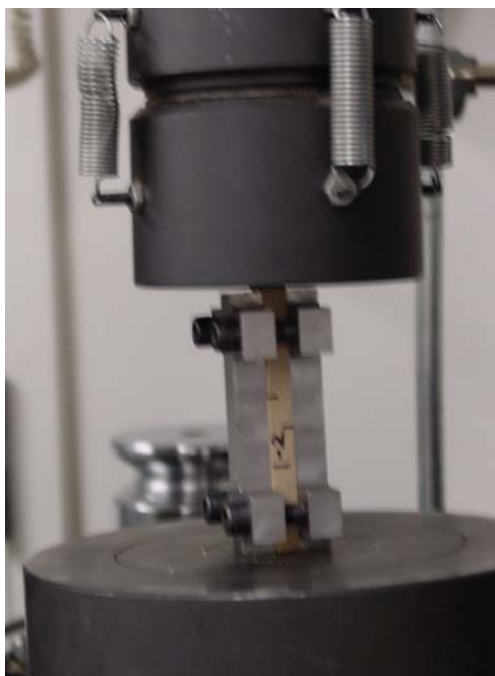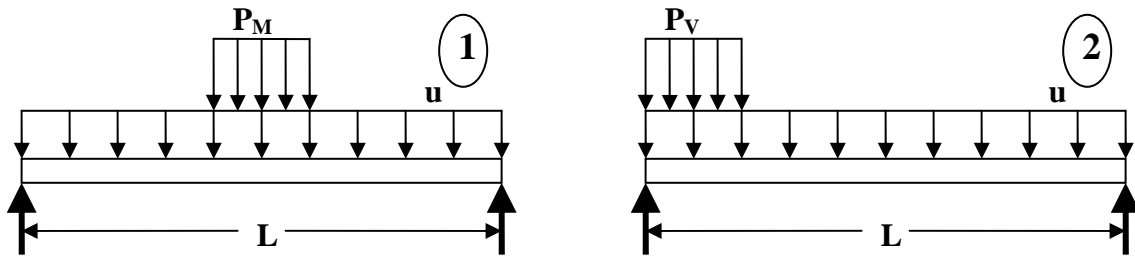Fig. B Typical test setup for static shear block tests

Fig. C Typical test setup for static coupon shear tests

APPENDIX C – APPLIED MOMENT AND SHEAR FORCE CALCULATIONS

FOR AASHTO BRIDGE DECK LOADING

Maximum Moment and Shear:

1.) **Maximum moment occurs at the center with wheel load at the center**

2.) **Maximum shear occurs at the support with the wheel load located over the same support**

Define Loads for HS20-44 Moment (M) and Shear (V):

$$P_M = \frac{18000lbf}{20in.} = 900\,{}^{lbf}\!/_{in.}$$

$$P_V = \frac{26000lbf}{20in.} = 1300\,{}^{lbf}\!/_{in.}$$

$$u = 640\,{}^{lbf}\!/_{ft} \cdot \left({}^{ft}\!/_{12in.}\right) = 53.3\,{}^{lbf}\!/_{in.}$$

If L ≤ 20-in.:

$$M_{\leq 20} = (0.8) \cdot \frac{(P_M + u) \cdot L^2}{8} = 95.33 \cdot L^2$$

$$V_{\leq 20} = \frac{(P_V + u) \cdot L}{2} = 676.67 \cdot L$$

If L > 20-in.:

$$M_{>20} = 0.8 \cdot \left[\left(\frac{u \cdot L}{2} + 9000\right) \cdot \left(\frac{L}{2}\right) - u \cdot \left(\frac{L}{2}\right) \cdot \left(\frac{L}{4}\right) - 9000 \cdot 5\right] = 5.34L^2 + 3600L - 36000$$

$$V_{>20} = P_V \cdot \left(1 - \frac{10}{L}\right) + \frac{u \cdot L}{2} = 26.67 \cdot L + 26000 - \frac{260000}{L}$$

APPENDIX D – EXAMPLE CALCULATION OF ALLOWABLE DESIGN

STRESS OF A WPC

Test Data: Moment: Shear:

$x_m := 7125\text{psi}$ $x_v := 320\text{lpsi}$ (mean of flat-wise specimen tests)

$nm \equiv 28$ $nv \equiv 29$ (sample size)

$km := 2.5632$ $kv := 2.5396$ (confidence level factor)

$COV_m := 0.0289$ $COV_v := 0.0553$ (standard deviation)

Determine characterictic Design Value, B:

$$B_m := x_m - x_m \cdot \left[km \cdot \left(COV_m \right) \right] \qquad\qquad B_v := x_v - x_v \cdot \left[kv \cdot \left(COV_v \right) \right]$$

$$B_m = 6597.2\text{lpsi} \qquad\qquad\qquad\qquad B_v = 2751.45\text{psi}$$

Define adjustment factors, see Chapter 3:

$X_{10yr} := 3$ (Load duration adjustment)

$C_a := \dfrac{1}{X_{10yr} \cdot 1.3}$ (Property adjustment factor)

$C_t := 0.75$ (Temperature adjustment factor)

$C_v := \left(\dfrac{1}{d} \right)^{0.05}$ (Volume adjustment factor; depth, $d \equiv 1$)

$C_m := 1.0$ (Moisture ajustment factor)

$C_D := 2.35$ (Load duration factor)

Allowable Design Stress:

$$F_b := B_m \cdot C_a \cdot C_t \cdot C_m \cdot C_v \cdot C_D \qquad\qquad F_v := B_v \cdot C_a \cdot C_t \cdot C_m \cdot C_v \cdot C_D$$

$$F_b = 2981.43\text{psi} \qquad\qquad\qquad\qquad F_v = 1243.44\text{psi}$$

Determine Moment Capacity, M: Determine Shear Capacity, V:

$I = 0.46\text{in}^4$ (Nominal moment of inertia)

$c = 0.5\text{in}$ (Assumed distance from N.A. to extreme fiber) $A = 5.4463\text{in}^2$ (Nominal area)

$S := \dfrac{I}{c}$ $M := F_b \cdot S$

                                        $V := \left(\dfrac{2}{3} \right) \cdot F_v \cdot A$

$M = 2730.99\text{lbf} \cdot \text{in}$

                                        $V = 4514.78\text{lbf}$

APPENDIX E – EXAMPLE CALCULATIONS FOR DETERMINATION OF

WEIBULL PARAMETERS

E.1 Two-parameter Weibull
(Law and Kelton, 1999)

	1
1	$6.6 \cdot 10^3$
2	$6.794 \cdot 10^3$

$X =$ (table above)

Data: Formulation PP-MAPP static tests (MOR, psi)

$n := rows(X)$ Number of data points

β = scale parameter
α = shape parameter

Maximum Liklihood Method (MLE), two equations must be satisfied:

Initial guess:

$$\alpha 0 := \left[\frac{\left(\frac{6}{\pi^2}\right) \cdot \left[\left[\sum_{i=1}^{n} \left(\ln\left(X_i\right)\right)^2\right] - \frac{\left[\sum_{i=1}^{n} \left(\ln\left(X_i\right)\right)\right]^2}{n}\right]}{n-1} \right]^{-\left(\frac{1}{2}\right)}$$

$\alpha 0 = 43.988$

Given

(Equation 1)

$$\left[\frac{\sum_{i=1}^{n} \left(X_i\right)^{\alpha 0} \cdot \ln\left(X_i\right)}{\sum_{i=1}^{n} \left(X_i\right)^{\alpha 0}}\right] - \frac{1}{\alpha 0} = \frac{\sum_{i=1}^{n} \ln\left(X_i\right)}{n}$$

$\alpha := Find(\alpha 0)$ $\alpha = 40.209$ Shape parameter for 2-parameter Weibull

(Equation 2)

$$\beta := \left[\frac{\sum_{i=1}^{n} \left(X_i\right)^{\alpha}}{n}\right]^{\frac{1}{\alpha}}$$

$\beta = 7218.9$ Scale parameter for 2-parameter Weibull

$\beta \cdot 1000 = 7.22 \times 10^6$

E.2 Three-parameter Weibull parameters
(Kline and Bender, 1990)

	1
1	$6.055 \cdot 10^3$
2	$6.103 \cdot 10^3$
3	$6.263 \cdot 10^3$
4	$6.304 \cdot 10^3$

$X =$ (table above)

Data: Formulation PP-MAPP static tests (MOR, psi)

$n := \text{rows}(X)$

$n = 30$

The log likelihood function of a 3-parameter Weibull:

$$L(\delta,\gamma,\eta) := \sum_{i=1}^{n} \left[\ln\left[\delta \cdot \gamma^{-\delta} \cdot \left(X_i - \eta\right)^{\delta-1} \cdot e^{-\left(\frac{X_i - \eta}{\gamma}\right)^{\delta}} \right] \right]$$

where,
δ = shape parameter
γ = scale parameter
η = location parameter

Weibull parameters are estimated by differentiating the above equation with respect to each of the parmeters,then setting each equation equal to zero.

Initial estimates:

$a := 0.97366$ $b := 0.16731$ $c := 0.63000$

$na := \text{ceil}(n \cdot a)$ $nb := \text{ceil}(n \cdot b)$ $nc := \text{ceil}(n \cdot c)$

$$\eta := \frac{\left[X_1 \cdot X_n - \left(X_2\right)^2\right]}{\left(X_1 + X_n - 2 \cdot X_2\right)}$$

$$\delta := \frac{\ln\left(\left(\frac{\ln(1-a)}{\ln(1-b)}\right)\right)}{\ln\left[\frac{\left(X_{na} - \eta\right)}{\left(X_{nb} - \eta\right)}\right]}$$

$$\gamma := -\eta + X_{nc}$$

$\eta = 6051.6$ $\delta = 2.502$ $\gamma = 528.062$

Given

$$\frac{d}{d\delta}L(\delta,\gamma,\eta) = 0 \qquad \frac{d}{d\gamma}L(\delta,\gamma,\eta) = 0 \qquad \frac{d}{d\eta}L(\delta,\gamma,\eta) = 0$$

$B := \text{Find}(\delta,\gamma,\eta)$

$\delta := B_1$ $\delta = 3.373$

$\gamma := B_2$ $\gamma = 689.787$ Estimates for 3-parameter Weibull distribution

$\eta := B_3$ $\eta = 5874.26$

E.3 References

Kline, D.E. and Bender, D.A. "Maximum Likelihood Method for Shifted Weibull and Lognormal Distributions." American Society of Agricultural Engineering. Transactions in Agriculture, 1990.

Law, A.M. and Kelton, W.D. "Simulation Modeling and Analysis." McGraw-Hill Inc., 3rd Edition, 1999.

APPENDIX F – EXAMPLE CALCULATION OF KOLMOGOROV-SMIRNOV

(K-S) GOODNESS-OF-FIT METHOD

Null Hyptothesis: A 3-parameter Weibull distribution adequately estimates the distribution of a wood-plastic composite sample tested in flexure.

Alternate Hyptothesis: A distrubtion other than a 3-parameter Weibull distribution is adequate.

$\delta = 3.373$ (Shape parameter)

$\gamma = 689.79$ (Scale parameter)

$\eta = 5874.3$ (Location parameter)

$F := 1 - e^{-\left(\frac{Q-\eta}{\gamma}\right)^{\delta}}$ (Cumulative distribution function for 3-parameter Weibull)

$n := rows(Q)$

$n = 17$

Calculate K-S statistic Dn:

$i := 1..n$

$D1_i := \left(\dfrac{i}{n}\right) - F_i$ $\qquad D11 := max(D1) \qquad D11 = 0.112$

$D2_i := F_i - \dfrac{(i-1)}{n}$ $\qquad D22 := max(D2) \qquad D22 = 0.18$

$Dn := max(D11, D22) \qquad Dn = 0.18$ (K-S statistic)

Reject or fail to reject the null hypothesis if the $\sqrt{n}\,Dn$ is greater than C (at a significance level, p)

$j := 1..5$

$$C := \begin{pmatrix} 0.74557 - \dfrac{0.17853}{\sqrt{n}} & p = 0.2 \\ 0.78064 - \dfrac{0.18820}{\sqrt{n}} & p = 0.15 \\ 0.82608 - \dfrac{0.19708}{\sqrt{n}} & p = 0.10 \\ 0.89906 - \dfrac{0.22601}{\sqrt{n}} & p = 0.05 \\ 1.04749 - \dfrac{0.29280}{\sqrt{n}} & p = 0.01 \end{pmatrix} \qquad C = \begin{pmatrix} 0.702 \\ 0.735 \\ 0.778 \\ 0.844 \\ 0.976 \end{pmatrix}$$

$$\sqrt{n} \cdot Dn = 0.741$$

$$R_j := \begin{cases} \text{"Reject Null Hypothesis"} & \text{if } \sqrt{n} \cdot Dn > C_j \\ \text{"Fail to Reject Null Hypothesis"} & \text{otherwise} \end{cases}$$

$$R = \begin{pmatrix} \text{"Reject Null Hypothesis"} \\ \text{"Reject Null Hypothesis"} \\ \text{"Fail to Reject Null Hypothesis"} \\ \text{"Fail to Reject Null Hypothesis"} \\ \text{"Fail to Reject Null Hypothesis"} \end{pmatrix} \begin{matrix} p = 0.2 \\ p = 0.15 \\ p = 0.10 \\ p = 0.05 \\ p = 0.01 \end{matrix}$$

F.1 References

Law, A.M. and Kelton, W.D. "Simulation Modeling and Analysis." McGraw-Hill Inc.,
3rd Edition, 1999.

APPENDIX G – FATIGUE DATA ANALYSIS

G.1 Introduction

Information presented herein is a supplement to the fatigue results presented in Chapter 4. As discussed in Chapter 4, load and crosshead data was collected at various cycles for each fatigue test including both couple (PP-MAPP) and uncouple (PP) formulations. This data was analyzed in order to assess the viscoelastic properties, modulus of elasticity, and damage behavior of each formulation during fatigue. In addition, the actual frequency and stress ratio were determined.

G.2 Calculations

A FORTRAN program was created to analyze load and deflection data acquired for each test. Data was acquired in groups of 5 to 10 waves at various cycles throughout testing. The program used average values from each group of waves and associated the average value with the cycle in which the data acquisition began. The FORTRAN program calculated various parameters associated with the fatigue test, and each parameter outputted from the programs is summarized below. The program source code is included in section G.6.

- *Cyclecount* and *time* are a direct read from the input files that indicate the cycle count and the time that cycle occurred.

- *Top, bot,* and *totaltemp* are the average temperatures across the specimen, top, bottom, and all four thermocouples, respectively.

- *xblockfreq* and *Rratio* calculate the actual test frequency and stress ratio.

- *Dispspan* is the difference between the maximum and minimum crosshead displacement.

- *Rate* is an estimate of the load rate of the specimen calculated from the actual frequency and the displacement span

- *Xloadmax, xloadmin, crossheadmax,* and *crossheadmin* reports the minimum and maximum load and crosshead displacement acquired from the test equipment, respectively.

- *Stressmax, stressmin, strainmax,* and *strainmin* are the calculated stress and strain assuming a linear stress-strain relationship and the crosshead deflection. The crosshead deflection was used for calculation of strain for the static tests as well to insure an accurate comparison. The following equations were utilized:

$$\sigma = \frac{PLy}{16} \qquad \varepsilon = \frac{27h\Delta}{5L^2}$$

where,

$P = $ load

$L = $ span

$y = h/2$

$d = $ specimen depth

$\Delta = $ crosshead deflection

- *Avgphase, Eloss, Estorage,* and *Ecomplex* represent the phase shift, loss modulus, storage modulus, and complex modulus, respectively. The phase shift measures the angle for which the stress and strain curves are out-of-phase. A perfectly elastic material exhibits a phase shift of 0° (i.e., the maximum stress occurs with maximum strain), whereas, a perfect fluid exhibits a shift of 90°. The complex modulus is viscoelastic a measure that is a function of the storage and loss moduli. The storage modulus is representative of the mechanical energy returned by a material during each cycle, while the loss modulus is a measure of the energy loss or the energy converted from mechanical to thermal forms.

$$E^* = E' + iE'' \qquad \left|E^*\right| = \frac{\sigma_0}{\varepsilon_0} = \sqrt{E'^2 + E''^2} \qquad \tan\delta = \frac{E''}{E'}$$

where,

$E^* =$ Complex modulus

$E' =$ Storage modulus

$E'' =$ Loss modulus

$\delta =$ Phase shift

- *Esecantult* and *Esecantapp* is the secant modulus of elasticity calculating using the slope of the load displacement curve between 20% and 40% of the ultimate and applied load, respectively.   The secant modulus is then determined using the following equation:

$$E_{secant} = \frac{5L^3}{324I} \cdot slope$$

Where,

$L =$ span

$I =$ moment of intertia

- *Damagec, Damgeult, Damageapp,* and *Dstor* is the damage calculated with the complex modulus, ultimate secant modulus, applied secant modulus, and the storage modulus, respectively, using the following equation for damage.

$$D = 1 - \frac{MOE}{MOEi}$$

Where,

$MOEi =$ initial modulus of elasticity

- *Xdispmax* and *xdispmin* are estimates of the midspan deflections, which was calculated by adding the expected difference between the crosshead location and mispan using the following equation:

$$\Delta_{midspan} = \Delta_{crosshead} + \frac{3P}{20Slope}$$

Where,

$P = $ load

$Slope = $ slope of the load deflection curve

G.3 – Results

The FORTRAN program was used to analyze each fatigue specimen. The laboratory experienced large temperature swings, which noticeably affected the fatigue specimens. As the temperature of the lab fluctuated, the specimen temperature responded, which affected the properties. It is important to note that these temperature effects did not seem to cause any outliers in the S-N data. Assessing the results in relation to application of the material on bridges, large temperature fluctuations exist in the field, and therefore may be assumed as reasonable for fatigue testing. On the other hand, when comparing damage plots the unstable environment is not desirable because it affects the results, therefore the results for the fatigue tests performed are difficult to compare or apply.

Nonetheless, a modulus of elasticity and temperature versus cycles plot for each fatigue test are included in section G.5. The included plots demonstrate that the fatigue and data analysis tools behaved as expected by demonstrating degradation in modulus during cycling, but the temperature of the specimen did not behave as expected. Specimen temperature tended to exhibit significant fluctuations, suggesting that temperature of the specimen decreased. This is not reasonable unless the lab conditions changed significantly to provide cooling of the specimen. These fluctuations in lab conditions caused abrupt changes in modulus of elasticity for some specimens that are obviously correlated to the specimen temperature (see figures). Therefore, any in-depth results or analysis is not reasonable.

G.4 – Conclusions

Overall, the specimen temperature is associated with the mechanical properties. The most effected property was the secant modulus of elasticity. The variation in mechanical properties with heating indicates that properties are functions of specimen temperature. Drawing conclusions are difficult because the lab conditions were not monitored or constant during the testing. Therefore, future fatigue research should be performed in a controlled environment to identify the true effects of temperature on the fatigue behavior of wood-plastic composites.

G.5 Modulus of Elasticity versus Cycle Plots
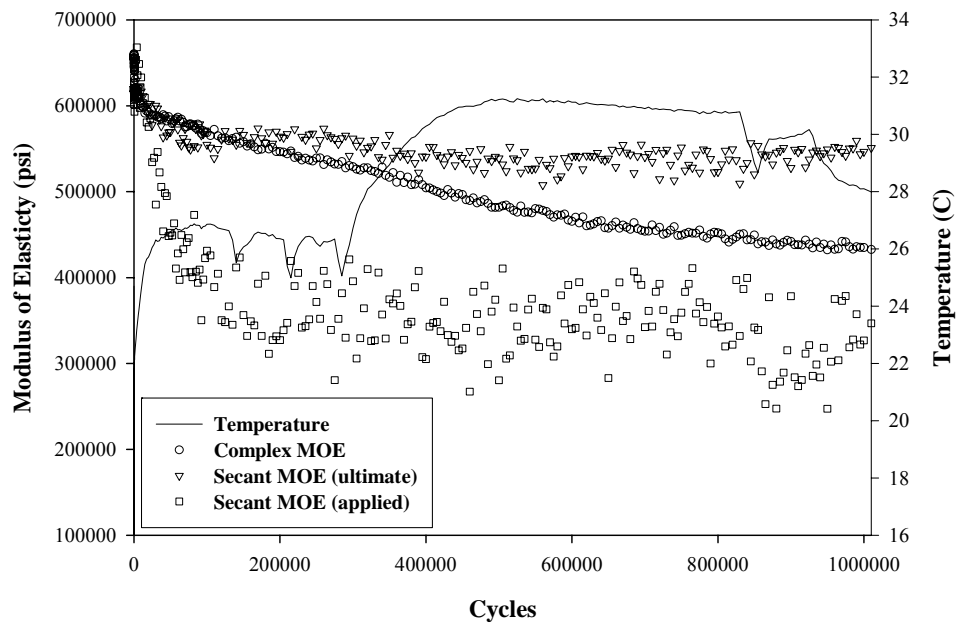
Fig. G.1. PP-MAPP modulus of elasticity and temperature plot at 40%, 10.4-Hz, R = 0.14, and N = 1,000,000 (test stopped)
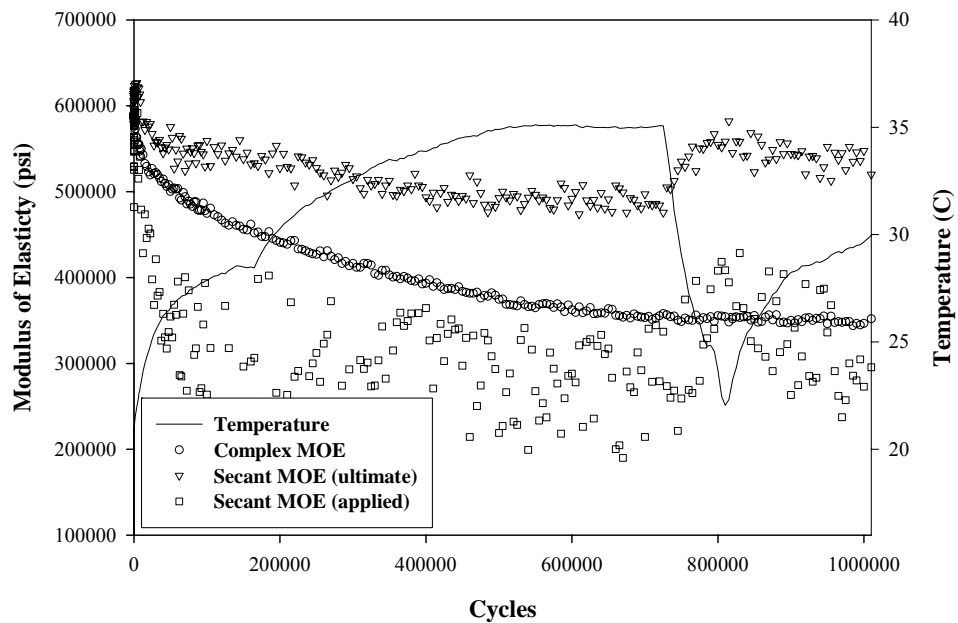
Fig. G.2. PP-MAPP modulus of elasticity and temperature plot at 40%, 10.4-Hz, R = 0.14, and N = 1,000,000 (test stopped)

110
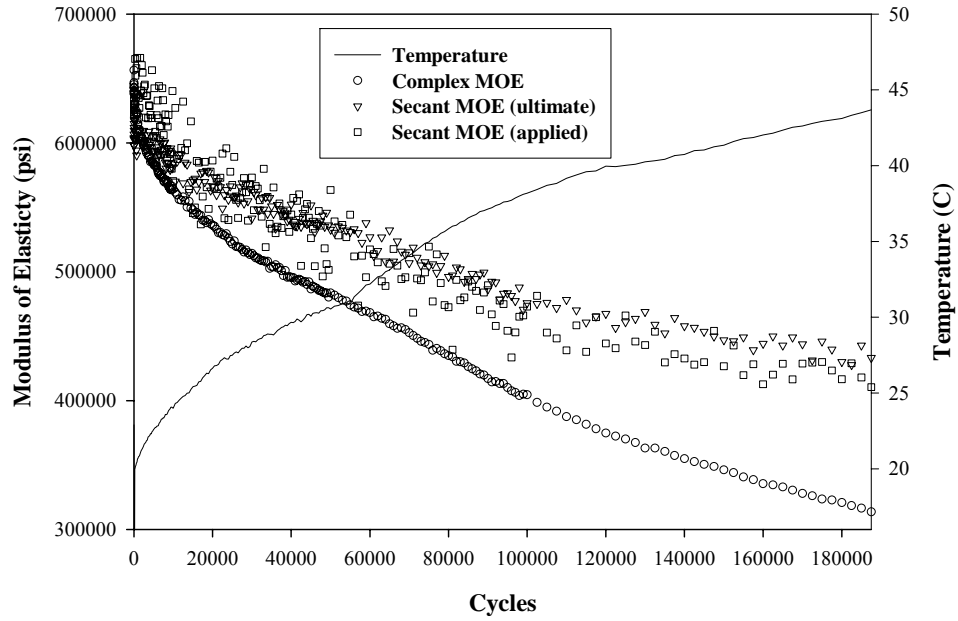
Fig. G.3. PP-MAPP modulus of elasticity and temperature plot at 48%, 10.4-Hz, R = 0.18, N = 188,912, and 0.95% strain at failure
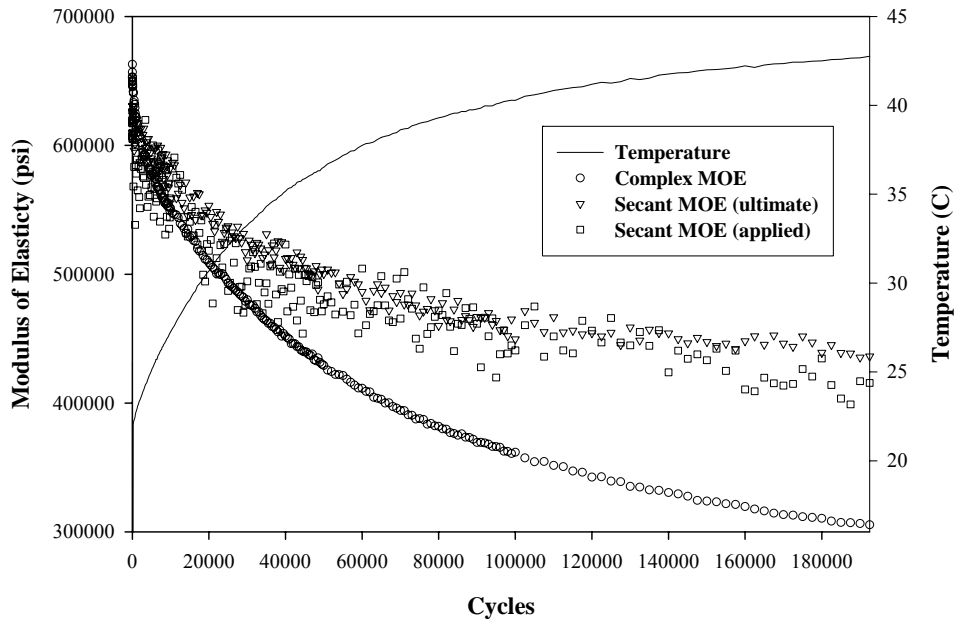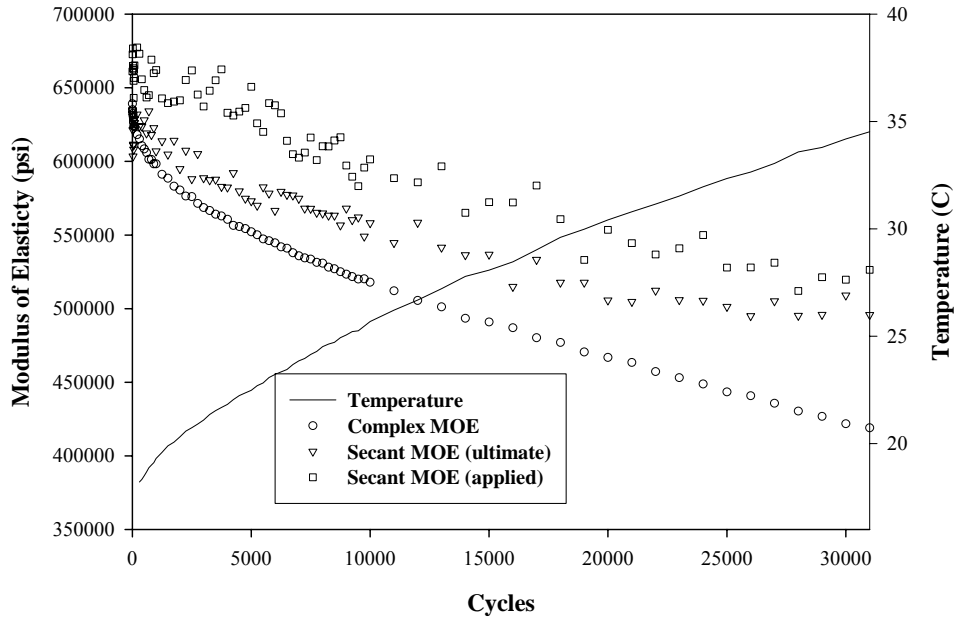

Fig. G.4. PP-MAPP modulus of elasticity and temperature plot at 48%, 10.4-Hz, R = 0.18, N = 194,898, and 0.95% strain at failure

111

Fig. G.5. PP-MAPP modulus of elasticity and temperature plot at 58%, 10.4-Hz, R = 0.17, N = 32,001, and 0.98% strain at failure
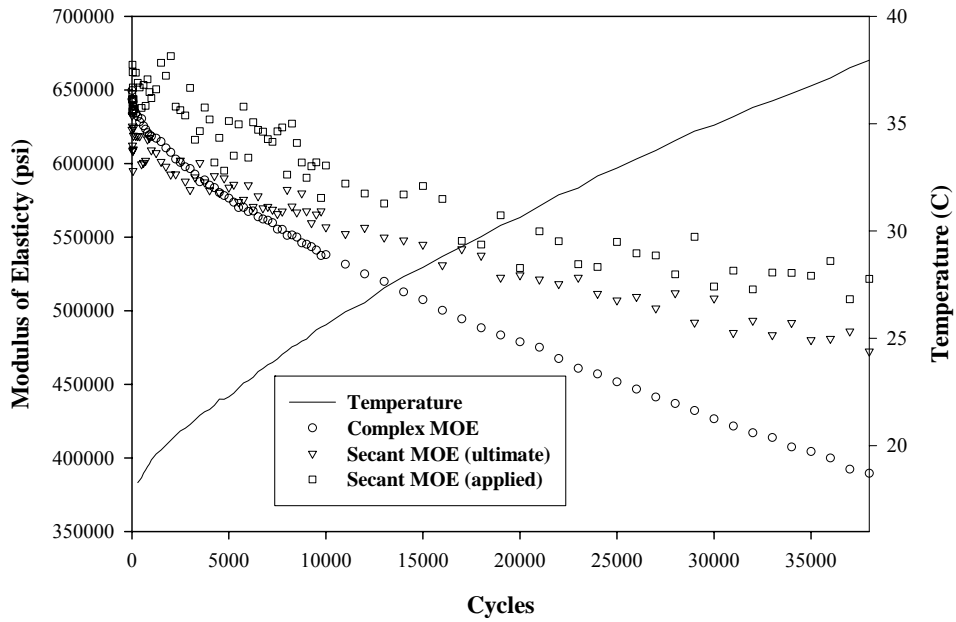

Fig. G.6. PP-MAPP modulus of elasticity and temperature plot at 57%, 10.4-Hz, R = 0.19, N = 38,688, and 0.85% strain at failure
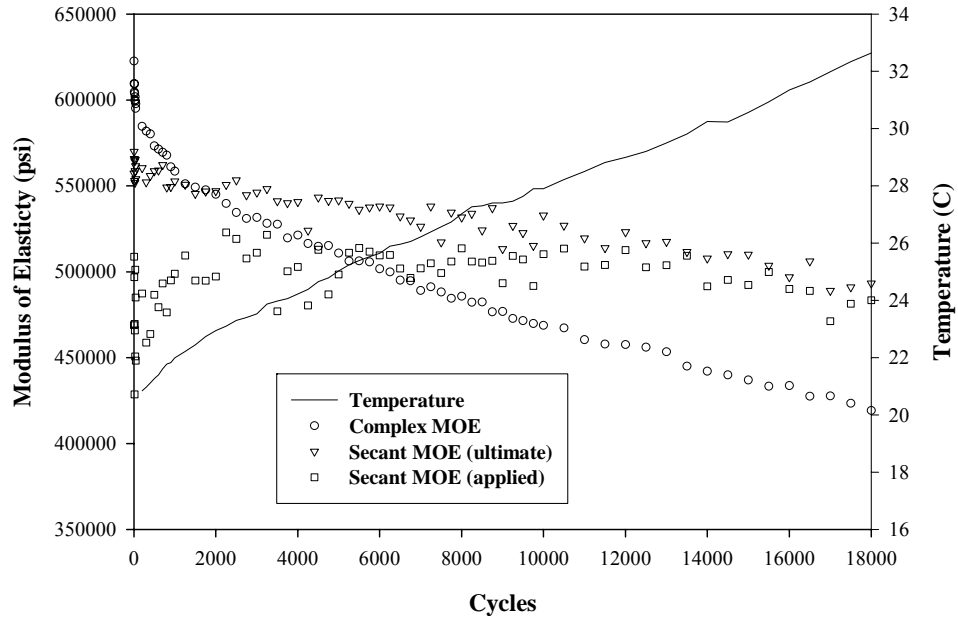
Fig. G.7. PP-MAPP modulus of elasticity and temperature plot at 58%, 10.4-Hz, R = 0.16, N = 18,268, and 0.91% strain at failure
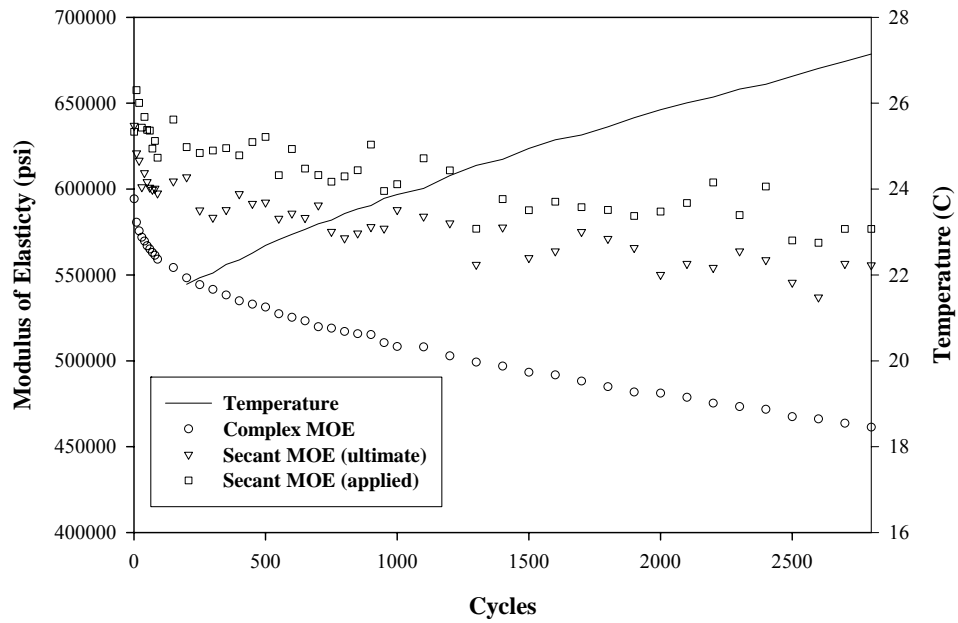

Fig. G.8. PP-MAPP modulus of elasticity and temperature plot at 66%, 10.4-Hz, R = 0.20, N = 2,884, and 0.90% strain at failure
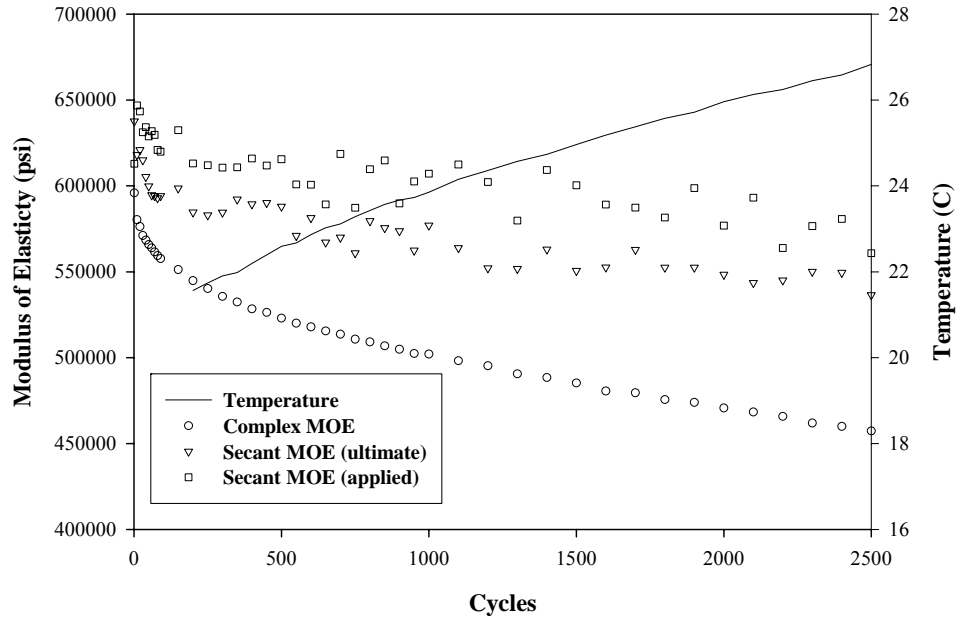
Fig. G.9. PP-MAPP modulus of elasticity and temperature plot at 66%, 10.4-Hz, R = 0.21, N = 2,545, and 0.91% strain at failure
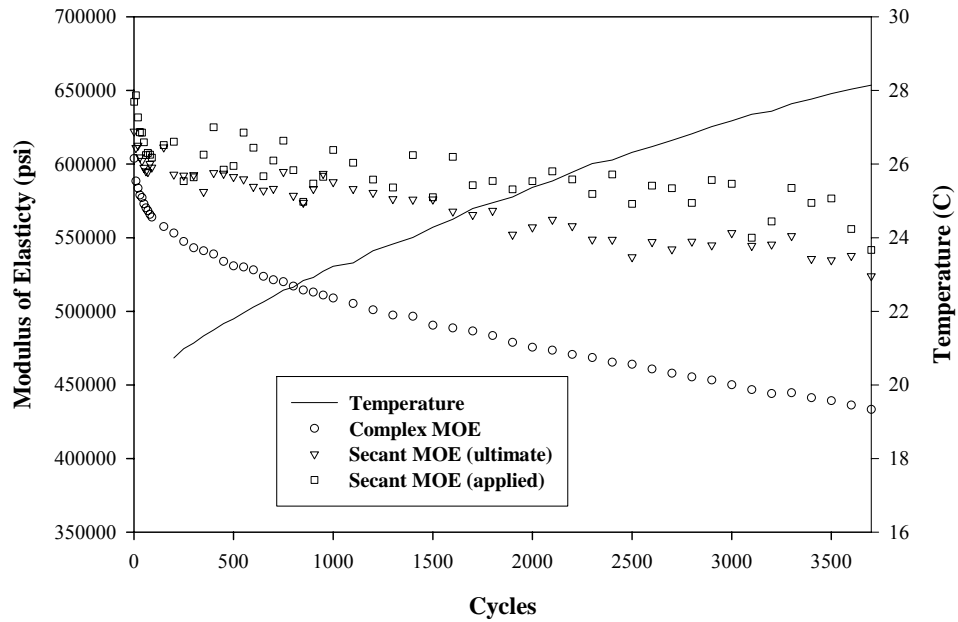

Fig. G.10. PP-MAPP modulus of elasticity and temperature plot at 70%, 10.4-Hz, R = 0.21, N = 3,776, and 1.02% strain at failure
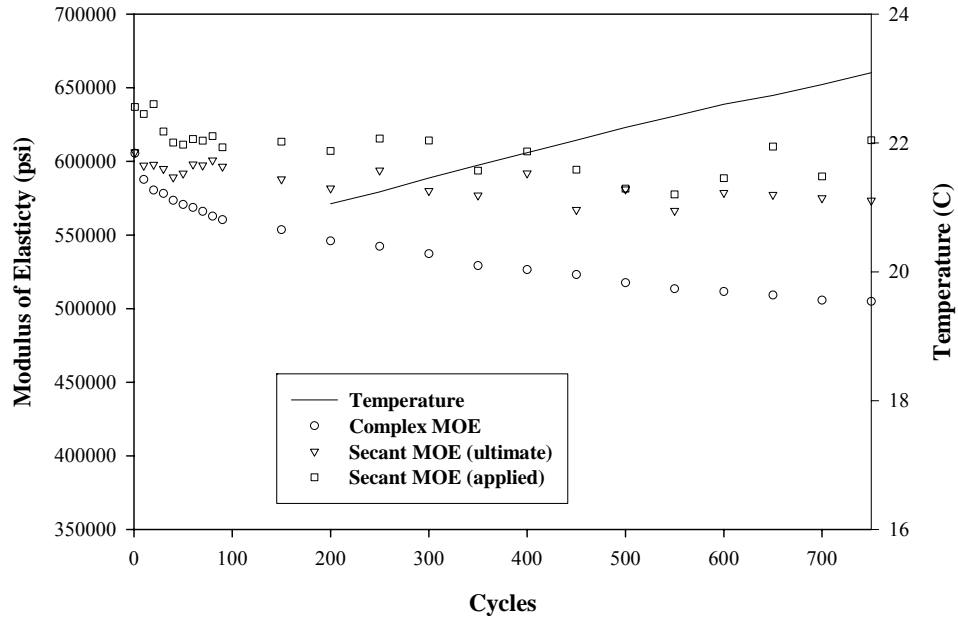
Fig. G.11. PP-MAPP modulus of elasticity and temperature plot at 70%, 10.4-Hz, R = 0.21, N = 808, and 0.89% strain at failure

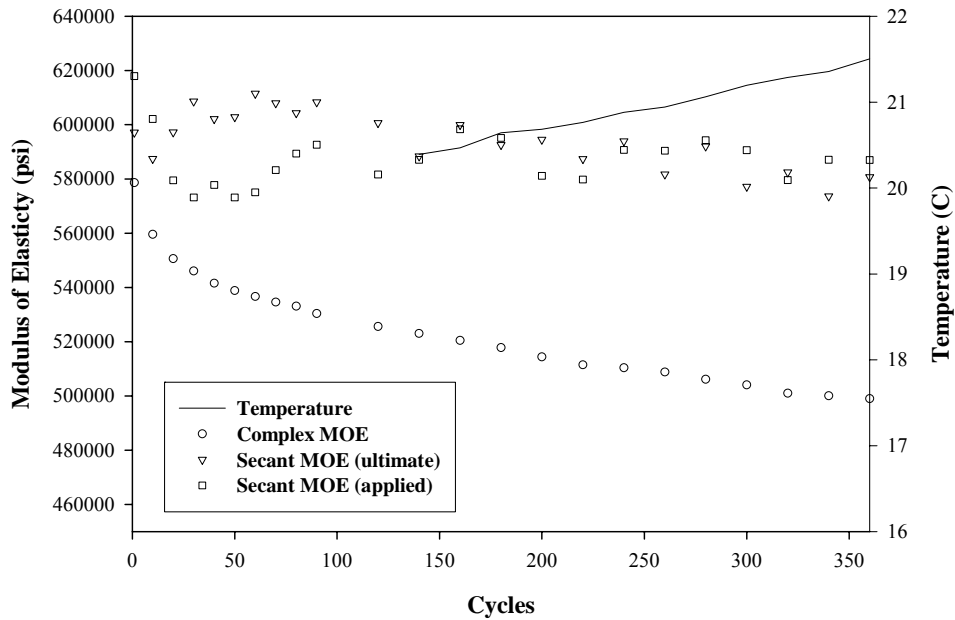**Fig. G.12**. PP-MAPP modulus of elasticity and temperature plot at 75%, 10.4-Hz, R = 0.21, N = 385, and 0.95% strain at failure

Fig. G.13. PP-MAPP modulus of elasticity and temperature plot at 75%, 10.4-Hz, R = 0.21, N = 1.054, and 1.06% strain at failure

Fig. G.14. PP-MAPP modulus of elasticity and temperature plot at 81%, 10.4-Hz, R = 0.19, N = 261, and 1.10% strain at failure

116

Fig. G.15. PP-MAPP modulus of elasticity and temperature plot at 80%, 10.4-Hz, R = 0.21, N = 200, and 1.00% strain at failure

Fig. G.16. PP-MAPP modulus of elasticity and temperature plot at 60%, 5.2-Hz, R = 0.11, N = 11,352, and 0.94% strain at failure
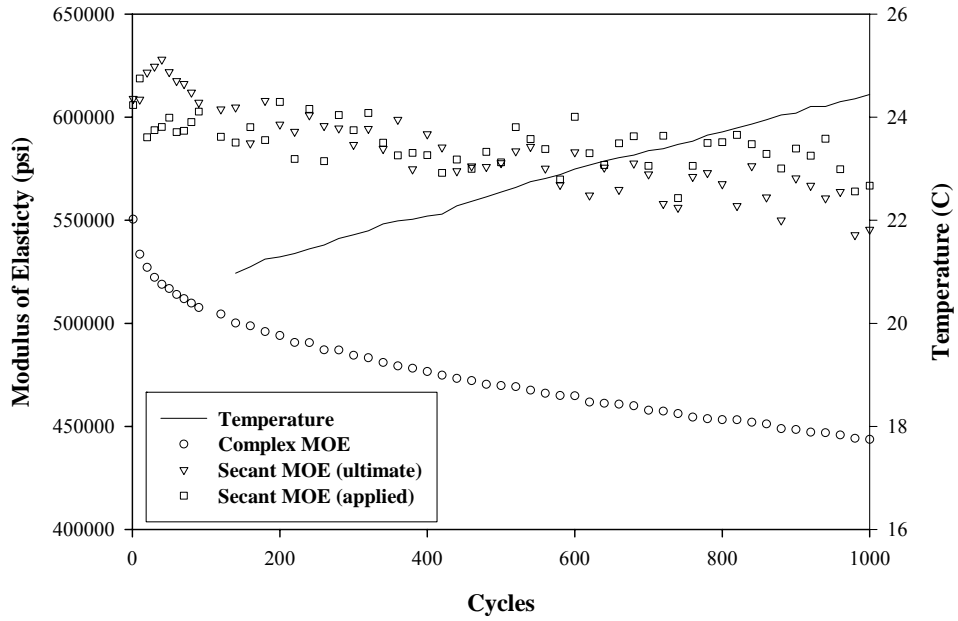
117

Fig. G.17. PP-MAPP modulus of elasticity and temperature plot at 61%, 5.2-Hz, R = 0.10, N = 11,356, and 0.93% strain at failure

Fig. G.18. PP-MAPP modulus of elasticity and temperature plot at 62%, 5.2-Hz, R = 0.10, N = 17,162, and 1.03% strain at failure

Fig. G.19. PP-MAPP modulus of elasticity and temperature plot at 62%, 1.04-Hz, R = 0.07, N = 9,412, and 1.09% strain at failure
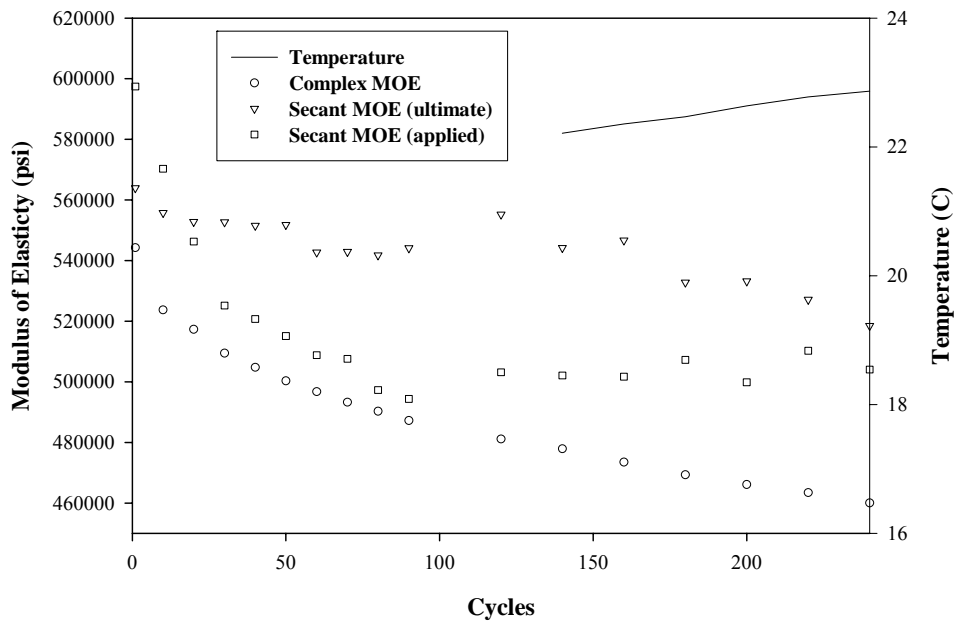

Fig. G.20. PP-MAPP modulus of elasticity and temperature plot at 59%, 1.04-Hz, R = 0.08, N = 6,390, and 0.93% strain at failure

Fig. G.21. PP-MAPP modulus of elasticity and temperature plot at 62%, 1.04-Hz, R = 0.07, N = 7,351, and 1.01% strain at failure
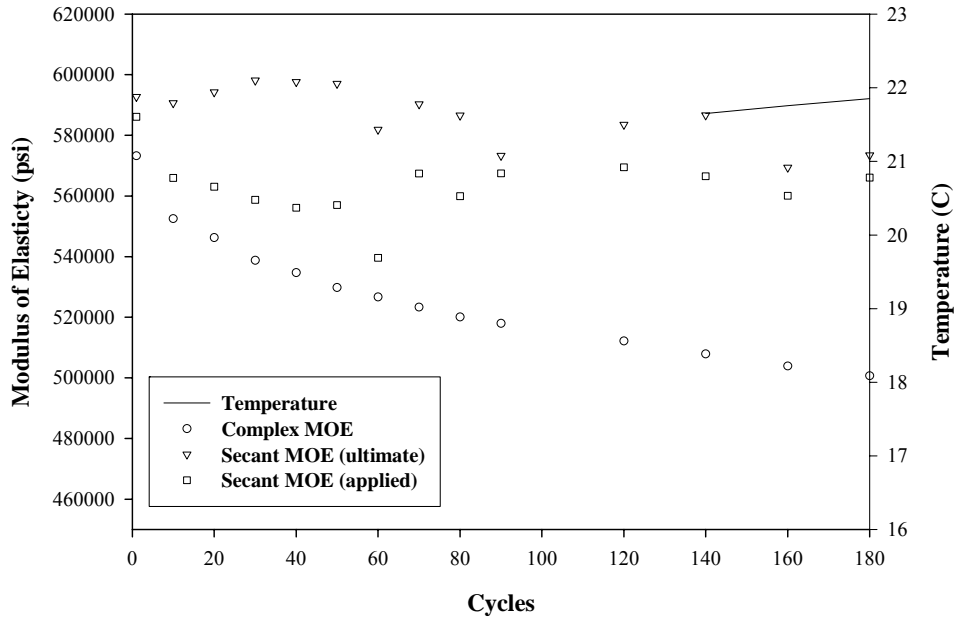

Fig. G.22. PP modulus of elasticity and temperature plot at 44%, 10.4-Hz, R = 0.27, and N = 3,421,837 (test stopped)

Fig. G.23. PP modulus of elasticity and temperature plot at 45%, 10.4-Hz,
R = 0.24, N = 658,907, and 1.27% strain at failure

Fig. G.24. PP modulus of elasticity and temperature plot at 45%, 10.4-Hz,
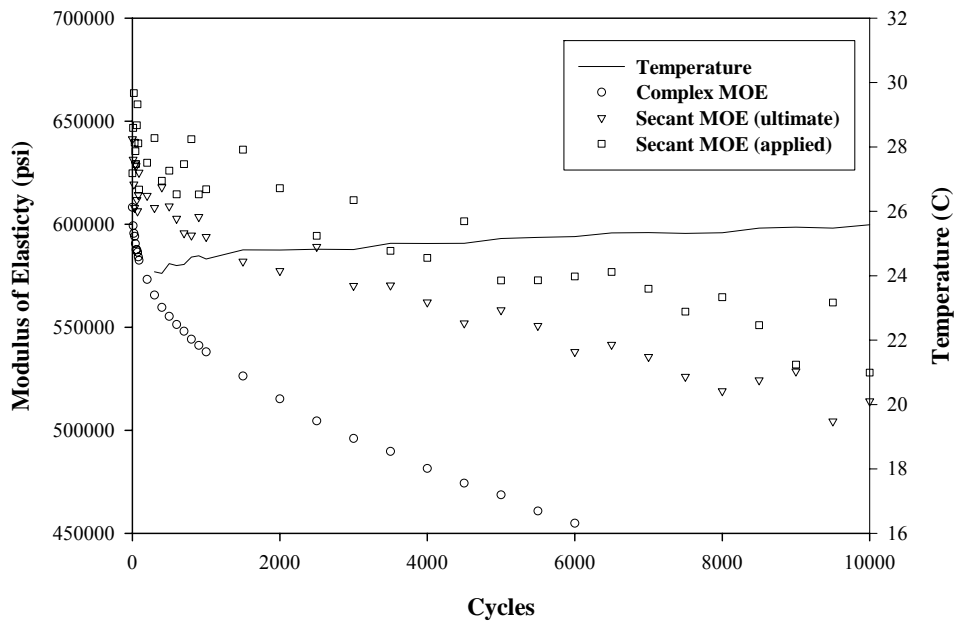R = 0.23, N = 802,049, and 1.19% strain at failure

Fig. G.25. PP modulus of elasticity and temperature plot at 51%, 10.4-Hz, R = 0.26, N = 152,494, and 1.35% strain at failure
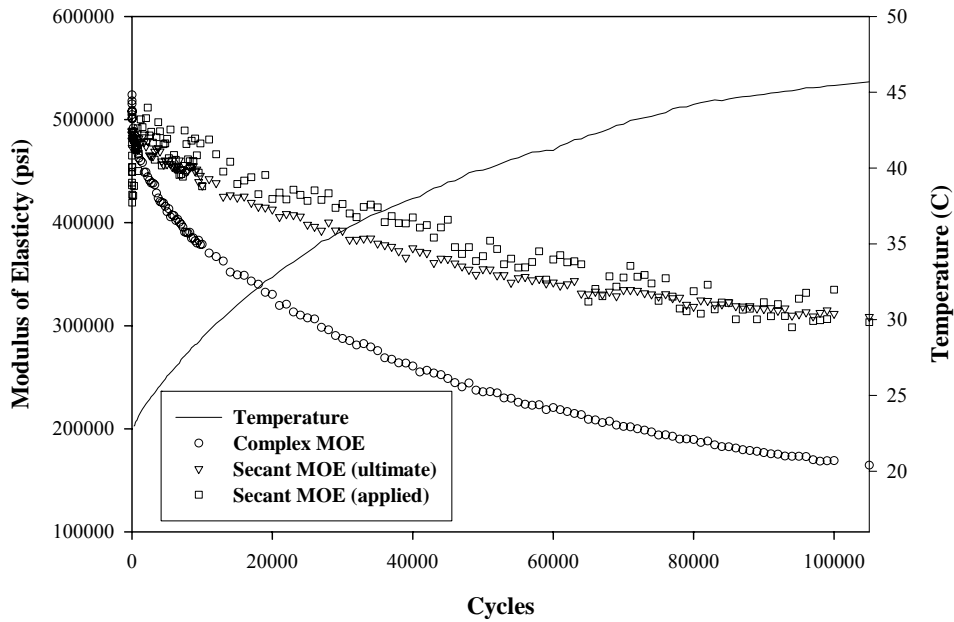
Fig. G.26. PP modulus of elasticity and temperature plot at 49%, 10.4-Hz, R = 0.24, N = 109,113, and 1.31% strain at failure
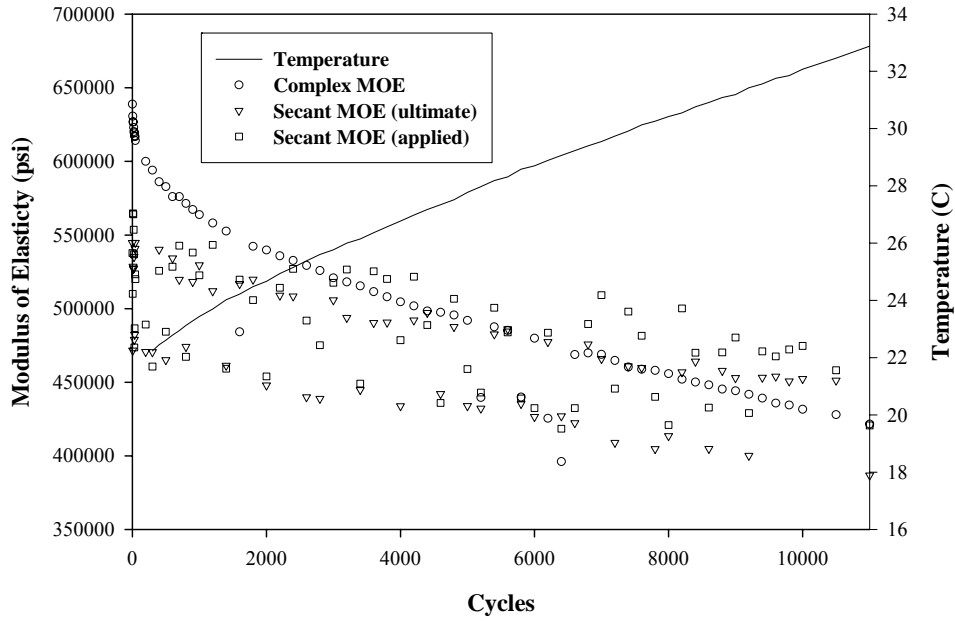
122
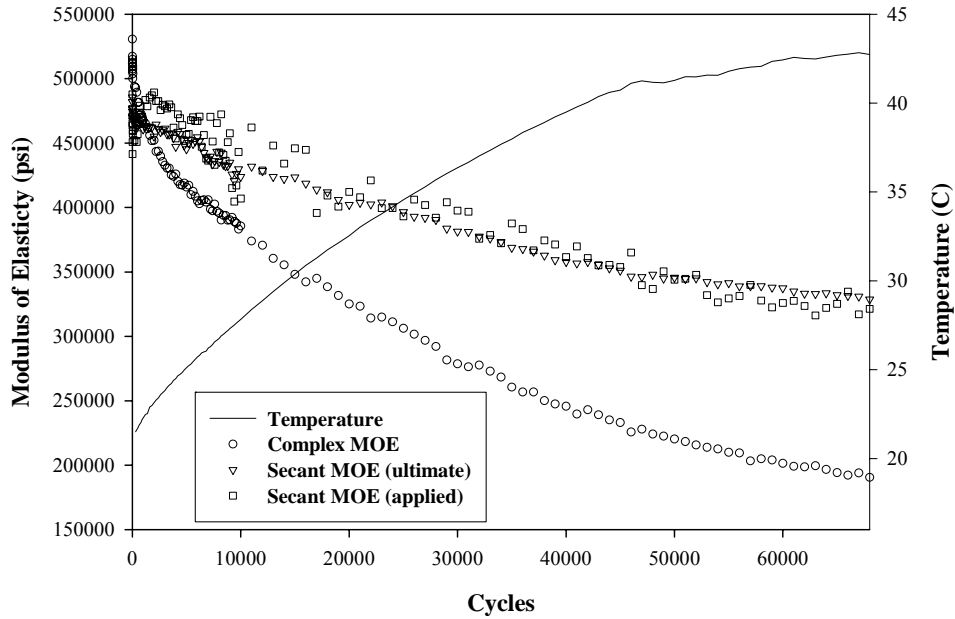
Fig. G.27. PP modulus of elasticity and temperature plot at 55%, 10.4-Hz, R = 0.23, N = 68,797, and 1.28% strain at failure
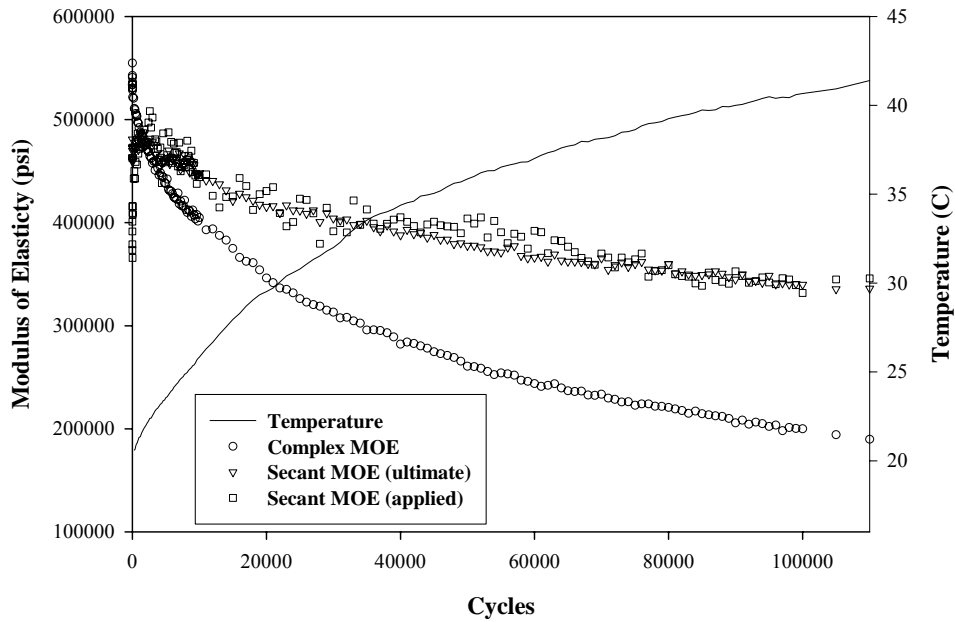
Fig. G.28. PP modulus of elasticity and temperature plot at 55%, 10.4-Hz, R = 0.22, N = 112,451, and 1.30% strain at failure
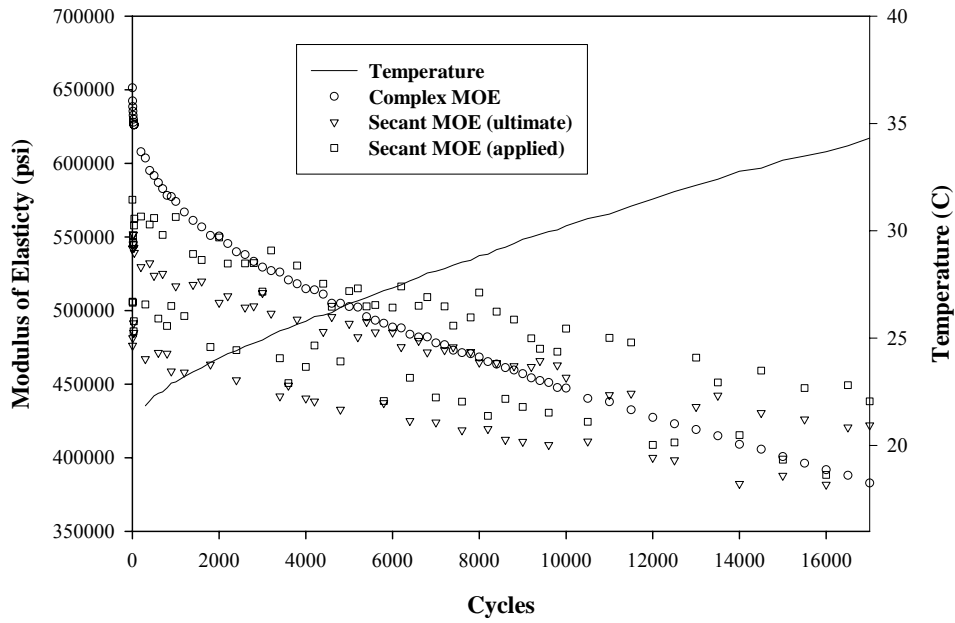
123
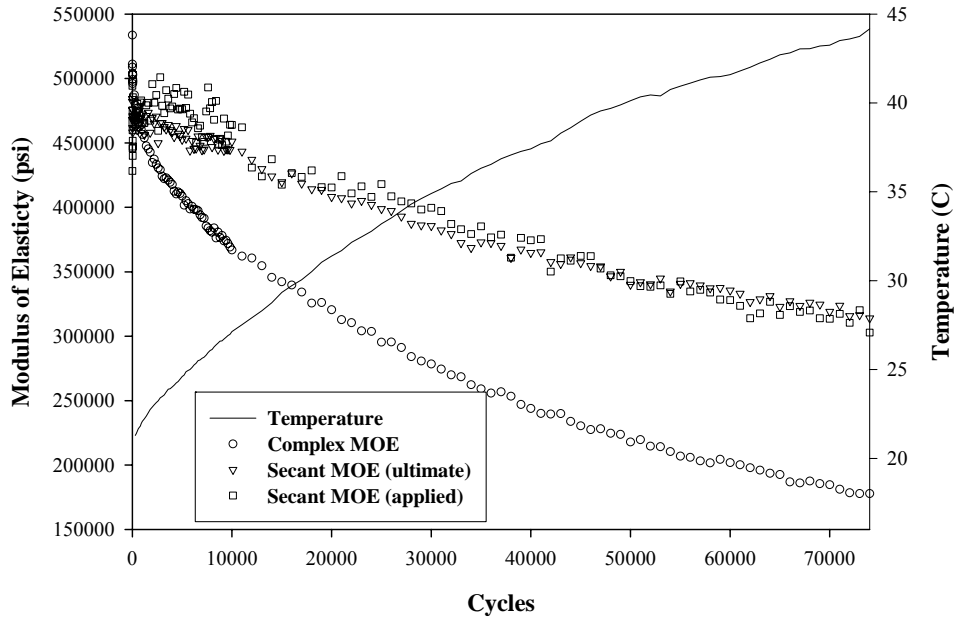
Fig. G.29. PP modulus of elasticity and temperature plot at 55%, 10.4-Hz, R = 0.23, N = 74,970, and 1.37% strain at failure
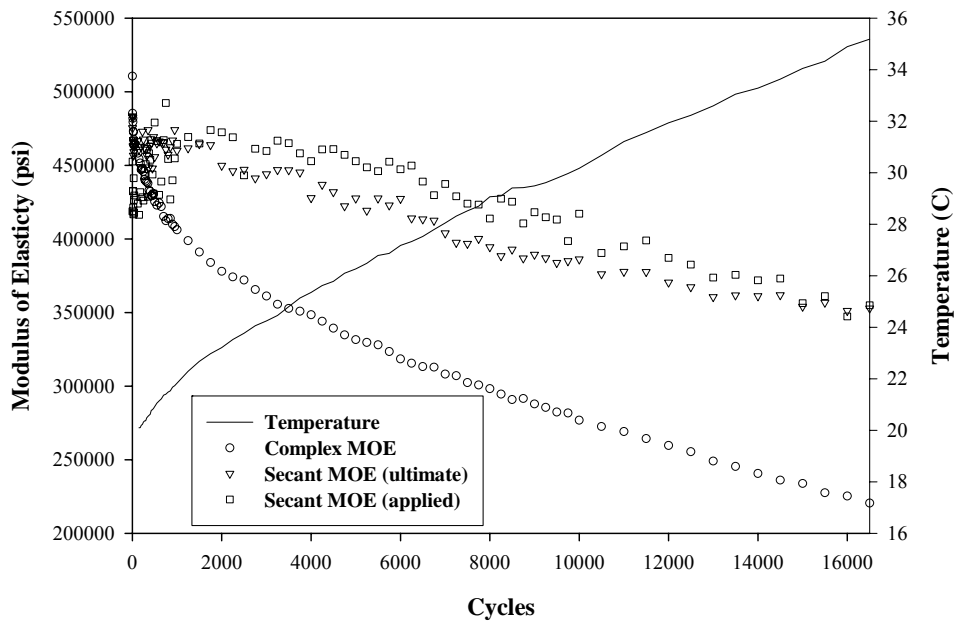
Fig. G.30. PP modulus of elasticity and temperature plot at 63%, 10.4-Hz, R = 0.23, N = 16,712, and 1.27% strain at failure
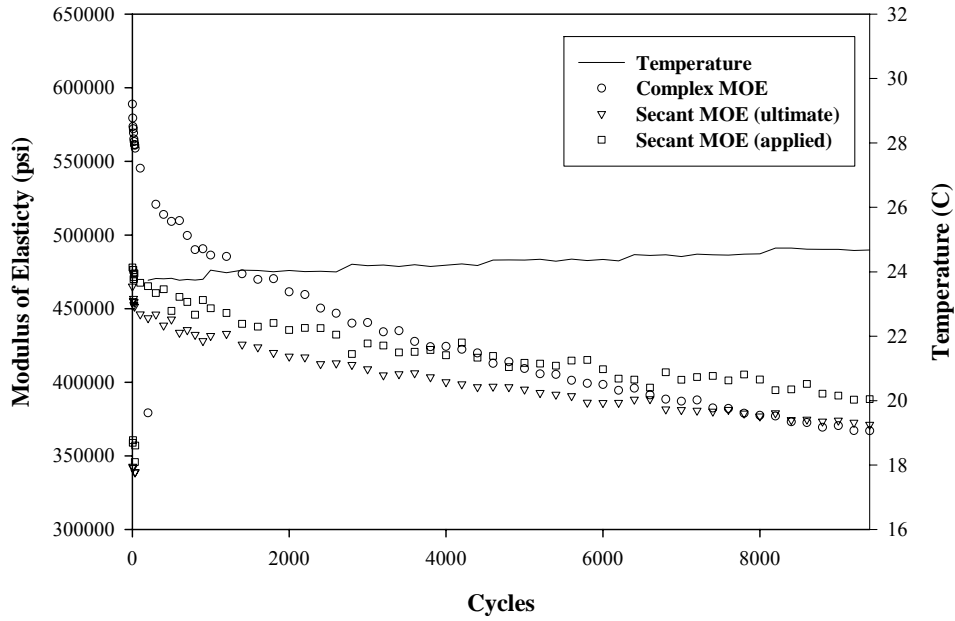
124
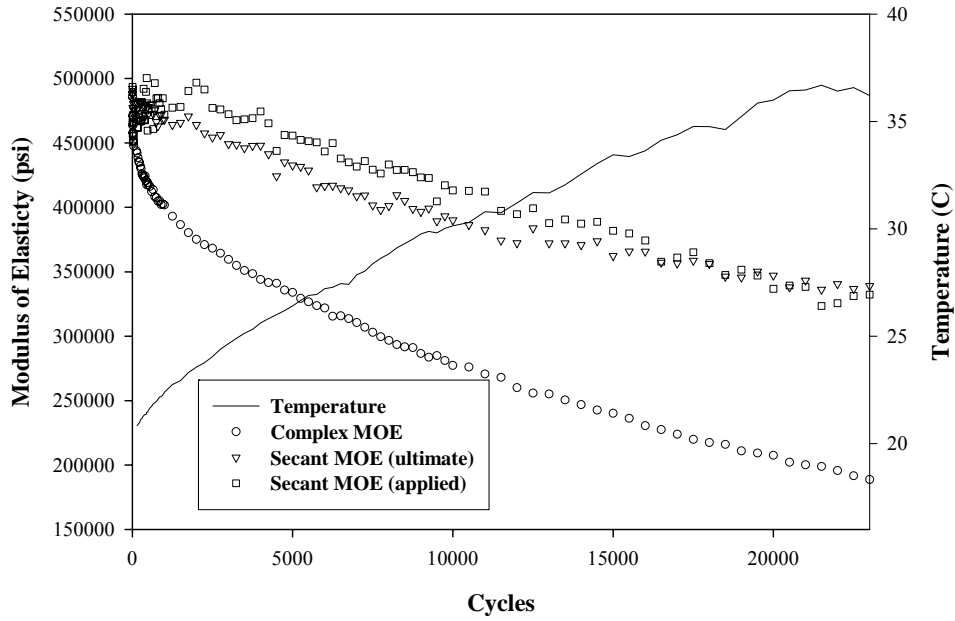
Fig. G.31. PP modulus of elasticity and temperature plot at 63%, 10.4-Hz, R = 0.24, N = 23,220, and 1.47% strain at failure
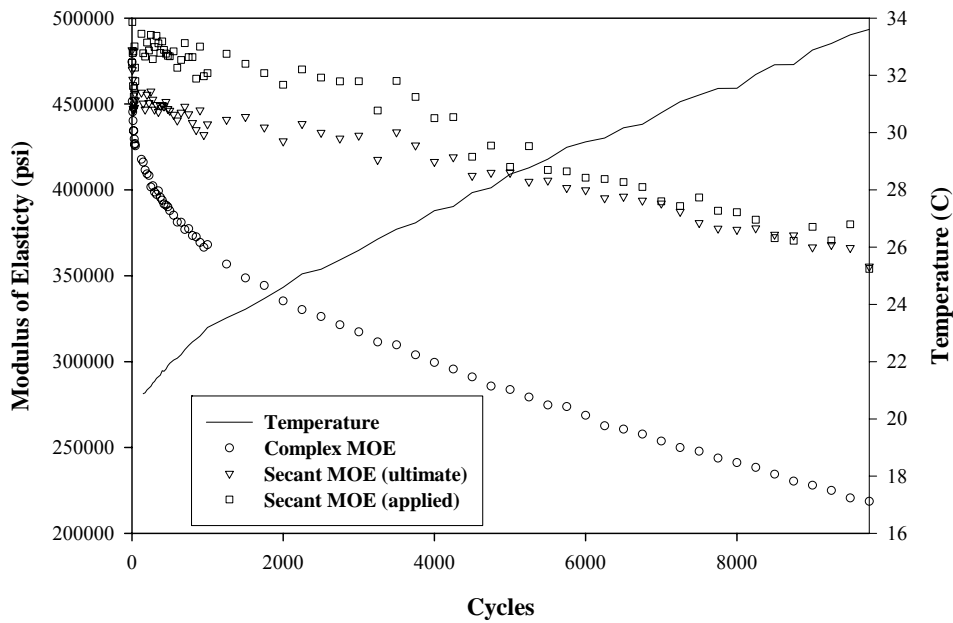
Fig. G.32. PP modulus of elasticity and temperature plot at 67%, 10.4-Hz, R = 0.25, N = 9,943, and 1.36% strain at failure
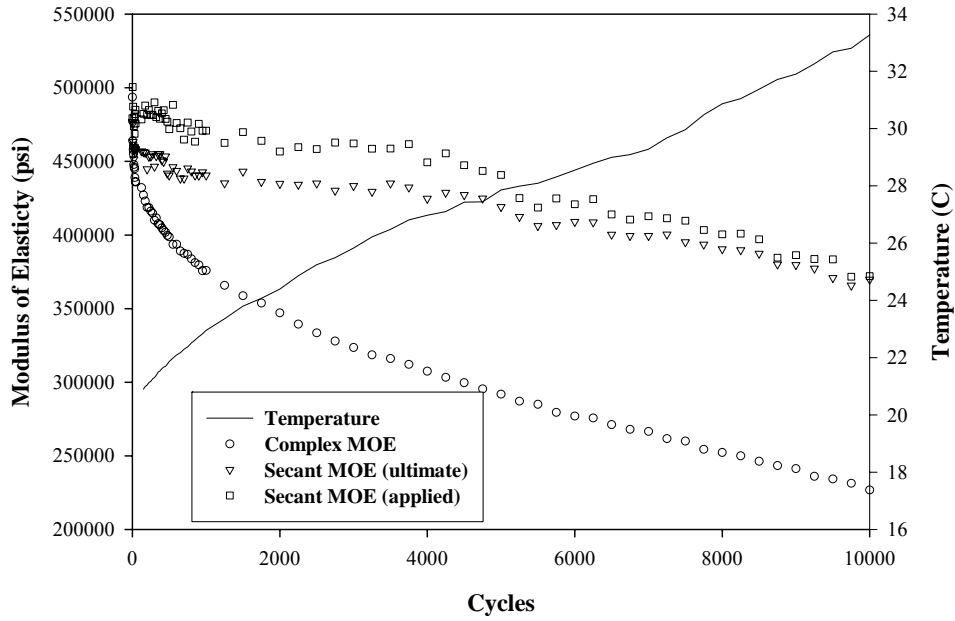
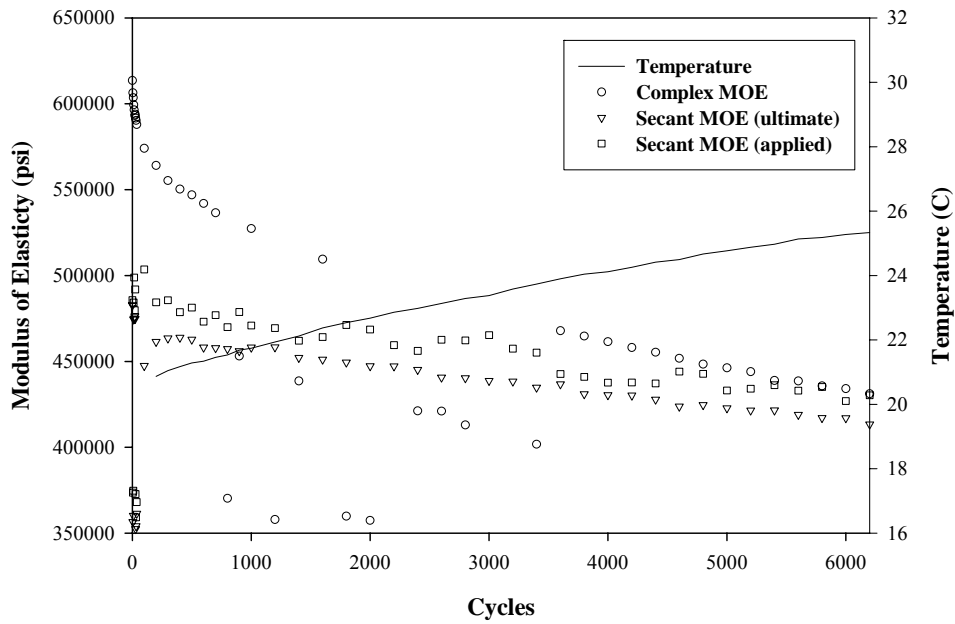**Fig. G.33**. PP modulus of elasticity and temperature plot at 67%, 10.4-Hz, R = 0.26, N = 10,031, and 1.30% strain at failure
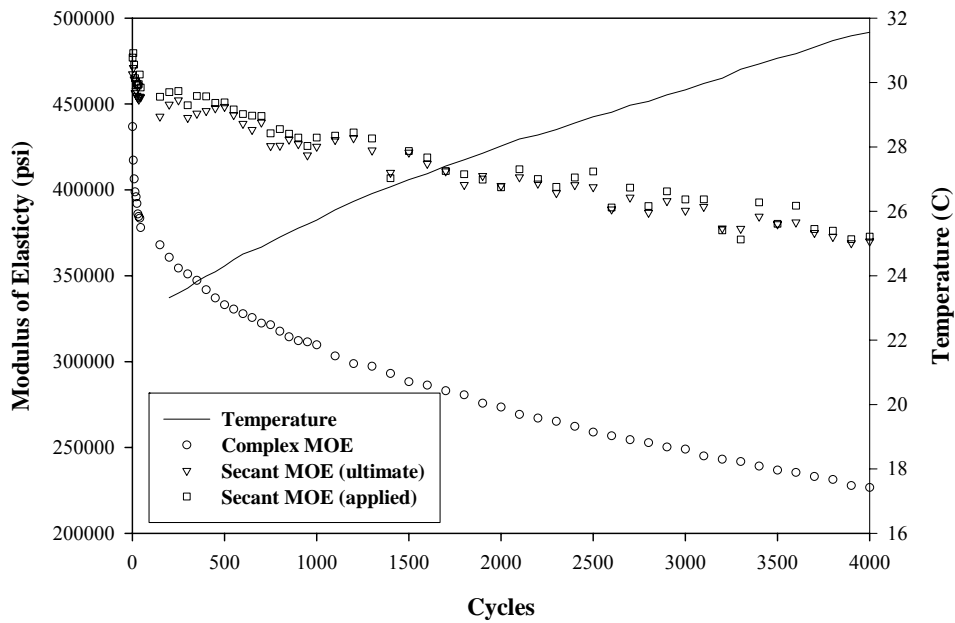
Fig. G.34. PP modulus of elasticity and temperature plot at 69%, 10.4-Hz, R = 0.30, N = 4,105, and 1.38% strain at failure
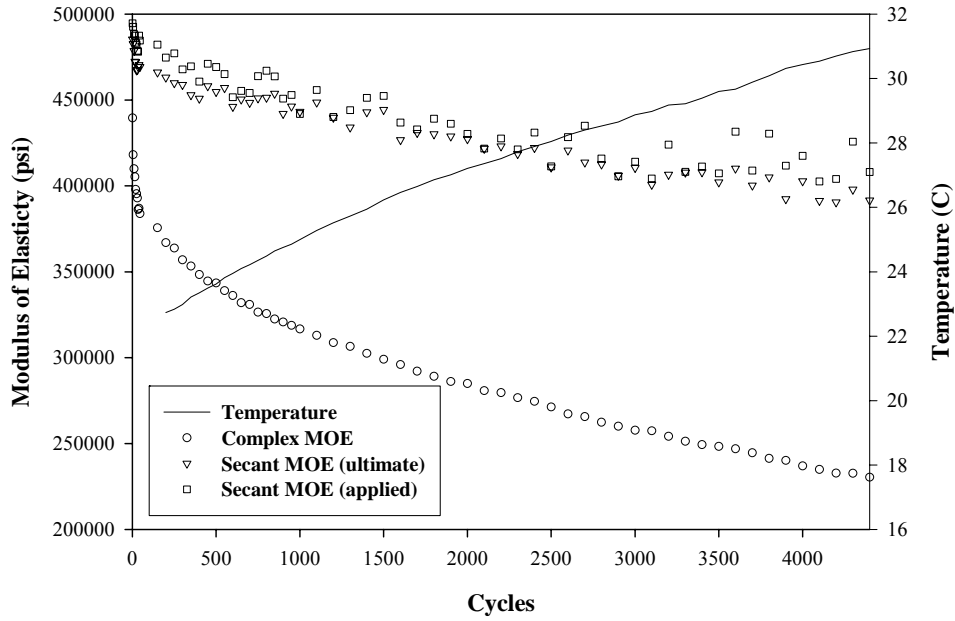
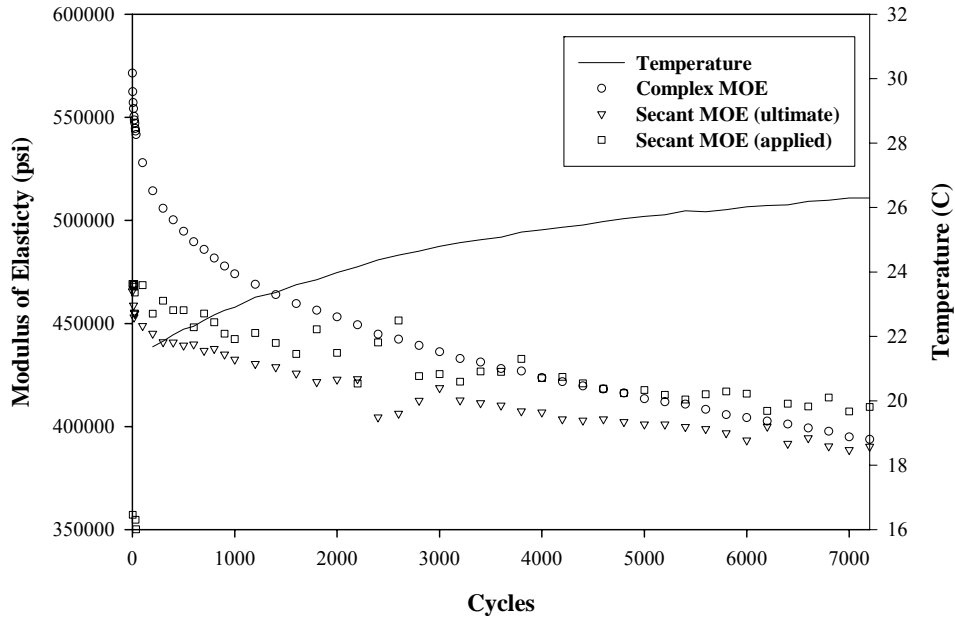**Fig. G.35**. PP modulus of elasticity and temperature plot at 69%, 10.4-Hz, R = 0.30, N = 4,435, and 1.36% strain at failure
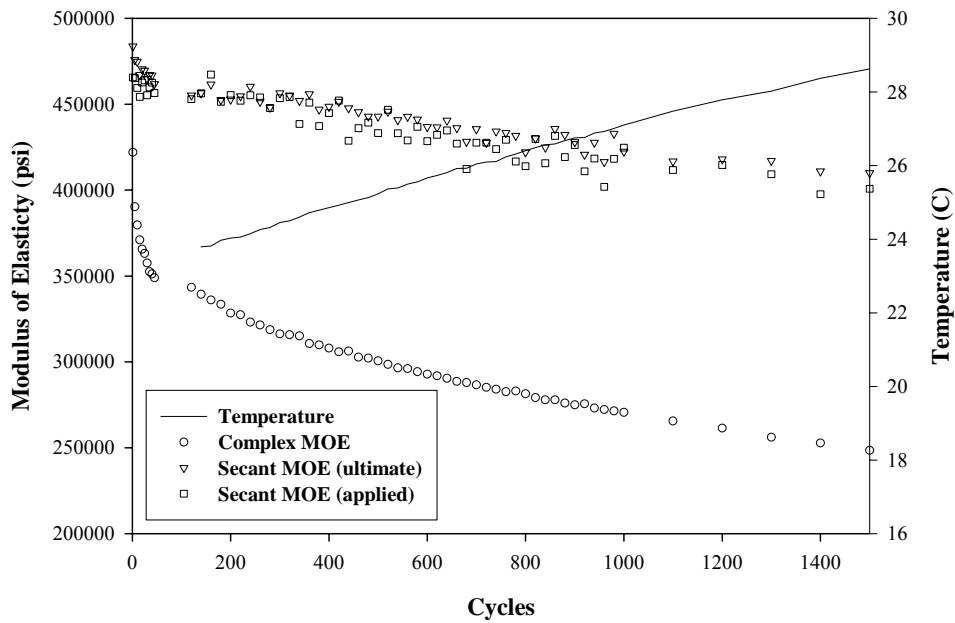
Fig. G.36. PP modulus of elasticity and temperature plot at 73%, 10.4-Hz, R = 0.28, N = 1,583, and 1.36% strain at failure
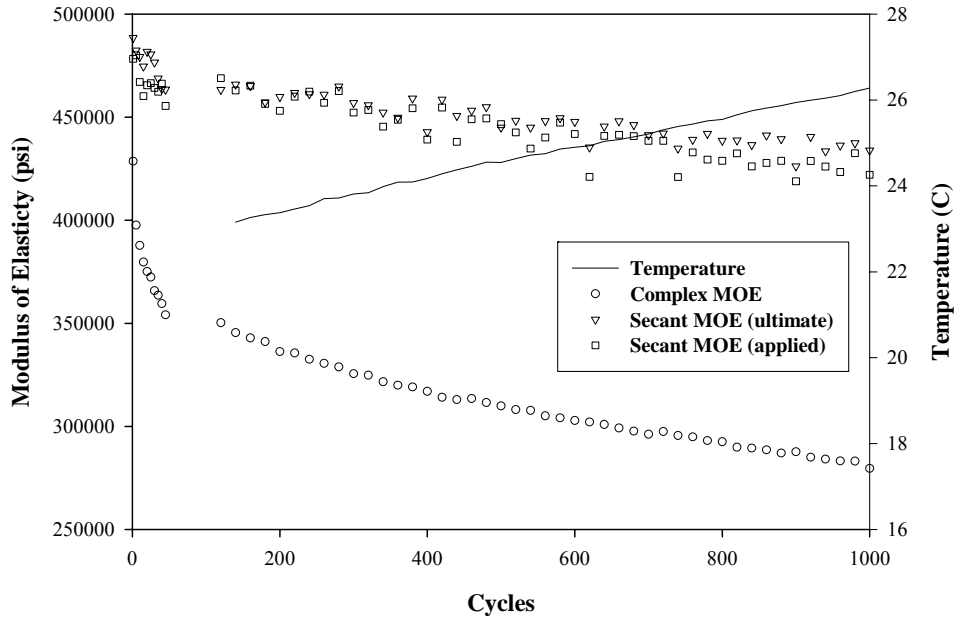
Fig. G.37. PP modulus of elasticity and temperature plot at 73%, 10.4-Hz, R = 0.30, N = 1,012, and 1.20% strain at failure
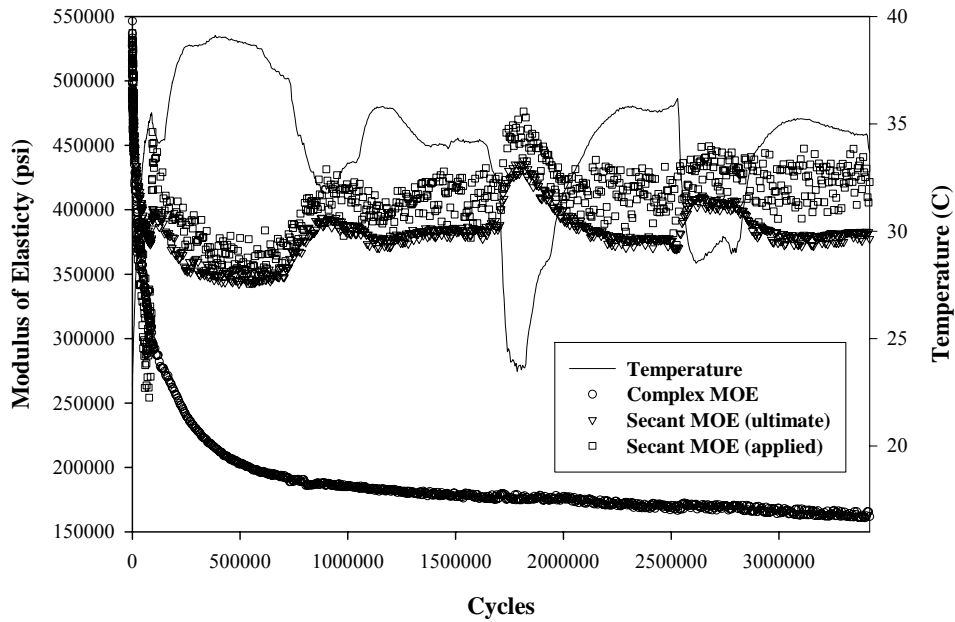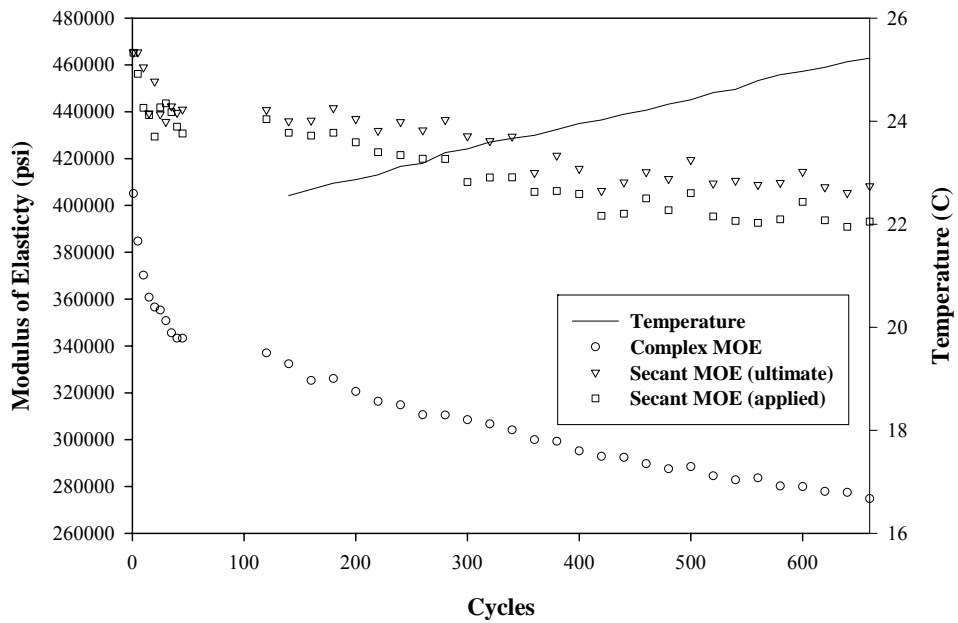

Fig. G.38. PP modulus of elasticity and temperature plot at 77%, 10.4-Hz, R = 0.29, N = 340, and 1.22% strain at failure
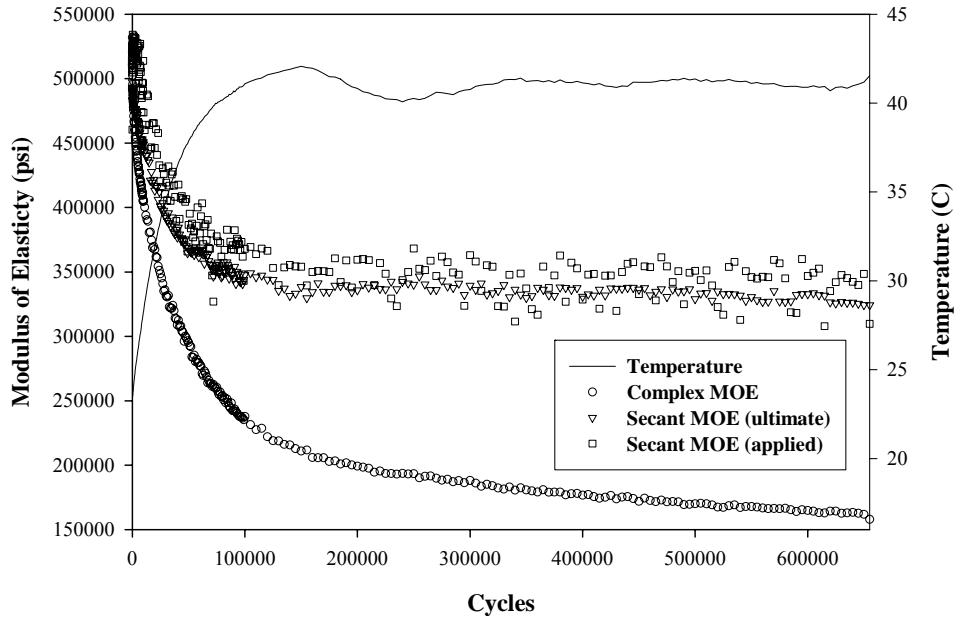
128
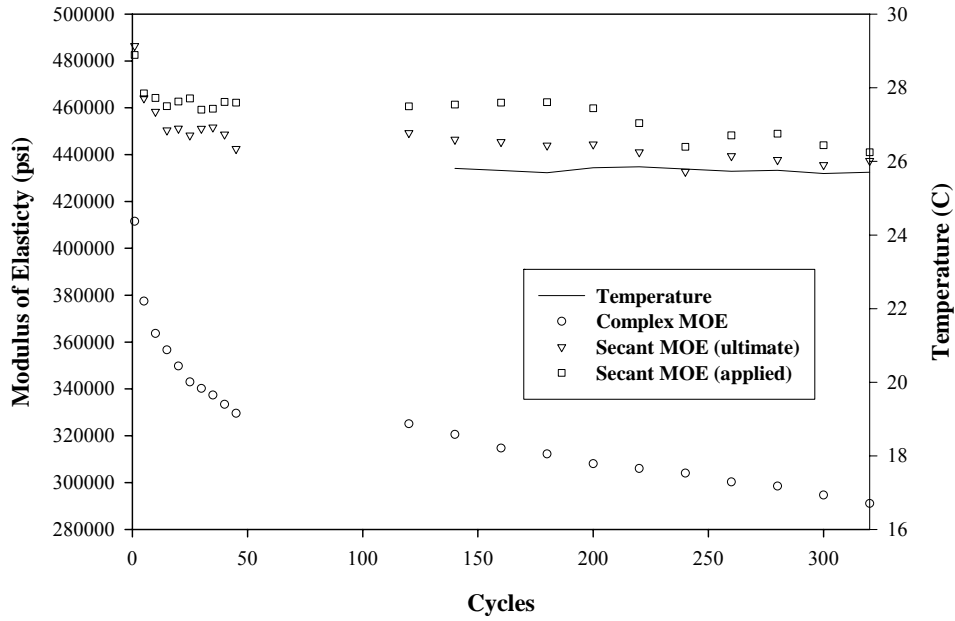
Fig. G.39. PP modulus of elasticity and temperature plot at 78%, 10.4-Hz, R = 0.29, N = 674, and 1.30% strain at failure
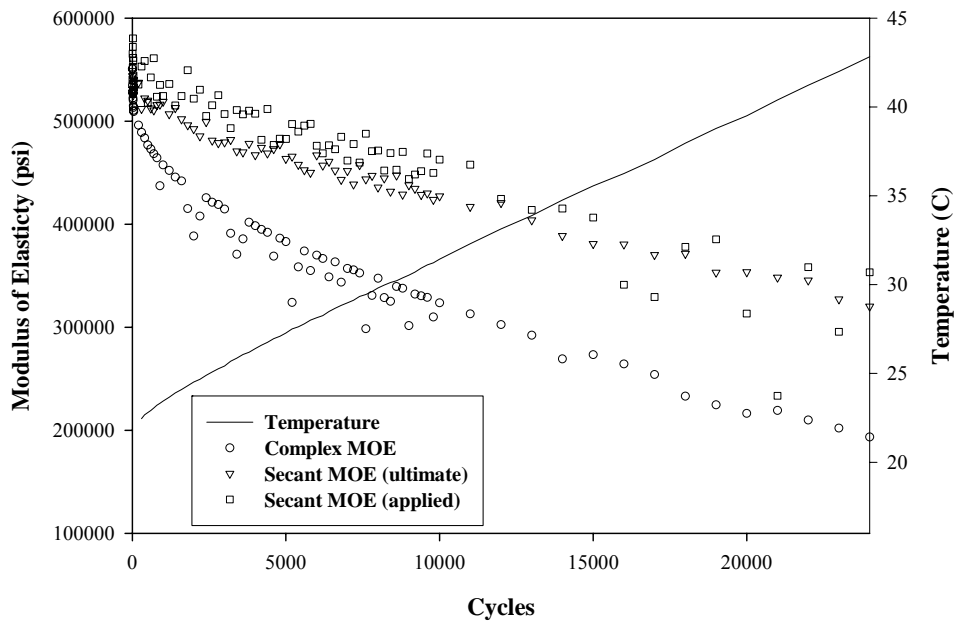
Fig. G.40. PP modulus of elasticity and temperature plot at 59%, 5.2-Hz, R = 0.11, N = 24,138, and 1.42% strain at failure
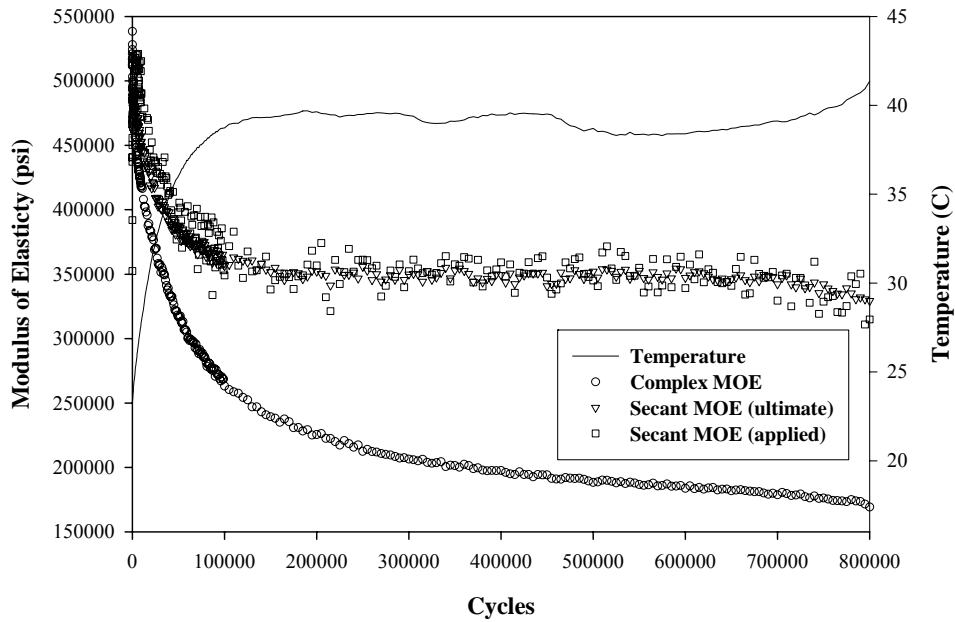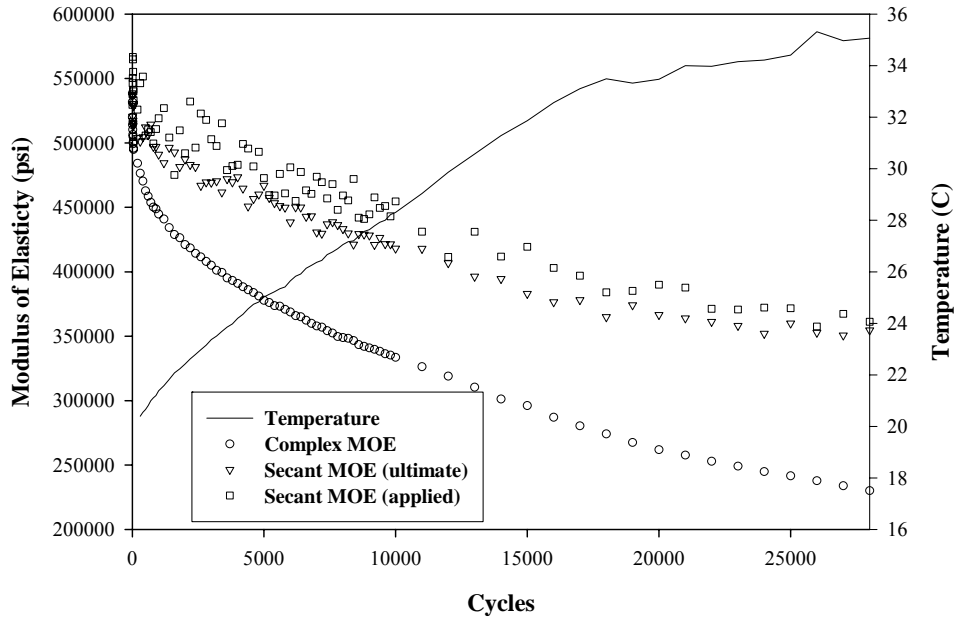
Fig. G.41. PP modulus of elasticity and temperature plot at 60%, 5.2-Hz, R = 0.11, N = 20,009, and 1.20% strain at failure
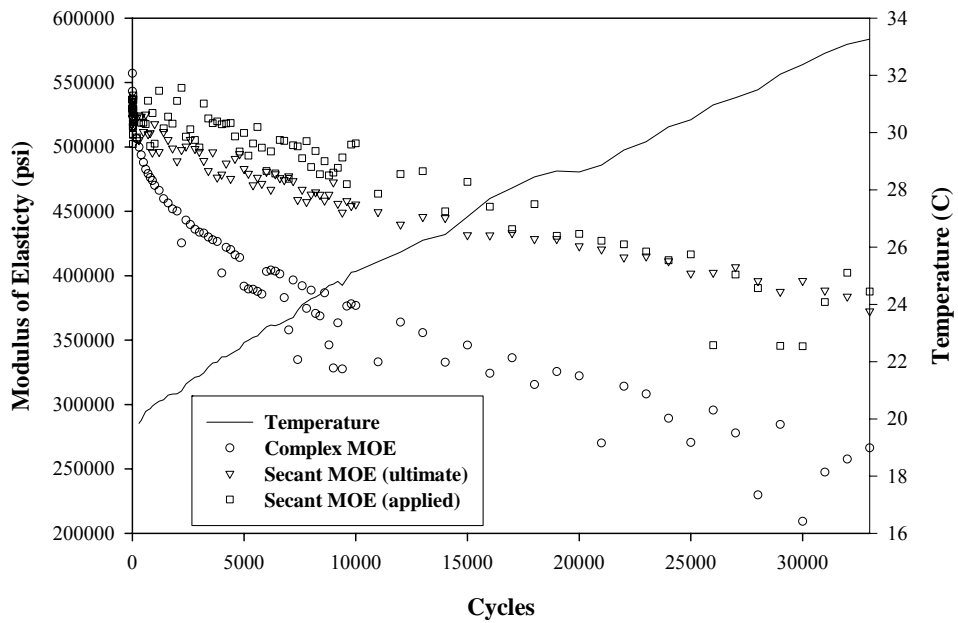
Fig. G.42. PP modulus of elasticity and temperature plot at 59%, 5.2-Hz, R = 0.10, N = 33,887, and 1.05% strain at failure
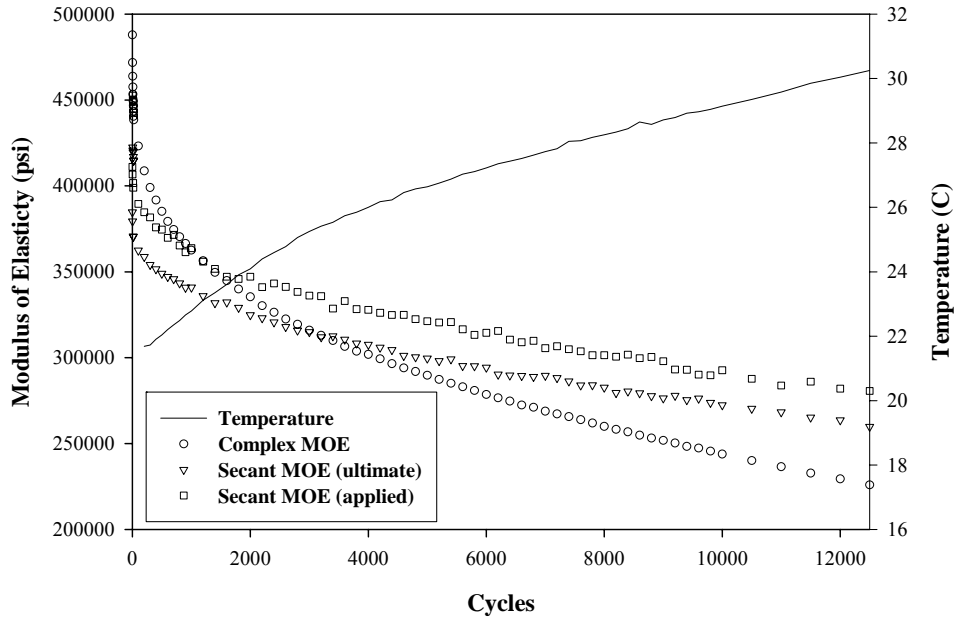
Fig. G.43. PP modulus of elasticity and temperature plot at 62%, 1.04-Hz, R = 0.06, N = 12,916, and 1.27% strain at failure
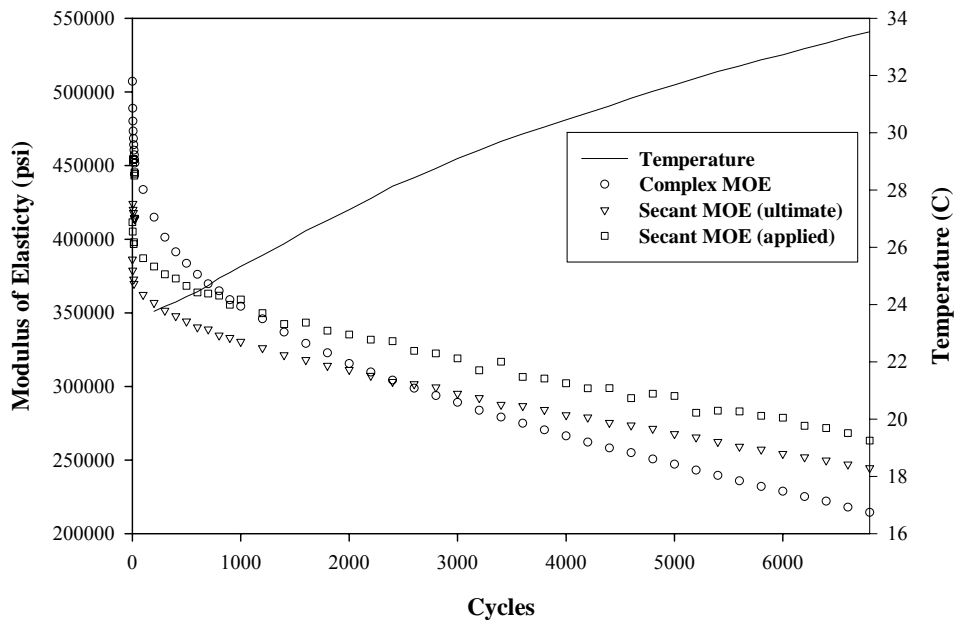
Fig. G.44. PP modulus of elasticity and temperature plot at 62%, 1.04-Hz, R = 0.07, N = 6,862, and 1.36% strain at failure
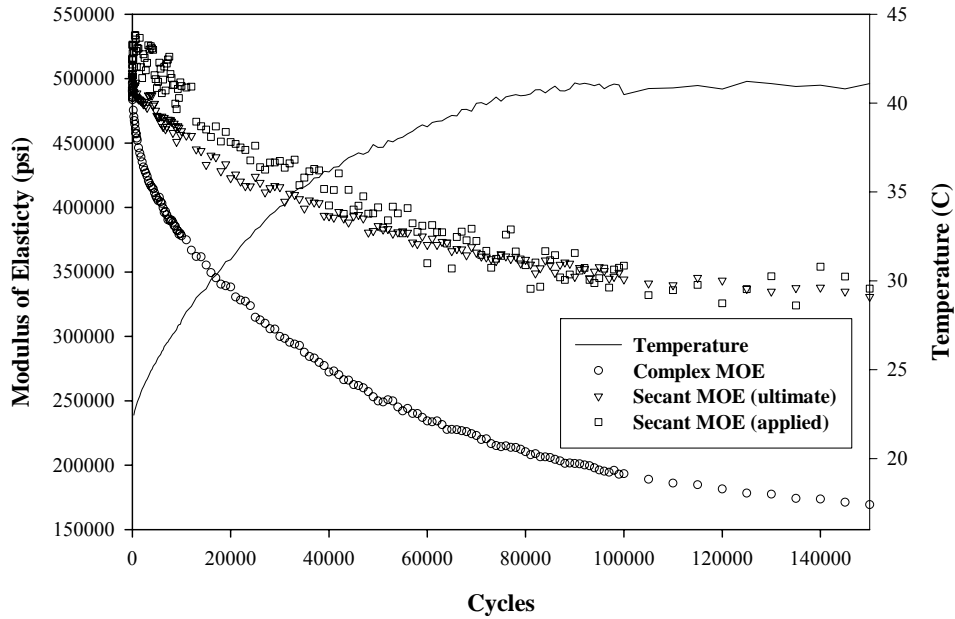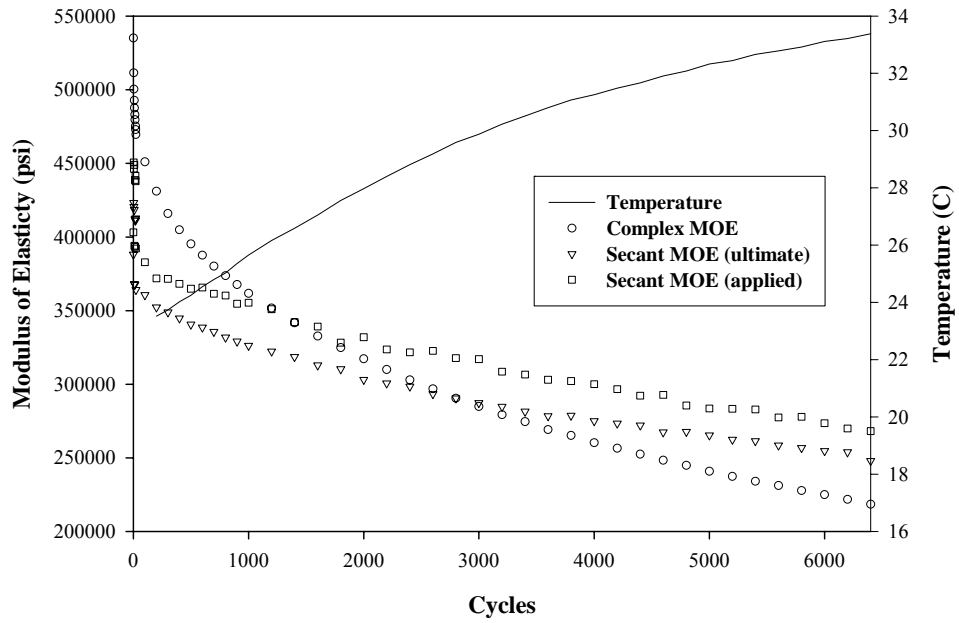
Fig. G.45. PP modulus of elasticity and temperature plot at 62%, 1.04-Hz, R = 0.06, N = 6,457, and 1.35% strain at failure

G.6 FORTRAN Source Code

```fortran
C=================================================================
      PROGRAM Analysis
      IMPLICIT double PRECISION (a-h,o-z)
      INTEGER i,j,k,l,m,n
      DIMENSION X(5000,2,10001),cyclecount(999),temp(4,999) !input
files

c Per data block variables
      COMMON iii,idatapts
      DIMENSION Pmax(50,2),Pmin(50,2),Dmax(50,2),Dmin(50,2)  !Max and
mins

c Temporay variables:
      DIMENSION Pmaxtemp(50),Pmintemp(50),Dmaxtemp(50),Dmintemp(50)
c
c Desired output variables:
      CHARACTER time(999)*11
c
c-----------------------------------------------------------------
c INPUT VALUES:
c     X(500,2,501) - Load(:,1,:) and Displacement(:,2:,) for index
(i,:,:)
c                         - (:,:,x) is data
c     temp = temperature at each index (4-across)
c
c CALCULATION VARIABLES:
c     Pmax,Pmin,Dmax,Dmin = Max and Min of load/disp, (value,location)
c
c-----------------------------------------------------------------
c OPEN STATEMENT IDENTIFERS
      iin=10          !load displacement data
      icycle=13 !cycle counts
      itemp=14   !temperature data
c
      ioutput=100


C=============================================
c INPUT
c---------------------------------------------
c Test Data:
      span=16                        !Beam span,in
c
      ult=2073.8   !Ulitmite static load,lbf
c
c
      idatapts=500          !number of points in a read block
      scan=250              !scans frequency
      freq=5                !Nominal test frequency
      test=0.60             !Decimal value of percent of ultimate
loading
c
      zeropt=0.247   !Actuator position with zero load-->zero
displacement
      ambient=26.1   !initial temperature in degrees C
c

      R=0.1
      depth=0.986          !depth of specimen,in    A=0.986, B=0.997
      xMOI=0.420           !Moment of intertia,in4  A=0.420, B=0.436
c
c
c
c OPEN INPUT FILES(iin is the data, iout is file)
      OPEN (unit=13,file='cyclecount.txt', status='old',    !cycle
count
```

```
       +form='formatted')

       OPEN (unit=10,file='A11_60_5Hz',status='old',              !Input
file
       +form='formatted')

       OPEN (unit=14,file='A11_60_5Hztemp', status='old',
       +form='formatted')
c
c OPEN OUTPUT FILES
       OPEN (unit=100,file='Yup.txt',status='unknown',
       +form='formatted')
c
c WRITE TITLES
       WRITE (ioutput,1100)'Cycle','Time','Top','Bottom','Temp(C)',
       +'Freq(Hz)','R-ratio','Phase','LoadMax',
       +'LoadMin','CHMax','CHMin','StrsMax',
       +'StrsMin','StrnMax','StrnMin','Eloss','Estor','Ecomp',
       +'Eult','Eapp','Dcomp','Dult','Dapp','Dstor','DispSpn',
       +'rate(in/min)','Dispmax','Dispmin'

1100   FORMAT(a7,',',a13,',',a6,',',a6,',',a8,',',a8,',',a6,',',a6,',',
       +a6,',',a6,',',a7,',',a7,',',a6,',',a6,',',a7,',',a7,',',
       +a5,',',a5,',',a9,',',a9,',',a9,',',a7,',',a7,',',a7,',',a12,
       +',',a8,',',a8,',',a8,',',a8)
c
c
C========================================================
c ANALYSIS
C--------------------------------------------------------
c
       setpt=(test*ult-R*test*ult)/2+R*test*ult   !The test setpoint
       app=ult*test                                            !applied
max load
       zero=zeropt - 0.0474                            !adjust for F-
zero
c
c
cREAD the data using subroutine
       CALL readdata(X,cyclecount,temp,time,iin,icycle,itemp,scan,
       +freq,zero,iblocks,idatapts)
c
c
c CYCLE THROUGH EACH READ GROUP
       DO iii=1,iblocks
c
       break=1.0+zero
       DO mk=1,idatapts    !Check for end of file, if specimen broke in
read
       IF(X(iii,2,mk).EQ.break)GOTO 55
       ENDDO
c
c
c Find Max and Min of Load
       CALL maxmin(X,Pmax,Pmin,iii,freq,scan,1,setpt,imax,imin,idatapts)
c
       IF(imax.LT.3.OR.imin.LT.3)GOTO 50 !Not enough data to continue
c
c Find Max and Min of Displacment
       CALL displacmentmaxmin(X,Dmax,Dmin,iii,freq,scan,imaxd,imind,
       +idatapts)
       !imaxd-count for disp max, assumed equal imax (dummy argument)
       !imind-""
c
```

135

```
c Calculate the actual frequency of test using maximum load
c
      CALL actualfrequency(Pmax,scan,xblockfreq,imax)
      pi=3.1415926535898
      angularfreq=2*pi*xblockfreq
c
c Calculate the average phase shift between load and disp plots
      CALL averagephaseshift(X,angularfreq,AvgPhase,scan,idatapts,
     +xblockfreq,iii)
c
c Calculate the slope of the load deflection data
c     -note that the third point deflectoin is used
c     -the slope will be used for calculating the secant modulus
c
      CALL avgslope(X,Pmin,ult,ultslope,iii,imin)


      CALL avgslope(X,Pmin,app,appslope,iii,imin)
c
c Find average min max crosshead and loads
      DO j=1,imax
      Dmaxtemp(j)=Dmax(j,1)
      Pmaxtemp(j)=Pmax(j,1)
      ENDDO
      DO j=1,imin
      Dmintemp(j)=Dmin(j,1)
      Pmintemp(j)=Pmin(j,1)
      ENDDO
c
      CALL average(Crossheadmax,Dmaxtemp,-1,imax)
      CALL average(Crossheadmin,Dmintemp,-1,imin)
      CALL average(xLoadmax,Pmaxtemp,-1,imax)
      CALL average(xLoadmin,Pmintemp,-1,imin)
c
c Calculate the actual R-ratio
      Rratio=xLoadmin/xLoadmax
c
c Determine centerpoint deflection,stress, strain,MOE's,and damage
c
      CALL centerdefl(xLoadmax,xLoadmin,Crossheadmax,Crossheadmin,
     +xdispmax,xdispmin,ultslope)
c
      CALL stressstrain(xLoadmax,xLoadmin,crossheadmax,crossheadmin,
     +stressmax,stressmin,strainmax,strainmin,xMOI,depth,span)
c
      CALL
MOE(stressmax,strainmax,appslope,ultslope,span,xMOI,avgphase,
     +Ecomplex,Esecantult,Esecantapp,Estorage,Eloss)
c
      CALL Damage(Ecomplex,Esecantult,Esecantapp,Estorage,
     +Damagec,Damageult,Damageapp,Dstor,iii)
c
c Find displacement span and loading rate
      dispspan=CHmax-CHmin
      rate=dispspan/(1/(2*xblockfreq))*60  !in/min
c
c Find the average temperature
      IF(iii.EQ.1) GOTO 440
      GOTO 450
c
440   totaltemp=ambient !uses the measured intial test as first
temperature
      top=ambient
      bot=ambient
```

```fortran
        GOTO 60
c
450     totaltemp=(temp(1,iii)+temp(2,iii)+temp(3,iii)+temp(4,iii))/4
        top=(temp(1,iii)+temp(2,iii))/2
        bot=(temp(3,iii)+temp(4,iii))/2
        GOTO 60
c
50      time(iii)='NoData'

60      CONTINUE
c Write the data:
        WRITE(ioutput,2100) cyclecount(iii),time(iii),top,bot,totaltemp,
     +xblockfreq,Rratio,avgphase,xloadmax,xloadmin,crossheadmax,
     +crossheadmin,stressmax,stressmin,strainmax*100,strainmin*100,
     +Eloss,Estorage,Ecomplex,Esecantult,Esecantapp,Damagec,Damageult,
     +Damageapp,Dstor,dispspan,rate,xdispmax,xdispmin

2100    FORMAT(F8.0,',',a13,',',F6.3,',',F6.3,',',F6.3,',',F6.3,',',F6.4,
     +',',F6.4,',',F7.2,',',F7.2,',',F6.4,',',F6.4,',',F7.2,',',F7.2,
     +',',F6.4,',',F6.4,',',F9.0,',',F9.0,',',F9.0,',',F9.0,',',F9.0,
     +',',F7.5,',',F7.5,',',F7.5,',',F7.5,',',F7.4,',',F9.4,',',F9.4,
     +',',F9.4)


        ENDDO
        GOTO 65
c
55      time(iii)='Broken'        !shows that piece is broken
        WRITE(ioutput,2200) time(iii)
2200    FORMAT(',',a13)
c
65      CONTINUE
        END
c
c*********************************************************************
        SUBROUTINE Damage(Ec,Eu,Ea,Es,Dc,Du,Da,Ds,iii)
        IMPLICIT double PRECISION (a-h,o-z)
        INTEGER i,j,k,l,m,n
c--------------------------------------------
c       Calculate damage variable, D
c
c       D=1-E/Ei  Ei=initial MOE, E=MOE at cycle
c
c--------------------------------------------
        IF(iii.EQ.1) GOTO 10  !Set inital MOE, which is assumed to come
from the
        GOTO 20                           !first set of data
10      Eci=Ec
        Eui=Eu
        Eai=Ea
        Esi=Es
20      CONTINUE
c
        Dc=1-Ec/Eci
        Du=1-Eu/Eui
        Da=1-Ea/Eai
c
        Ds=1-Es/Esi
c
        RETURN
        END
c
c
c*********************************************************************
```

137

```
      SUBROUTINE MOE(strs,strn,app,ult,s,xMOI,phase,Ec,Esult,Esapp,
     +Estor,Eloss)
      IMPLICIT double PRECISION (a-h,o-z)
      INTEGER i,j,k,l,m,n
C-------------------------------------------------
c     Determine 3 differenct MOE values
c          Ec = Complex modulus = maxstress/masxtrain
c          Esult = Secant modulus = 5L^3/324I*(ultimateslope)
c          Esapp = Secant modulus = 5L^3/324I*(appliedloadslope)
C-------------------------------------------------
      Ec=strs/strn
      Esult=((5*s**3)/(324*xMOI))*ult
      Esapp=((5*s**3)/(324*xMOI))*app

      Estor=Ec/(sqrt(1+(tan(phase))**2))
      Eloss=sqrt(Ec**2-Estor**2)


C
      RETURN
      END
C
C*********************************************************************
      SUBROUTINE stressstrain(xloadmax,xloadmin,CHmax,CHmin,
     +strsmax,strsmin,strnmax,strnmin,xMOI,depth,span)
      IMPLICIT double PRECISION (a-h,o-z)
      INTEGER i,j,k,l,m,n
C-------------------------------------------------------------
c     stress = My/I = PLy/I6
c     strain = 27hDmax/5L^2*100 (in percent)   -Based on Crosshead
deflection
c
C-------------------------------------------------------------
c
      strsmax=(xloadmax*span*(depth/2))/(xMOI*6)
      strnmax=(27*depth*CHmax)/(5*span**2)
      strsmin=(xloadmin*span*(depth/2))/(xMOI*6)
      strnmin=(27*depth*CHmin)/(5*span**2)
C
      RETURN
      END
C
C
*********************************************************************
*
      SUBROUTINE centerdefl(xloadmax,xloadmin,CHmax,CHmin,xdispmax,
     +xdispmin,slope)
      IMPLICIT double PRECISION (a-h,o-z)
      INTEGER i,j,k,l,m,n
C--------------------------------------------------------
c     D = center deflection
c     Dmax--Crosshead deflectin
c
c     Crosshead deflection is converted assuming a radius of curvature
c     within the moment free region.
c
c     E=23L^3/1296I (slope)   slope is taken between 20%and40% of
ultimate as done in static
c
c     D = Dcrosshead+PL^3/432EI
c     E = 5L^3/324I*slope
c
c     so, D = Dcrosshead + 3P/(20slope)
C--------------------------------------------------------
```

```
c
      xdispmax=CHmax+(3*xloadmax)/(20*slope)
      xdispmin=CHmin+(3*xloadmin)/(20*slope)
c
      RETURN
      END
c
c
c*********************************************************************
      SUBROUTINE avgslope(X,Pmin,ultimate,slope,iii,ipts)
      IMPLICIT double PRECISION (a-h,o-z)
      INTEGER i,j,k,l,m,n
      DIMENSION X(5000,2,10001),Pmin(50,2),Pmax(50,2),tempslope(50)
c------------------------------
c Calculate the slope of each cycle within the block between the 20 and
c 40% of ultimate
c   - based on linear regression model
c   - calculates slopes from the first minimum to the last minimum-1
c     X(:,1,:) -->load
c     X(:,2,:) -->disp
c
c     x-disp
c     y-load
c     sumx = sum of the load between values
c     sumy = sum of the disp between values
c     sumxy = sum of disp*load between values
c     sumxsq = sum of load*load
c------------------------------
c Count data
      ierror=0
      icount=ipts-1          !do not use last data point, they can have
bad data
      xlow=0.2*ultimate
      xhigh=0.4*ultimate
c
      DO nn=1,20
      tempslope(nn)=0
      ENDDO

c
222   DO k=2,icount   !loop thru each cycle in the block, skip 1st&last

          mstart=Pmin(k,2)
          mend=Pmin(k,2)+(Pmin(k+1,2)-Pmin(k,2))/2  !stops halfway
          m=mstart

          n=0             !data points for slope

          sumxy=0         !initialize sumations
          sumx=0
          sumy=0
          sumxsq=0

          DO WHILE(m.LT.mend)

          DO WHILE(X(iii,1,m).GT.xlow.AND.X(iii,1,m).LT.xhigh)
          yy=X(iii,1,m)
          xx=X(iii,2,m)
c
          sumxy=sumxy+xx*yy
          sumx=sumx+xx
          sumy=sumy+yy
          sumxsq=sumxsq+xx*xx
c
```

```
                    m=m+1   !absolulte position
                    n=n+1   !data point count
                  ENDDO
101               m=m+1
                ENDDO
                IF(n.EQ.0)GOTO 200
                sxy=sumxy-(sumx*sumy)/n
                sxx=sumxsq-(sumx*sumx)/n
                tempslope(k-1)=sxy/sxx
200     CONTINUE
        ENDDO

        CALL average(slope,tempslope,0,icount)

        RETURN
        END
c
c
c********************************************************************
        SUBROUTINE averagephaseshift(X,w,avg,scan,idatapts,freq,iii)
        IMPLICIT double PRECISION (a-h,o-z)
        INTEGER i,j,k,l,m,n
        DIMENSION X(5000,2,10001),xloadtime(100),xdisptime(100)
c--------------------------------
c Determines the difference in the location of the load and displacment
c plots using the
c     mean of the wave
c--------------------------------
c
        waves=idatapts/scan*freq
        ipts=scan/waves
c
c Find maximum and minimum overall
c
        xlmax=0
        xlmin=9999
        xdmax=0
        xdmin=9999
c
        DO j=1,idatapts
             IF(X(iii,1,j).GT.xlmax) xlmax=X(iii,1,j)
             IF(X(iii,1,j).LT.xlmin) xlmin=X(iii,1,j)
             IF(X(iii,2,j).GT.xdmax) xdmax=X(iii,2,j)
             IF(X(iii,2,j).LT.xdmin) xdmin=X(iii,2,j)
        ENDDO
c
        xloadmean=((xlmax-xlmin)/2)+xlmin
        xdispmean=((xdmax-xdmin)/2)+xdmin
c
c
        iload=0
        idisp=0
c
c Find the phase from the mean value (increasing load side only)
        kk=2
        DO WHILE (kk.LE.idatapts)    !loop thru all data in block
        Xupload=X(iii,1,kk)                !upper value
        Xloload=X(iii,1,kk-1)        !lower value

             IF(Xupload.GE.xloadmean.AND.Xloload.LT.xloadmean) GOTO 5000
             GOTO 5001
5000         iload=iload+1
             Rx=Xupload-Xloload
             Rt=xloadmean-Xloload
```

```fortran
                xloadtime(iload)=Rt/Rx+(kk-1)
                kk=kk+ipts/2
5001    CONTINUE
        kk=kk+1
        ENDDO

        kk=2
        DO WHILE(kk.LE.idatapts)
        Xupdisp=X(iii,2,kk)
        Xlodisp=X(iii,2,kk-1)

                IF(Xupdisp.GE.xdispmean.AND.Xlodisp.LT.xdispmean) GOTO 6000
                GOTO 6001
6000            idisp=idisp+1
                Rxx=Xupdisp-Xlodisp
                Rtt=xdispmean-Xlodisp
                xdisptime(idisp)=Rtt/Rxx+(kk-1)
                kk=kk+ipts/2
6001    CONTINUE
        kk=kk+1
        ENDDO
c
c Find the average phase
c
c
        Diff=xdisptime(1)-xloadtime(1)
        IF(abs(Diff).GT.0.5*ipts)GOTO 700 !check if one wave is offset by
one mean
        GOTO 800                                              !crossing
c
700     IF(Diff.LT.0) GOTO 771           !need to eliminate first value
of disp
        GOTO 772
771     DO m=1,idisp
                xdisptime(m)=xdisptime(m+1)
        ENDDO

772     IF(Diff.GT.0) GOTO 773
        GOTO 800
773     DO m=1,iload
                xloadtime(m)=xloadtime(m+1)
        ENDDO

800     CONTINUE

        IF(iload.GE.idisp) iloop=iload
        IF(iload.LT.idisp) iloop=idisp

        sumA=0
        icount=0

        DO nn=2,iloop-1  ! leave out the first and last data point in
average
                icount=icount+1
                sumA=sumA + abs(xdisptime(nn)-xloadtime(nn))
        ENDDO

        avgA=sumA/icount
c
        avg=(1/scan)*avgA*w
c
        RETURN
        END
c
```

```fortran
C****************************************************************
      SUBROUTINE average(avg,thedata,jj,icount)
      IMPLICIT double PRECISION (a-h,o-z)
      INTEGER i,j,k,l,m,n
      DIMENSION thedata(50)
C----------------------------
c   Finds the average of a set of data
c   jj=-1 to remove last 2 peices of data
c   jj=0 to count all data
C----------------------------
c
      total=0
      ii=icount+jj  !removes last piece if required
      nn=1-jj       !removes first piece if required
      DO k=nn,ii
           total=total+thedata(k)
      ENDDO
c
      avg=total/(ii+jj)
c
      CONTINUE

      RETURN
      END
c
c
C****************************************************************
      SUBROUTINE displacmentmaxmin(X,Dmax,Dmin,iii,freq,scan,imax,imin,
     +idatapts)
      IMPLICIT double PRECISION (a-h,o-z)
      INTEGER i,j,k,l,m,n
      DIMENSION X(5000,2,10001),Dmax(50,2),Dmin(50,2)
C--------------------
c Finds the displacment setpoint for the given block of data, then call
c the maxmin subroutine to calculate
C--------------------
c
      tempmax=0
      tempmin=1000
      DO kk=1,20
      Dmax(kk,1)=0
      Dmin(kk,2)=0
      Dmax(kk,1)=0
      Dmin(kk,2)=0
      ENDDO
c
      DO mmm=1,idatapts
           IF(X(iii,2,mmm).GT.tempmax)GOTO 10
           GOTO 11
10         tempmax=X(iii,2,mmm)
           themax=tempmax
11         CONTINUE
c
           IF(X(iii,2,mmm).LT.tempmin)GOTO 20
           GOTO 21
20         tempmin=X(iii,2,mmm)
           themin=tempmin
21         CONTINUE
      ENDDO
c
      thesetpoint=(themax-themin)/2+themin
c
c Find the max and min of each cycle
      CALL maxmin(X,Dmax,Dmin,iii,freq,scan,2,thesetpoint,imax,imin,
```

```
     +idatapts)
c
      RETURN
      END
c
c
c*******************************************************************
      SUBROUTINE actualfrequency(P,scan,output,imax)
      IMPLICIT double PRECISION (a-h,o-z)
      INTEGER i,j,k,l,m,n
      DIMENSION P(50,2)
c----------------------------------------------------
c This subroutine calculates the actual frequency of
c each block of data using the set of maximum values and the locations
c The subroutine passes back a single value, which is the average freq
c for this block
c The first and last maximum is neglected b/c it might occur becasue of
c the end of block
c----------------------------------------------------
c Count the number of full cycles present in data
c
      istart=2    !skip first piont
      iend=imax-1 !skip last piont
      waves=iend-istart
c
      tstart=P(istart,2)      !location of the first max
      tend=P(iend,2)       !location of the last maximum
c
      output=waves/((tend-tstart)*1/scan)  !calculate freq
c
      RETURN
      END
c
c
c*******************************************************************
      SUBROUTINE
maxmin(X,themax,themin,iii,freq,scan,m,setpt,imax,imin,
     +idatapts)
      IMPLICIT double PRECISION (a-h,o-z)
      INTEGER i,j,k,l,m,n
      DIMENSION X(5000,2,10001),themax(50,2),themin(50,2)
c----------------------------------------------------------------------
c Determine maximum and minimum of the load and displacement data
c      - Subroutine searches sets of 500 only, it must be run for each
c set
c      - Use the first point of the data to determine a limit to check
c        above
c         to usure that each cycle has a max and min
c      - the relative position of the value is also stored
c
c xmin(i,1) = value
c xmin(i,2) = location
c j = 1....n (refrence index)
c iii = the group number
c freq = nominal test frequency, used for compensating for noisy data
c m = 1 for load
c m = 2 for displacement
c----------------------------------------------------------------------
c
      B=(500/scan)*freq     !Cycles per read
      C=500/B                        !Nominally a maximum occurs every C
data pts
      js=C/3                  !If the data file moves SF data pts from
max it is
```

```
c                                           !waiting for the next value
c
c zero data
      DO mm=1,20
      themax(mm,1)=0
      themax(mm,2)=0
      themin(mm,1)=0
      themin(mm,2)=0
      ENDDO
c
      y=setpt !must be GT or LT, first point is near setpoint
c
c FIND MAXIMUM VALUES AND LOCATIONS
      k=0    !first data point
      j=1                   !index number
      DO WHILE(k.LT.idatapts)
c
             k=k+1
         temp=0   !temporary storage for maximum value

             DO WHILE(X(iii,m,k).GT.y)
c
             IF(X(iii,m,k).GT.temp)GOTO 101
             GOTO 102
101          themax(j,1)=X(iii,m,k) !use actual values for max
             themax(j,2)=k
             temp=themax(j,1)
             jk=k  !temp location of maximum
c
102          k=k+1 !Go to next value
             IF(k.GT.idatapts) GOTO 203     !Exits if k exceeds data
points in block
             IF(k.EQ.jk+js)GOTO 201    !This statement checks if the
data is
             ENDDO
             IF(k.EQ.jk+js)GOTO 201
             GOTO 202                          !obviously past the
maximum, if so the
201          j=j+1                            !the index is changed to
accept a new value
202          CONTINUE
c
203   ENDDO
c
c FIND MINIMUM VALUES AND LOCATIONS(same as maximum except use lt temp)
      k=0
      j=0
      DO WHILE(k.LT.idatapts)
c
             k=k+1
             temp=99999  !temporary storage for minimum
c
             DO WHILE(X(iii,m,k).LT.y)
c
             IF(X(iii,m,k).LT.temp) GOTO 1001
             GOTO 1002
1001         themin(j,1)=X(iii,m,k) !use actual data for min
             themin(j,2)=k
             temp=themin(j,1)
             jk=k  !temp location of the minimum
c
1002         k=k+1
             IF(k.GT.idatapts) GOTO 2003
             IF(k.EQ.jk+js)GOTO 2001
```

```fortran
              ENDDO
              IF(k.EQ.jk+js)GOTO 2001
              GOTO 2002
2001          j=j+1
2002          CONTINUE
2003    ENDDO
c
c       Count the number of min's and max's
        nn=1
        mm=1
        DO WHILE(themax(nn,1).NE.0)
        nn=nn+1
        ENDDO
        DO WHILE(themin(mm,1).NE.0)
        mm=mm+1
        ENDDO
        imax=nn-1
        imin=mm-1
c
        RETURN
        END
c
c***********************************************************************
        SUBROUTINE readdata(X,cyclecount,temp,time,iin,icycle,itemp,scan,
     +freq,zero,iblocks,idatapts)
        IMPLICIT double PRECISION (a-h,o-z)
        INTEGER i,j,k,l,m,n
        DIMENSION X(5000,2,10001),xtemp(2,50001),cyclecount(999)
        DIMENSION temp(4,999)
        CHARACTER time(999)*11
c----------------------------------------------------------------------
c               -reads data from two columns in the form of:
c load,displacement
c               -data is from fatigue tests
c               -The file is ogranized as follows:
c
c                       7:00:00 AM  !time which reading begins
c                       xxxx,xxxx   !Data,1st block has 5000 pairs
c                       xxxx,xxxx
c                       -9999       !Time block break
c                       7:00:10 AM  !Next time
c                       xxxx,xxxx   !2nd and above time blocks contain 500
c pairs
c                       xxxx,xxxx
c----------------------------------------------------------------------
c       X(i,j,k) is an array of arrays
c                       i = the cycle index
c                       j = 1 or 2 (1=load,2=disp)
c                       k = data per a given block
c
c       i<500 b/c all tests have less than 500 reads
c
c       k=5001 1st block    (1-5000 is data, 5001 is the -9999 break)
c        =501 all other blocks (1-500 is data, 501 is the -9999 break)
c
c       time(i) = time stamp extraxted from the data, i = cycle index
c (same as for X())
c       xtemp(2,5001) = temp file used to extract then organize data into
c X()
c       temp(4,500) = thermocouple 1,2,3,4 etc
c----------------------------------------------------------------------
c
cREAD THE INTIAL TIME
        k=1
```

145

```fortran
      READ(iin,1001) time(1)
c
c READ 1st time block (5000 data points, plus one break)
      jend=(10*idatapts)+1
      DO j=1,jend                                !Data + break
          READ(iin,2000,end=100) xtemp(1,j), xtemp(2,j)  !Read--
>load,disp
      ENDDO

      CONTINUE
c
c READ the remainder of the data blocks 2 thru 500
      nend=idatapts+1
      DO k=11,999
!cycle index loop
          READ(iin,1001,end=100)time(k)               !read the time
print
c
              DO n=1,nend                                    !read the
500pts in block
              READ(iin,2000,end=100) X(k,1,n), X(k,2,n)
              ENDDO
      ENDDO
c
100   CONTINUE
      iblocks=k-1
c
c READ the cycle counts
c      - The first cycle represents 10 sets of 500, this is not in file
c           the file starts begins with the first set of 500 which is
the
c           11th group of 500
c
      DO ii=11,999
          READ(icycle,3000,end=200) cyclecount(ii)
      ENDDO
c
200   CONTINUE
c
c READ Temperatures (same situation as above)
c
c       READ(itemp,4001,end=300)temptitle
c
c
      DO jj=11,999
          READ(itemp,4000,end=300)temp(1,jj),temp(2,jj),temp(3,jj),
      +     temp(4,jj)
      ENDDO
c
300   CONTINUE
c
c TRANSFER xtemp data into X()
c      -break the 5000 points into 10 sets of 500 points, each which
c       represents 1s of data
c
      l=0 !index for xtemp

      DO i=1,10 !Cycle count index of X()
          DO j=1,idatapts
              l=l+1
              X(i,1,j)=xtemp(1,l)       !load
              X(i,2,j)=xtemp(2,l)       !deflection
          ENDDO
      ENDDO
```

146

```
c
c INSERT mising cycle counts
      count=500/scan*freq
      w=0
      DO kk=1,10
      cyclecount(kk)=w
      w=w+count
      ENDDO
      cyclecount(1)=1
c
c ADD compensation for actuator's initial position too the displacments
      DO nn=1,999        !Reads
      DO ii=1,idatapts      !Data points
          X(nn,2,ii)=X(nn,2,ii)+zero
      ENDDO
      ENDDO
c
c
c FORMAT STATEMENTS:
1001  FORMAT(a11)           !Time output file format
2000  FORMAT(2F10.5)       !Load/Disp data
3000  FORMAT(F10.0)
4000  FORMAT(4F10.5)
c
      RETURN
      END
```

APPENDIX H – EXAMPLE CALCULATIONS FOR T-TEST OF MEAN

MECHANICAL PROPERTIES

H.1 T-test example calculation

Hypthosis: H_0: $X_1 = X_2$ (means of the two samples are equal)

              H_a: $X_1 \ne X_2$ (means of the two samples are not equal)

Mean, COV, and Sample size:

$X_1 := 1.19$ $COV_1 := 20\%$ $N_1 := 5$

$X_2 := 1.68$ $COV_2 := 20.1\%$ $N_2 := 5$

Standard Deviation: $s_1 := X_1 \cdot COV_1$ $s_2 := X_2 \cdot COV_2$

Test Statistic:

$$T := \frac{X_1 - X_2}{\sqrt{\dfrac{(s_1)^2}{N_1} + \dfrac{(s_2)^2}{N_2}}} \qquad T = -2.652$$

Degress of Freedom:

$$dof := \frac{\left(\dfrac{s_1^{\,2}}{N_1} + \dfrac{s_2^{\,2}}{N_2}\right)^2}{\left[\dfrac{\left(\dfrac{s_1^{\,2}}{N_1}\right)^2}{N_1 - 1} + \dfrac{\left(\dfrac{s_2^{\,2}}{N_2}\right)^2}{N_2 - 1}\right]} \qquad dof = 7.187$$

Significance Level and probability: $\alpha := 20\%$ $p := 1 - \alpha$

Critical value of t-distribution: $t :=$

Probabilty:	0.8
D.O.F.	7.187484
t (α/2,dof)	0.26

$t = 0.263$

(utilizes Microsoft Excel t-statsitic function)

$(p \quad dof)$

Reject or Fail to Reject Null if:

$P := $ "Reject"   if $T < -t$

         "Reject"   if $T > t$ $P = $ "Reject"

         "Fail to Reject"   otherwise

H.2 T-test results

I.D.	Strain to Failure			Modulus of Elasticity		
	Test statisitc	**Critical Value**	**Fail or Reject Null Hypotheis**	**Test statisitc**	**Critical Value**	**Fail or Reject Null Hypotheis**
			α = 20%			*α= 20%*
1	1.45	0.256	Reject	-5.10	0.256	Reject
2	3.03	0.257	Reject	-9.53	0.257	Reject
3	7.68	0.256	Reject	15.46	0.256	Reject
4	-3.82	0.256	Reject	2.61	0.256	Reject
5	5.64	0.256	Reject	0.01	0.256	Fail to Reject
6	8.44	0.256	Reject	26.03	0.256	Reject
7	0.41	0.256	Reject	-5.05	0.256	Reject
8	1.06	0.256	Reject	2.39	0.256	Reject
9	-0.77	0.256	Reject	-2.25	0.256	Reject
10	-7.07	0.257	Reject	1.35	0.257	Reject
11	-3.85	0.256	Reject	7.71	0.256	Reject

I.D.	Modulus of Rupture			Shear Block		
	Test statisitc	**Critical Value**	**Fail or Reject Null Hypotheis**	**Test statisitc**	**Critical Value**	**Fail or Reject Null Hypotheis**
			p = 20%			*p = 20%*
1	1.42	0.256	Reject	0.14	0.256	Reject
2	-1.24	0.257	Reject	-4.36	0.256	Reject
3	15.21	0.256	Reject	10.63	0.256	Reject
4	1.52	0.256	Reject	-5.52	0.257	Reject
5	17.53	0.256	Reject	0.77	0.258	Reject
6	24.23	0.256	Reject	0.67	0.256	Reject
7	-2.29	0.256	Reject	4.93	0.256	Reject
8	6.34	0.256	Reject	-3.27	0.256	Reject
9	-0.27	0.256	Reject	13.41	0.256	Reject
10	-2.27	0.257	Reject	-1.55	0.256	Reject
11	4.35	0.256	Reject	-3.91	0.257	Reject